Shun Hing Institute of Advanced Engineering
信興高等工程研究所

Report and Research Highlights
2018 - 2019

June 2019

香　港　中　文　大　學
The Chinese University of Hong Kong

Printed in June 2019, this report contains information known as at June 2019.

Every effort has been made to ensure that the information contained in this report is correct at the time of printing. Shun Hing Institute of Advanced Engineering (SHIAE) – CUHK, reserves the right to make appropriate changes to the materials presented in this report without prior notice.

For further information, please visit our website: http://www.shiae.cuhk.edu.hk

Contents

INTRODUCTION OF SHIAE **4**

ORGANIZATION **6**

COMPOSITION OF INTERNATIONAL ADVISORY BOARD 6
COMPOSITION OF MANAGEMENT COMMITTEE 9
SHUN HING VISITING SCHOLARS/ FELLOWS 10

FINANCIAL STATUS OF SHIAE **11**

RESEARCH **14**

OUTSTANDING RESEARCH HIGHLIGHTS 14
ACADEMIC PUBLICATIONS 14
PROJECT EXHIBITION 15
RENEWABLE ENERGY TRACK 17
Research Reports *17*
BIOMEDICAL ENGINEERING TRACK 44
Research Reports *44*
MULTIMEDIA TECHNOLOGIES & AI TRACK 95
Research Reports *95*

SHUN HING DISTINGUISHED LECTURE SERIES **103**

Introduction of SHIAE

Mission of SHIAE

The MISSION of the Institute is to spearhead, conduct, promote and co-ordinate research in advanced engineering. There is no end to the list of areas to be explored and the plan is to give priority to research topics that are both exciting and innovative. The Institute also aspires to transferring its research results to industry for practical application and to put across to the community at large the role of engineering as a driving force for human development through educational activities.

As a pioneering institute exploring the forefront of the engineering science, The Shun Hing Institute of Advanced Engineering will

- spearhead state-of-the-art advanced engineering research
- create and sustain synergy with world-class researchers
- develop with and transfer to industries cutting edge technologies
- promote appreciation of engineering in society through educational programmes

The Shun Hing Education and Charity Fund was founded the late by Dr. William Mong Man Wai with the aim of enhancing educational opportunities for the younger generations. The Fund has already sponsored numerous educational and research programmes in Hong Kong, the Mainland, and overseas educational institutions. Himself an engineer and a firm believer in advancing the quality of life through the development of science and technology, Dr. Mong had been there to support the establishment and growth of this Institute from the beginning.

Centre of Excellence at CUHK

The Chinese University of Hong Kong is an internationally renowned institution of higher learning devoted to quality teaching and both academic and applied research. The University has established 29 research institutes and a number of research centres with a view to pursuing up-front research endeavours with focused goals and objectives. The Shun Hing Institute of Advanced Engineering plays a crucial part in the research infrastructure of the Chinese University which is committed to exciting research programmes in advanced engineering areas. The Institute is now in its second decade of development, and we are particularly pleased to have received continual staunch support and guidance from Mr. David Mong Tak Yeung, Chairman and CEO of the Shun Hing Group and the Shun Hing Education and Charity Fund.

As a strategic centre of excellence at The Chinese University of Hong Kong, the Institute supports greater regional and international research collaborations, and strives to attract talent from the world over to achieve greater internationalization, a vision strongly advocated by every member of the University.

Commitment of the Faculty of Engineering

The Faculty of Engineering was founded in 1991 and was built upon existing strengths with added talent from all over the world. The Faculty has been able to attract some of the best minds. Many received their training in leading universities in North America, Great Britain and Australia. Most of them have extensive experience in industry and many are leaders in their fields. This team of top-notch talent is gathered to nurture local talent through educational programmes, and break new frontiers in research through innovative and exciting research endeavours.

The positioning of The Shun Hing Institute of Advanced Engineering in the William M.W. Mong Engineering Building is deliberate as a key nucleating point to integrate research endeavours in the Engineering Faculty and its neighbours. Our members join hands with their counterparts from the Faculties of Science and Medicine in many interesting research collaborations. It is the ambitious goal of the Faculty of Engineering that the Institute should become a lighthouse for the local technology landscape to herald the migration towards high value-added technology and an information economy.

The mission of the Institute is to spearhead, conduct, promote and co-ordinate research in advanced engineering. There is no end to the list of areas to be explored and the plan is to give priority to research topics that are both exciting and innovative. The Institute also aspires to transferring its research results to industry for practical application and to put across to the community at large the role of engineering as a driving force for human development through educational activities.

Building on Strength and The Way Ahead

Many of the Institute's research projects are built upon areas in which the Faculty has already achieved outstanding performance. These are areas that have great potential for further technological advancement and in line with industrial development in Hong Kong. The Institute provides a vibrant R&D environment to spur new discoveries and speed up their translation into applications. Since 2012, we have expanded our scope to cover new frontiers in Renewable Energy striving to answer tomorrow's energy challenges. In year 2017, we further expand the research scope in Multimedia Technologies to include Artificial Intelligence, Big Data Analytics and Deep Learning as well.

Technology Transfer

Synergy with industry is the ultimate goal of research and development in Hong Kong. External experts have been brought in to the Institute to lead research projects that could benefit the industrial sector.

The technology transfer arm of the Faculty of Engineering plays an important role in the traffic between the Institute and industry. The Institute houses an array of top-notch research and development activities encompassing contract research, spin-off companies, and consultancies.

Contribution to Society

The Institute has been making contributions to the progress of Hong Kong through a wide range of educational activities like training courses, seminars, symposiums which disseminate the latest technologies to promote appreciation of engineering in society and arouse interest of the younger generations in engineering.

Organization of SHIAE

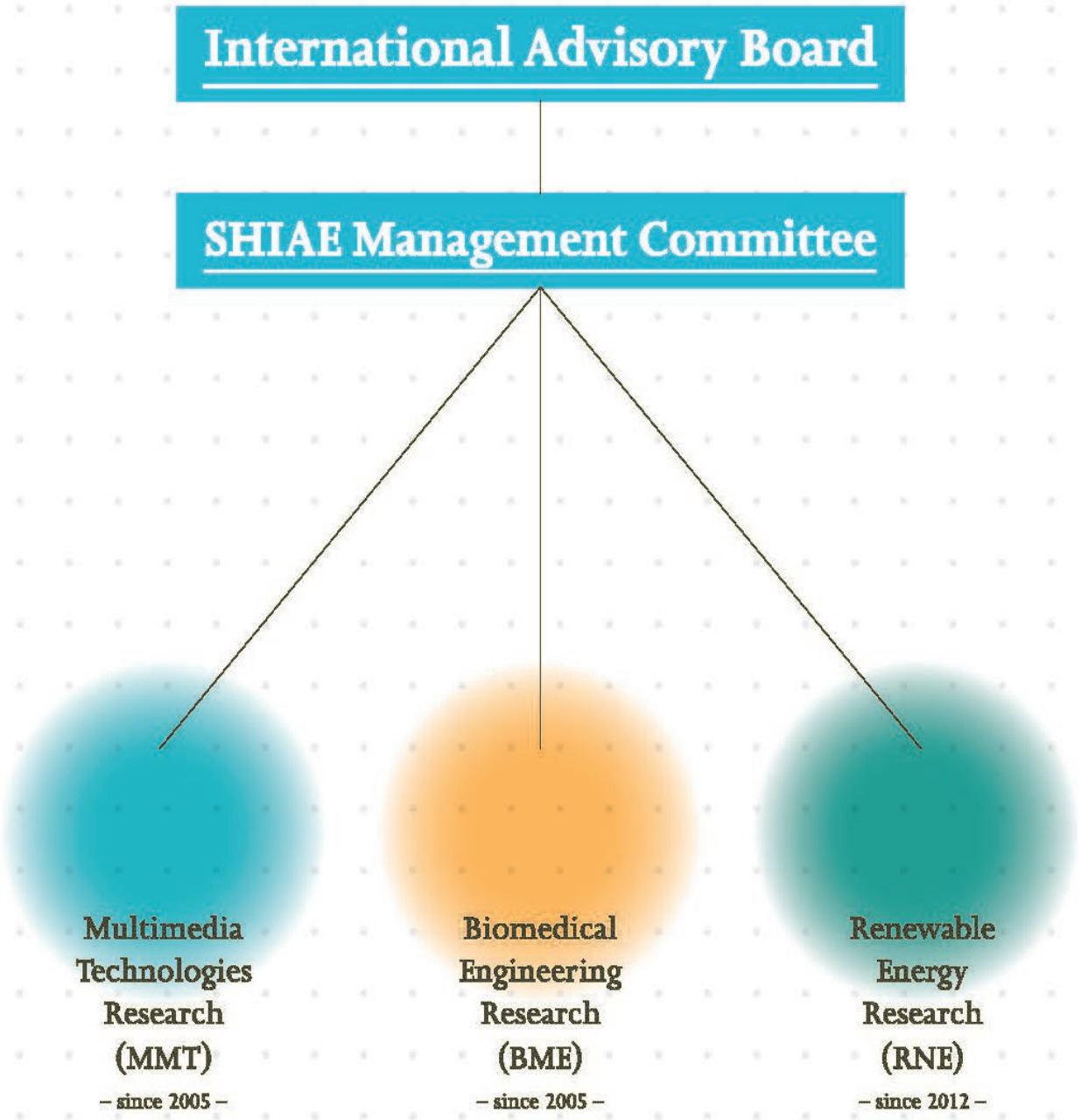

We also provide support and sponsorship to the Faculty of Engineering in organizing prestigious academic conferences in Hong Kong so as to raise our international profile.

Composition of International Advisory Board

Chairman:

Dr. David T.Y. MONG 蒙德揚先生

Chairman & Group CEO
Shun Hing Electronic Holdings Limited
Hong Kong

Members:

Professor Victor ZUE

Delta Electronics Professor of Electrical Engineering and Computer Science
Massachusetts Institute of Technology
U.S.A

Dr. Harry SHUM 沈向洋博士

Executive Vice President, Technology and Research
Microsoft Corporation
U.S.A.

Professor Yongmin KIM

Affiliate Professor
University of Washington
U.S.A.

Professor C.C. Jay KUO

Professor of Electrical Engineering and Computer Science
University of Southern California
U.S.A.

Professor Paul, Kit-lai YU

Provost, Revelle College, Jacobs School of Engineering
University of California, San Diego
U.S.A.

Professor Tai Fai FOK 霍泰輝教授

Pro-Vice-Chancellor
The Chinese University of Hong Kong
Hong Kong

Professor Wing-shing WONG 黃永成教授

Choh-Ming Li Professor of Information Engineering
The Chinese University of Hong Kong
Hong Kong

Professor Ching Ping WONG 汪正平教授

Emeritus Professor of Electronic Engineering
The Chinese University of Hong Kong
Hong Kong
(till 31 July 2019)

Professor Martin Ding Fat WONG 黃定發教授

Dean of Engineering
The Chinese University of Hong Kong
Hong Kong
(from 1 August 2019)

Professor Pak Chung CHING 程伯中教授

Director of Shun Hing Institute of Advanced Engineering
Choh-Ming Li Professor of Electronic Engineering
The Chinese University of Hong Kong
Hong Kong

Composition of Management Committee

Chairman:

Professor Pak Chung CHING *(ex-officio)*
Director of SHIAE, and Choh-Ming Li Professor of Electronic Engineering

Members:

Professor Martin Ding Fat WONG *(ex-officio)*
Dean of Faculty of Engineering
(from 4 January 2019)

Professor Ching Ping WONG *(ex-officio)*
Dean of Faculty of Engineering
(till 3January 2019)

Mr. Terrence CHAN
Managing Director of Shun Hing Electronic Holdings Limited
Hong Kong

Professor Jack C.Y. CHENG
Department of Orthopaedics and Traumatology

Professor Jianwei HUANG
Department of Information Engineering

Professor Tan LEE
Department of Electronic Engineering

Professor Wei-Hsin LIAO
Department of Mechanical and Automation Engineering

Professor Anthony Man-cho SO
Department of Systems Engineering and Engineering Management

Professor Raymond Kai-yu TONG
Department of Biomedical Engineering

Member and Secretary:

Professor John C.S. LUI
Choh-Ming Li Professor of Computer Science and Engineering

Shun Hing Visiting Scholars/ Fellows

The Institute has launched a Shun Hing Distinguished Scholar Program with an aim to attract distinguished scholars to pursue research collaboration with our faculty and to strengthen our research profile. The following scholars visited to work either on a short term or on a longer term engagement with the Institute between 2018 and 2019.

Shun Hing Fellows and Research Associate:
(in alphabetical order)

Mr. HUANG Peiyuan 2018-2019
University of Texas Southwestern Medical Centre, USA

Dr. LEE Chinghuan 2016-2018
National Chung Kung University, Taiwan

Mr. LEUNG Wing Cheong 2017-2018
Hong Kong Polytechnic University, Hong Kong

Dr. LI Qiang 2018-2019
School of Communication and Information Engineering, China

Dr. LI Xiaoyi 2018-2019
Tsinghua University, China

Dr. LIU Huikang 2018-2019
The Chinese University of Hong Kong, Hong Kong

Dr. Wang Jianjian 2018-2019
Tsinghua University, China

Dr. WANG Jiaqi 2019-2020
Hong Kong University of Science and Technology, Hong Kong

Ms. XIAO Qinru 2018-2019
The Chinese University of Hong Kong, Hong Kong

Dr. XIN Zhen 2018-2019
Aalborg University, Denmark

Mr. ZHANG Haiqiang 2018-2019
Tsinghua University, China

Mr. ZHAO Shirui 2017-2019
Ocean Unversity of China, China

Financial Status of SHIAE

INCOME AND EXPENDITURE STATEMENT 2018-2019

(Fiscal Year: April 1, 2018 – March 31, 2019)

	Notes	As at 31 March 2019	As at March 31, 2018
INCOME			
Funding Source			54,500,000
Accumulated fund brought forward		19,345,287	-
Interest and investment income		222,422	7,142,755
Sub-total:		19,567,709	61,642,755
EXPENDITURE			
Research Funding	(2)	2,962,000	40,649,200
Remaining fund from completed projects		-317,704	-3,191,128
Operating cost		413,786	4,839,396
Sub-total:		3,058,082	42,297,468
BALANCE as at 31 March 2019		**16,509,627**	**19,345,287**

APPROVED BUDGET 2019-2020

(Fiscal Year: April 1, 2019 – March 31, 2020)

	Notes	
INCOME		
Accumulated fund brought forward		16,509,627
Projected interest and investment income		200,000
Sub-total:		16,709,627
EXPENDITURE		
Research Funding		
On-going projects (Year 2018 batch)	(2)	1,527,000
Newly funded projects (Year 2019 batch)	(2)	1,550,000
Operating cost		
Staff and Admin. cost		430,000
Distinguished lectures		10,000
Activities Sponsorship		100,000
Sub-total:		**3,617,000**
Projected Balance in March 2020		**13,092,627**

Note (1) Annualized Research Funding to each research areas granted since 2010

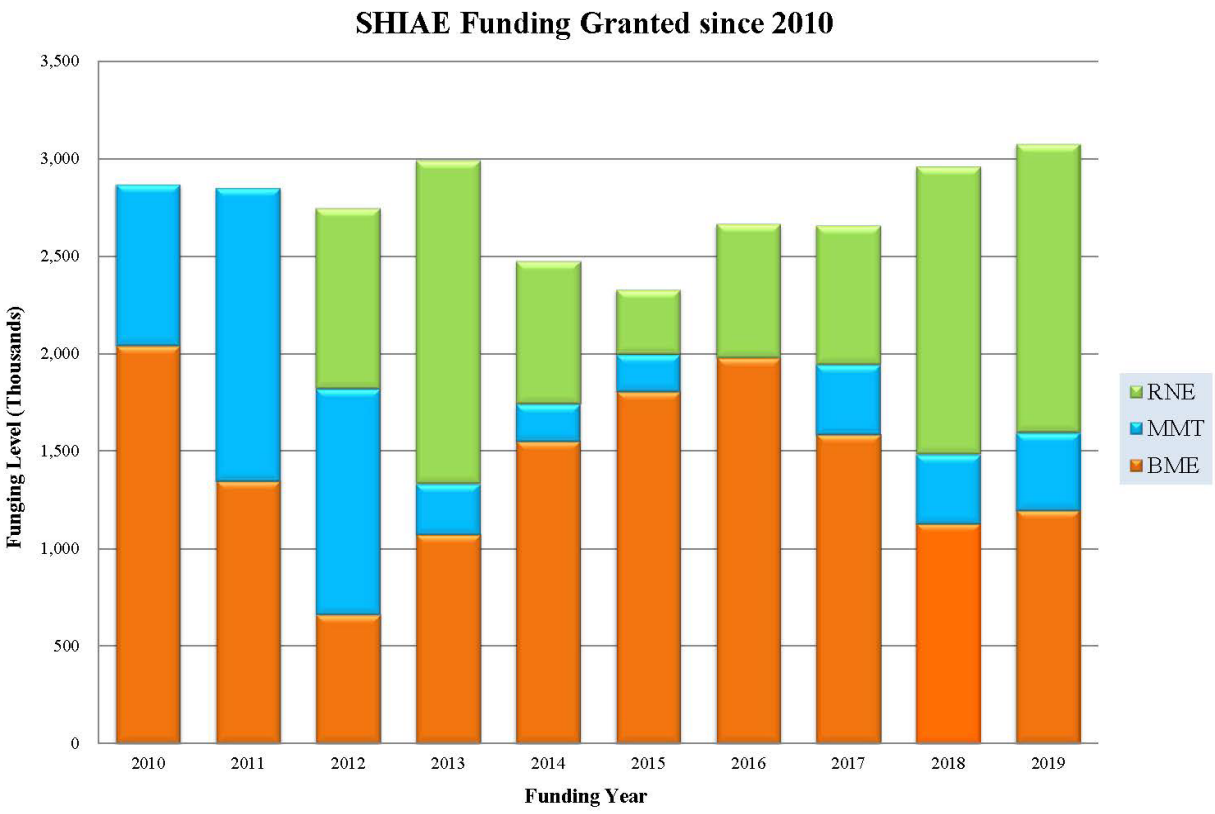

This figure shows the distribution of the SHIAE funding granted to each track of research projects, namely Biomedical Engineering (BME), Multimedia Technology (MMT) and Renewable Energy (RNE) annually.

Note (2) Total funding for each batch of projects (in HK$ '000)

Funding Year / No. of projects	2020 (committed)	2019	2018	2017	2016	2005 - 2015
Year 2005 / 6 Projects	-	-	-	-	-	6,108
Year 2006 / 5 Projects	-	-	-	-	-	3,175
Year 2007 / 7 Projects	-	-	-	-	-	4,146
Year 2008 / 4 Projects	-	-	-	-	-	3,976
Year 2009 / 5 Projects	-	-	-	-	-	3,306
Year 2010 / 5 Projects	-	-	-	-	-	2,789.2
Year 2011 / 4 Projects	-	-	-	-	-	2,476
Year 2012 / 5 Projects	-	-	-	-	-	3,040
Year 2013 / 4 Projects	-	-	-	-	-	2,948
Year 2014 / 3 Projects	-	-	-	-	-	2,004
Year 2015 / 4 Projects	-	-	-	-	1,328	1,328
Year 2016 / 4 Projects			-	1,213	1,340	-
Year 2017 / 4 Projects			1,447	1,447	-	
Year 2018 / 4 Projects		1,527	1,515	-	-	
Year 2019 / 4 Projects	1,550	1,550		-	-	
WOSP2007			-	-	-	25
	1,550	3,077	2,962	2,660	2,668	35,321.2

Accumulated Total: **HK$48,238,200.00**

This table shows the detail amount of SHIAE funding granted to each batch of research projects. The subtotal amount of **1.550 million** budgeted for 2020 is committed to support research projects in July 2020.

Research - *Outstanding Research Highlights*

Academic Publications

So far **56 projects** have been successfully completed and **433 articles** arising from the results of these research projects have been published in international conference proceedings and journals. The other **8 on-going projects** are also progressing well with encouraging results produced. All publications generated by each individual projects are kept in the archive of SHIAE office. The chart below shows the number of academic publications produced from 2010 onward.

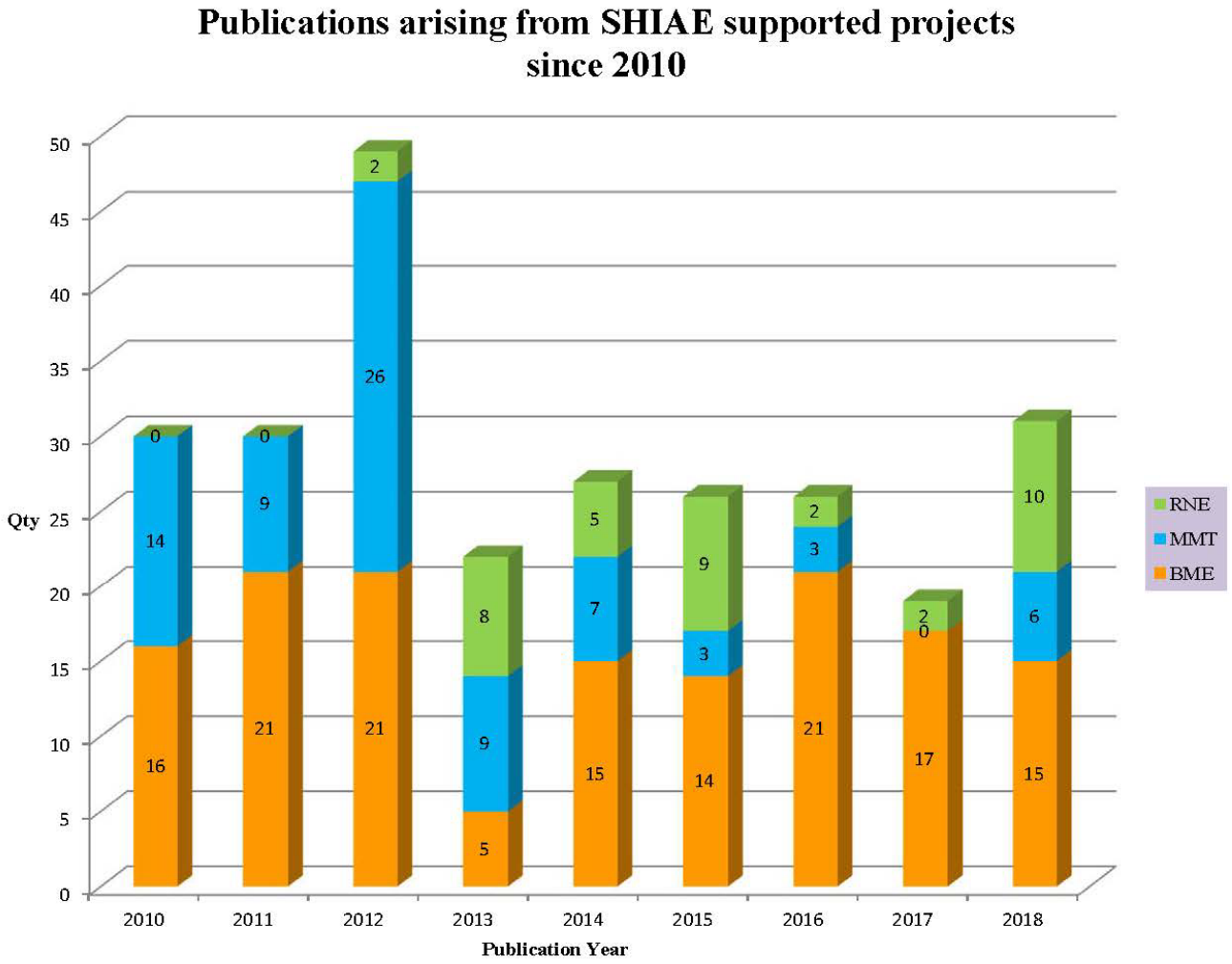

The full list of publications can also be downloaded from the webpage of SHIAE at www.shiae.cuhk.edu.hk/research.htm

Project Exhibition

One of the project prototype showcased in the Shun Hing Group 65th Anniversary cum Panasonic Corporation 100th Anniversary Exhibition during 7-10 November 2018 in HKCEC.

Intention-driven shoulder rehabilitation for targeted neuro-muscular training using an exo-musculoskeletal robot

by Professor Dawin TM Lau

(page 75-84)

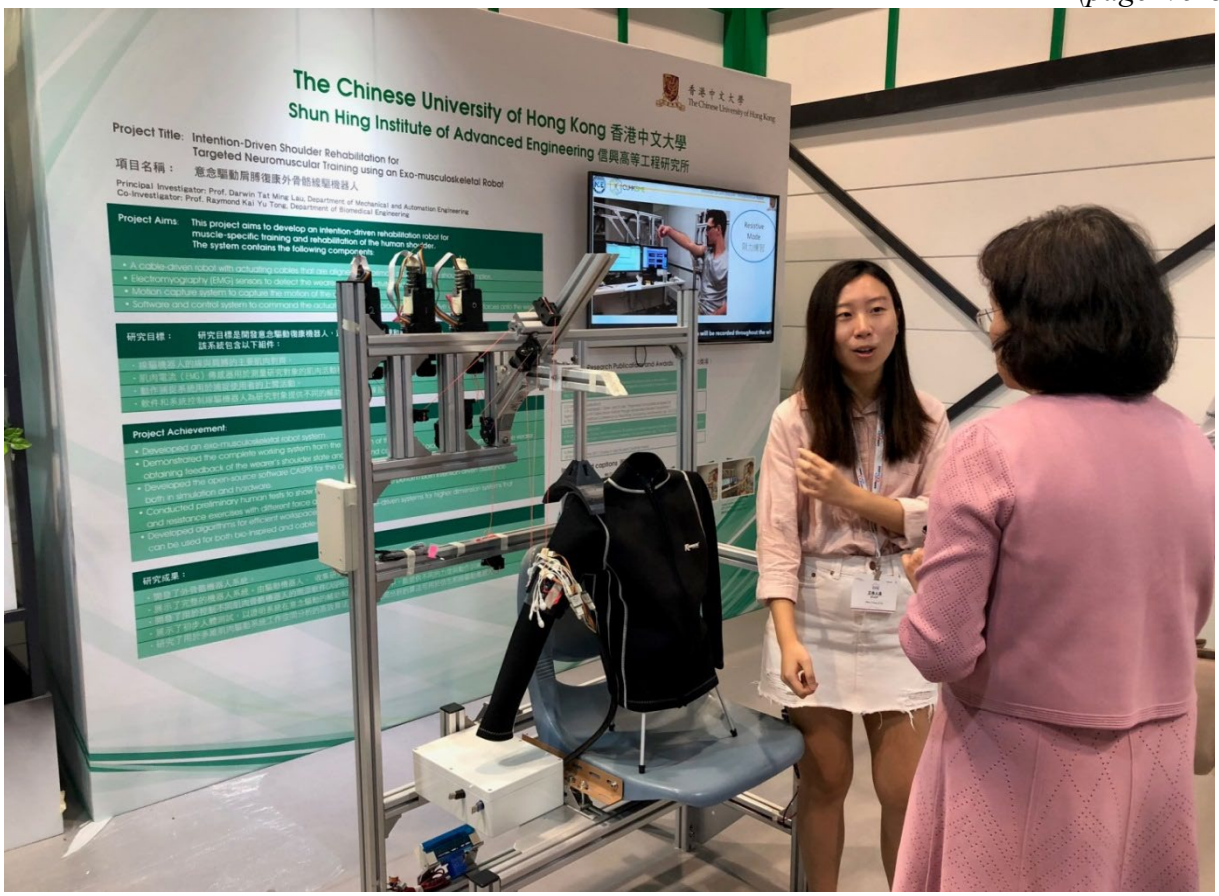

Mrs. Kao (right) visited the CUHK booth

Renewable Energy Track

Research Reports In Renewable Energy

Newly Funded Projects (2019-2021)	* Energy Management System for Large-scale Electric Vehicle Charging with Renewable Generation and Energy Storage
Continuing Projects (2018-2020)	* Development of a Novel Cooling Tower with Free Daytime Radiative Cooling for Reducing Energy Consumption in Buildings
	* Megahertz Current Sensor for Megahertz Renewable Energy Converter
	* Development of High-Performance Triboelectric Nanogenerators for Renewable Blue Energy Harvesting
(2017-2019)	* Tunable Spindle Using Self-excited Vibration for High Efficiency Renewable Electric Generators
Completed Projects (2016-2018)	* Robust NiMo–yttria Stabilized Zirconia (NiMo–YSZ) Anode Materials for Solid Oxide Fuel Cells

The following reports are enclosed in “Research Highlights” printed in November 2017.

Completed Projects (2015-2017)	* Experimental and modeling study of biodiesel combustion

The following reports are enclosed in “Research Highlights” printed in November 2017.

Completed Projects (2013-2015)	* Earth-Abundant Metal/Metal Oxide Nanostructures for Rechargeable Li-Air Batteries: Catalyst Design and Mechanistic Investigation * Graphene-based asymmetric supercapacitors with high energy density for clean energy storage systems

The following reports are enclosed in “Research Highlights” printed in July 2015.

Completed Projects (2012)	* Vibration Energy Harvesting Utilizing Multifunctional Phononic Meta-Materials and Structures
Completed Projects (2012)	* Understanding Electron and Phonon Transport in Boron Carbide Nanowires for Thermoelectric Energy Conversion * Ternary Hybrid Polymer/Nanocrystal Bulk Heterojunction Solar Cells with Cascade Energy-Level Alignmen

(Funded Year)

ENERGY MANAGEMENT SYSTEM FOR LARGE-SCALE ELECTRIC VEHICLE CHARGING WITH RENEWABLE GENERATION AND ENERGY STORAGE

Principal Investigator: Professor Yunjian XU
Department of Mechanical & Automation Engineering
CUHK

Project Start Date: 1 July 2019

ABSTRACT

This project aims to develop an energy management system for electric vehicle (EV) charging stations equipped with an energy storage system (e.g., reused EV batteries) and distributed renewable generation (e.g., rooftop solar and small-scale wind generation). The quickly growing adoption of EVs and intermittent renewable generation will impose significant challenges on the secure and efficient operation of electric power systems. We will develop a novel approach (that combines the advantages of stochastic optimal control techniques and data-driven approaches) to harness the inherent flexibility in (deferrable) EV charging load for renewable generation integration and operational cost reduction. Success of the proposed research would maximize the economic and environmental benefits of EV adoption for Hong Kong.

This project will develop i) a software package that optimally coordinates the charging of a large number of (up to 1000) EVs and the operation of an energy storage system to minimize the long-term expected system cost, under random renewable generation, EV arrivals, and electricity prices, and ii) a hardware-in-the loop (HIL) demonstrator that implements and tests the developed computational approaches and power electronic controllers in a realistic hardware environment simulating real-world EV charging station and power distribution system conditions.

INNOVATION AND PRACTICAL SIGNIFICANCE:

Hong Kong has more than 11,000 plug-in EVs in late July 2017. Many major countries, including the U.S. and China, have witnessed fast-growing adoption of plug-in EVs and intermittent renewable generation. The intermittency and stochasticity of renewable generation (from solar and wind) impose significant challenges on the real-time supply-demand balance of electric power system operation. The key innovation of the proposed project is two-fold: i) a stochastic optimal control based computational approach that optimally schedules the charging of a large number of EVs by explicitly taking into account the stochasticity in future renewable generation, EV arrivals, and electricity prices, and ii) a hardware-in-the loop (HIL) simulator that demonstrates the advantages of the developed energy management system (over existing technical approaches) with actual hardware components simulating real-world power system conditions. The developed HIL demonstrator will facilitate the technology transfer and follow-up funding applications for the potential commercialization of our research results on the cost-minimizing coordinated charging of a large number of EVs for a power distribution system with significant renewable generation.

PROJECT OBJECTIVES:

1. Develop scalable algorithmic approaches to compute the optimal scheduling policies for up to 1000 EV chargers and an energy storage system with intermittent renewable generation.

2. Develop a software module that trains and updates probabilistic models describing future renewable generation and EV arrivals with real-world data.

3. Develop a software package for real-time decision making on the charging of (up to 1000) EVs, based on the updated probabilistic information about future renewable generation and EV arrivals.

4. Implement the developed software package in a hardware-in-the-loop (HIL) simulation platform that verifies the performance of the developed energy management system with actual hardware components in real-world power distribution system environment.

WORK IN PROGRESS

DEVELOPMENT OF A NOVEL COOLING TOWER WITH FREE DAYTIME RADIATIVE COOLING FOR REDUCING ENERGY CONSUMPTION IN BUILDINGS

Principal Investigator: Professor CHEN Chun
Department of Mechanical & Automation Engineering
CUHK

Research Team Members:
Xinxian Yu, Ph.D. Student [(1)],
Haiqiang Zhang, Research Assistant [(1)]

[(1)] Dept. of Mechanical and Automation Engineering

Reporting Period: 01 July 2018– 30 April 2019

INNOVATION AND PRACTICAL SIGNIFICANCE:

Conventional cooling towers drag the outdoor air to cool the cooling water for rejecting heat to the atmosphere. Lower cooling water temperature results in a higher COP of chillers. Therefore, it is worthwhile to enhance the heat rejection in cooling towers without consuming additional energy. The innovation of this work is to develop a cooling tower with free daytime radiative cooling. The proposed cooling tower utilizes free and renewable cooling to lower the cooling water temperature. Consequently, the COP of chillers is expected to increase by 10 to 20%. A prototype will be fabricated and tested in this project. With the collaboration with the heating, ventilation, and air-conditioning (HVAC) industry, we will actively see further development of the prototype and potential technology transfer. If successful, the novel cooling towers can be potentially used in commercial and residential buildings to reduce the energy consumption and the associated carbon dioxide emissions.

ABSTRACT

The air-conditioning systems in buildings consume about 30% of the total electricity in Hong Kong. In a typical heating, ventilation, and air-conditioning (HVAC) system, the conventional cooling tower drags the outdoor air to cool the cooling water for rejecting heat to the atmosphere. To reduce the energy consumption, this project proposed to develop a novel cooling tower with renewable sky radiative cooling. A basin coated with a film of radiative cooling metamaterial, as a sky radiative cooler, will be implemented into the cooling tower. The film can reflect the solar irradiance and draw the heat from the water through the infrared transparency window of the atmosphere to the cold sink of outer space. The radiative cooling is free and renewable because the cold sink of outer space can be effectively regarded as a cooling reservoir. Consequently, the cooling water temperature will decrease without consuming additional energy, so that the coefficient of performance (COP) of chillers will increase. The design of the proposed cooling tower will be supported by thermodynamic modeling. Experiments will be conducted to evaluate the performance of the sky radiative cooler. The proposed project will offer a novel cooling tower that can utilize renewable cooling and reduce the energy consumption in buildings.

1. OBJECTIVES AND SIGNIFICANCE

1.1. Objectives

The first objective is to propose a novel cooling tower with renewable sky radiative cooling. The proposed cooling tower will utilize sky radiative cooling to reduce the condenser temperature, so that the COP of the chillers can be increased. Thus, the new system can be potentially applied in buildings to reduce the energy consumption.

The second objective is to develop a numerical thermodynamic model for predicting the performance of the cooling tower with renewable sky radiative cooling. The developed model will be used to support the design of the cooling tower to achieve the optimal energy performance.

The third objective is to evaluate the system performance under various working conditions using the numerical model. This work can identify the key influencing factors on the energy performance and propose the suitable application working environment of the cooling tower with sky radiative cooling.

The fourth objective is to fabricate a sky radiative cooler and conduct experimental measurements of the cooling capacity under various conditions. The obtained experimental data can be used to support and verify the design of cooling tower with sky radiative cooling.

1.2. Significance of this project

Conventional HVAC cooling towers drag the outdoor air to cool the cooling water for rejecting heat to the atmosphere. Lower cooling water temperature results in a higher COP of chillers. Therefore, it is worthwhile to enhance the heat rejection in cooling towers without consuming additional energy. The innovation of this work is to develop a cooling tower with renewable sky radiative cooling. The proposed cooling tower utilizes free and renewable sky radiative cooling to lower the cooling water temperature. Consequently, the COP of chillers is expected to increase by 5 to 10%. A prototype sky radiative cooler will be fabricated and tested in this project. With the collaboration with the HVAC industry, we will actively see further development of the prototype and potential technology transfer. If successful, the novel cooling tower with sky radiative cooling can be potentially used in commercial and residential buildings to reduce the energy consumption and the associated carbon dioxide emissions.

2. RESEARCH METHODOLOGY

2.1 Cooling tower with sky radiative cooling

This study proposed to implement a passive sky radiative cooler between the cooling tower and the condenser. Figure 1 shows a schematic of the system setup. This investigation focused on a counterflow cooling tower without the fan speed control. The high-temperature cooling water from the condenser entered into the cooling tower, and the spray water droplets had heat and mass transfer with the included air. The water leaved the cooling tower with a lowest possible temperature of the outdoor wet-bulb temperature. The cool temperature then entered into a radiative cooler, which consisted of a basin covered by a metamaterial film with radiative materials. Through radiative heat transfer to the outer space, the cooling water was further cooled before flowing back to the condenser. Through this process, the condenser temperature was decreased, so that the COP of chiller could be improved.

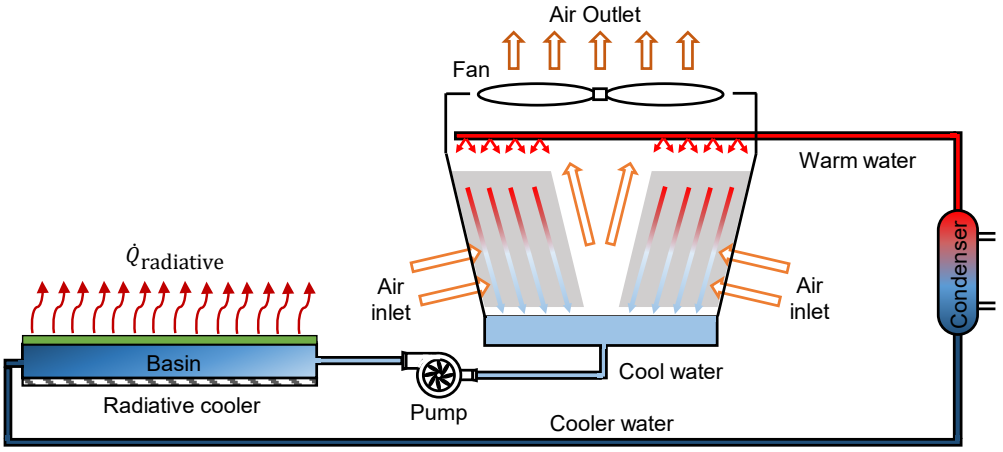

Figure 1. Schematic of the proposed cooling tower with renewable passive radiative cooling.

Figure 2 shows the schematic of the metamaterial film with radiative materials. The upper layer can reject heat through the infrared irradiance to the cold sink of outer space. The radiative material has strong emission between 8 and 13 μm, the atmospheric transmission window. The lower layer can reflect the solar irradiance so that the radiative cooler can still work in the daytime. With the use of the radiative cooler, the system may achieve a cooling water temperature lower than outdoor wet-bulb temperature. However, it is still unknown if the proposed cooling tower with passive sky radiative cooling could actually improve the COP of chiller. Therefore, this study will develop a numerical model for the analysis in the following section.

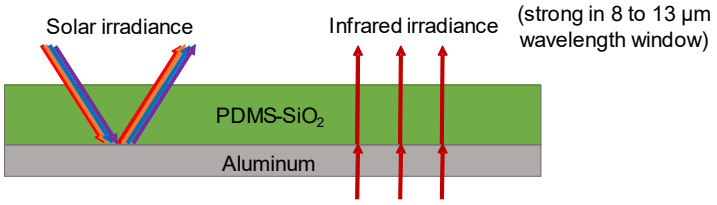

Figure 2. Schematic of the metamaterial film that can reflect the solar irradiance and reject heat through the infrared irradiance to the cold sink of outer space.

2.2 Mathematical model

Considering the steady-state condition, the radiative emission power of the cooler is equal to the net incident power absorbed by the cooler:

$$2\pi A_{rc,a}\int_0^{\pi/2}\sin\theta\cos\theta\int_0^{\infty} I_{BB}(T_{rc},\lambda)\varepsilon_{rc}(\lambda,\theta)d\lambda d\theta = A_{rc,a}\int_0^{\infty} I_{AM1.5}\varepsilon_{rc}(\lambda)d\lambda$$
$$+2\pi A_{rc,a}\int_0^{\pi/2}\sin\theta\cos\theta\int_0^{\infty} I_{BB}(T_{atm},\lambda)\varepsilon_{rc}(\lambda,\theta)\varepsilon_{atm}(\lambda,\theta)d\lambda d\theta + A_{rc,a}h_{rc,a}(T_{atm}-T_{rc}) + m_w c_{p,w}(T_{w2}-T_{w1}) \quad (1)$$

where A_{rc} (m^2) is the cooling surface area exposed to the sky, θ (sr) is the radiation angle, I_{BB} ($W/m^2 \cdot sr \cdot m$) is the spectral radiance of a blackbody, T_{rc} (K) is the temperature of the radiative cooler, ε_{rc} (unitless) is the emissivity of the radiative cooling material, $I_{AIM1.5}$ ($W/m^2 \cdot m$) is the solar illumination, T_{atm} (K) is the temperature of the ambient air, $\delta_{w,atm}$ (atm-cm) is the absolute vertical water vapor column in the atmosphere, ε_{atm} (unitless) is the emissivity of the atmosphere, $h_{rc,a}$ ($W/m^2 \cdot K$) is the convective heat transfer coefficient between the cooler and the surrounding air, T_{w1} (K) is the temperature of the water entering the radiative cooler (or leaving the cooling tower), and T_{w2} (K) is the temperature of the water leaving the radiative cooler (or entering the condenser). The spectral radiance of a blackbody can be calculated by

$$I_{BB}(T,\lambda)=\frac{2hc^2}{\lambda^5}\frac{1}{\exp(\frac{hc}{\lambda k_B T})-1}$$

(2)

where h is the Planck's constant (6.626×10^{-34} J·s), c is the speed of light (2.998×10^{8} m/s), λ (m) is the wavelength, and k_B is the Boltzmann constant (1.381×10^{-23} $m^2\cdot kg/s^2\cdot K$). The emissivity of the atmosphere, which can be calculated based on the "box model" proposed by Granqvist and Hjortsberg:

$$\varepsilon_{atm}(\lambda,\theta)=\begin{cases}1 & \lambda<8\ \mu m\\ 1-t(\lambda,\delta_{w,atm})^{1/\cos\theta} & 8\ \mu m\le\lambda\le13\ \mu m\\ 1 & \lambda>13\ \mu m\end{cases}$$

(3)

where t (unitless) is the atmospheric transmittance, which can be calculated using the software MODTRAN.

This study focused on counterflow cooling tower with a constant fan speed. Based on the cooling tower theory proposed by Merkel, the heat and mass transfer process occurs between water, interfacial film, and air. The interfacial film was assumed to be of saturated air. Under steady-state condition, the water heat loss is equal to the air heat gain:

$$m_w c_{p,w} dT_w = m_a dh_a = K\alpha(h_{film}-h_a)dV \Rightarrow \frac{K\alpha V}{m_w}=\int_{T_{w1}}^{T_{w3}}\frac{c_{p,w}}{h_{film}-h_a}dT_w$$

(4)

where m_w (kg/s) is the inlet water mass flow rate, $c_{p,w}$ (kJ/kg·K) is the specific heat of water, T_w (K) is the water temperature, m_a (kg/s) is the air mass flow rate, h_a (kJ/kg) the enthalpy of bulk air, K ($kg/s\cdot m^2$) is the unit conductance of mass transfer from the water-air interface to main airstream, α (m^2/m^3) is the ratio of water-air interface area to the cooling tower volume, h_{film} (kJ/kg) is the enthalpy of saturated air at the bulk water temperature, V (m^3) is the cooling volume of the tower, and T_{w3} (K) is the temperature of water leaving the cooling tower (or entering the radiative cooler).

The COP of the chiller can be calculated by:

$$COP=\frac{Q_{evap}}{m_w c_{p,w}(T_{w,3}-T_{w,2})-Q_{evap}}=\frac{T_{evap}}{\beta_1\cdot T_{w,3}+\beta_2-T_{evap}}\eta$$

(5)

where Q_{evap} (W) is the heat absorbed by the evaporator, T_{evap} (K) is the average temperature of evaporator, T_{cond} (K) is the average temperature in condenser, β_1 and β_2 are constants, and η (unitless) is the internal efficiency of the chiller. Solving the equations above, the temperatures, including T_{rc}, T_{w1}, T_{w2}, T_{w3}, and T_{cond}, can be obtained.

3. RESULTS ACHIEVED SO FAR

This study used the developed numerical model to predict the improvement in COP of chiller and reduction in chiller electricity use for several buildings. The outdoor air temperature and relative humidity were set the monthly average values in Hong Kong for a whole year. The cooling load per unit floor area was set at 60 W/m^2. The rooftop area available for the sky radiative cooler was assumed to be 80%. The cooling tower volume and water flow rate were set at the average value from the data collected from the literature. The K·α

was set at 0.445 according to the U.S. Department of Energy (DOE) report. The radiative cooler material was selected to be of high emissivity in the wavelength range of 8 to 13 μm, while very low emissivity in other wavelength ranges. Figure 3 plots the percentage of reduction in chiller electricity use and increase in chiller COP for the buildings with different numbers of floor. When the number of floor increased, the corresponding cooling load increased, so that the cooling water flow rate tended to increase. In that case, with the same sky radiative cooling area, the reduction in cooling water temperature decreased. Thus, the cooling tower with sky radiative cooling performed better for lower floor buildings. Although the results show significant reduction in chiller electricity use, more parametric studies are needed in the second year of this project.

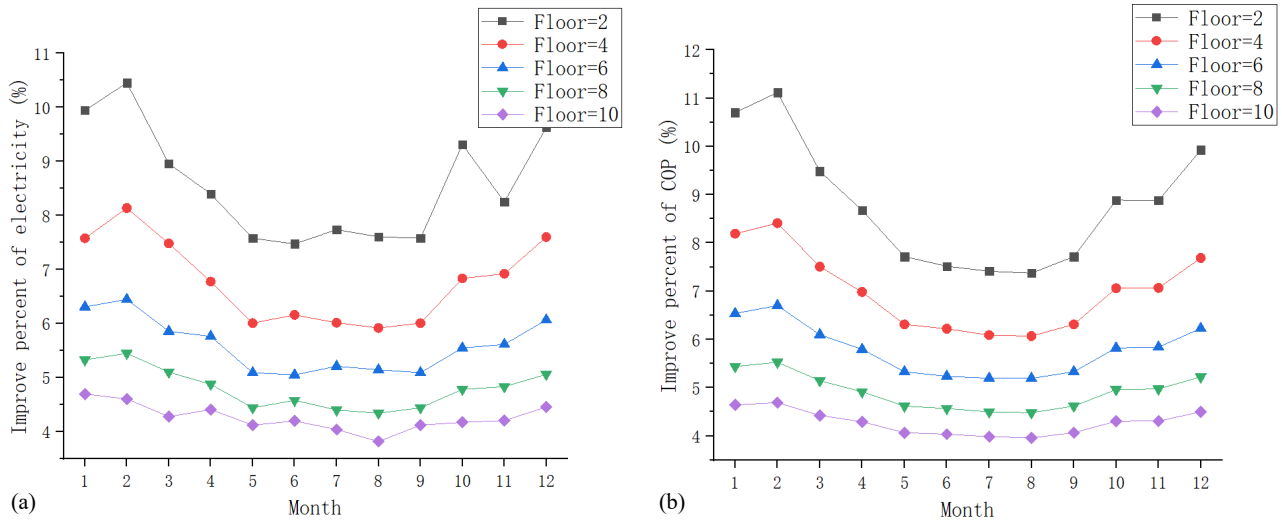

Figure 3. (a) Percentage of reduction in chiller electricity use, and (b) percentage of increase in chiller COP.

A preliminary experiment has also been carried out. The fabricated sky radiative cooler consisted of a water tank covered by a sky radiative cooling material film. In the second year of this project, a water flow loop with a controllable heater will be added to the radiative cooler to simulate the cooling water circuit. More experiments will be conducted to obtain data to support the design of the cooling tower with sky radiative cooling.

4. PUBLICATION AND AWARDS

J[1] X. Yu, H. Zhang, and C. Chen, "Numerical model of the performance of HVAC cooling tower with passive sky radiative cooling," *Energy Conservation and Management*, under preparation.

WORK IN PROGRESS

MEGAHERTZ CURRENT SENSOR FOR MEGAHERTZ RENEWABLE ENERGY CONVERTER

Principal Investigator: Professor LOH Poh Chiang Andrew
Department of Electronic Engineering, CUHK

Co-Investigator: XIN Zhen [(1)]

Research Team Members: MING Lei, Ph.D. Student [(1)]

[(1)] Department of Electronic Engineering, CUHK

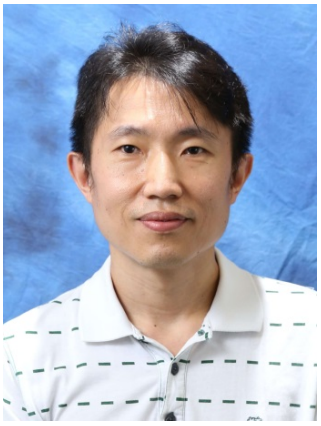

Reporting Period: 01 July 2018– 30 April 2019

INNOVATION AND PRACTICAL SIGNIFICANCE:

The developed current sensor will have a frequency bandwidth up to 10 megahertz. It is thus around 40 times wider than that of a commonly used Hall current sensor. Such wide bandwidth permits the realization of fast control and reliable protection in the newest generation of power converters built using WBG devices. The resulting converters can be sized for renewable energy generation or miniaturized for routinely used laptop adapter, EV charger and phone charger to name only a few. There will be a revolutionary reduction of size and weight, enabled by the high-frequency operation of WBG devices. In addition, the developed sensor is of great commercial competitiveness due to its small size and low cost, made possible by its integration into an inexpensive printed circuit board. This merit will promote the coming era of WBG devices with extremely high efficiency, but has its commercialization hindered many years due to its high price. Moreover, the substantial market volume and the all-important cost factor have led to the development of a wide range of alternative current sensing methods. The market demand for isolated current sensors will, in fact, hit 100 million in 2020. This is roughly equivalent to the amount of iPhones produced in 2012 [1]. Therefore, the developed current sensor is revolutionary, yet with great potential and competitiveness to be converted into a commercial product.

ABSTRACT

Power converter is an essential interface for tying a renewable source (e.g. solar and wind) to the power system. It usually consists of three main components, respectively known as microprocessor, power semiconductor devices and sensors. If its microprocessor is then analogously viewed as its “brain”, its sensors and power devices are then its “sense organs” and “limbs”, respectively. Recently, technological progress has pushed operational speed of its “brain” to the ***gigahertz*** range, while the development of wide bandgap (WBG) devices has allowed its “limbs” to reach the ***megahertz*** range with both high efficiency and power density (power per unit volume). The next trend of rapid development will hence likely be related to its “sense organs”, or more precisely, its current sensors, presently limited to below hundreds of ***kilohertz***. The ***megahertz*** responses of the “limbs” are thus not sensed properly for control, protection and monitoring of the power converter. These are nontrivial issues, judging from the amount of power generated by a typical renewable source. An intense need for advanced current sensing techniques that can sense from DC to a few ***megahertz*** with both high noise immunity and low manufacturing cost is thus prevailing, but presently cannot be met by existing commercial sensors. Development of an advanced current sensor is thus timely, albeit challenging.

1. OBJECTIVES AND SIGNIFICANCE

The developed current sensor must have the following objective features, which upon materialized, will fasten the era of highly efficient WBG usage in miniaturized power converters. Possible applications include renewable energy generation, laptop / phone adapter, and electric vehicle charger to name only a few. Its commercialization has however been hindered by high component prices, including that of the current sensor, whose market demand will likely reach 100 million in 2020. This is roughly the number of iPhones produced in 2012. Therefore, the developed current sensor is revolutionary with great potential as a commercial product.

Ultrafast with a bandwidth up to 10 MHz: WBG devices can operate at an extremely high frequency (up to megahertz), which in essence, is the key towards realization of high-efficiency and high-power-density renewable energy generation. But, in terms of their short-circuit protection, operating current measurement becomes a significant challenge, which practically, cannot be achieved with the widely used Hall current sensors due to their limited 250-kHz bandwidth. A megahertz current sensor is thus essential.

Nonintrusive with a very low insertion inductance of less than 1nH: High-speed WBG power devices are highly sensitive to parasitic inductances, which in the extreme, can downgrade their performances towards those of silicon devices. Therefore, very low insertion parasitic, especially inductance, is necessary.

Compact with the target of embedding within highly dense power converter: High power density has always been the packaging target of power converters, in order to fully utilize energy resources and lessen operating costs. It has to date roughly doubled every 10 years since 1970, but can now be impeded by existing bulky current sensors. For instance, recent photovoltaic inverter invented through the Google Little Box Challenge has achieved a 2-kW power rating with its volume being the same as two iPhone5s. Further reduction of its size is however not easy, since it depends on the current sensor, which presently is larger than an Apple watch. Development of newer current sensors is thus an immediate challenge to resolve.

Low cost: Instead of explicitly mounting a (e.g. hall-effect) current sensor, it is conceptually cheaper to have the current sensor embedded within the print-circuit board (PCB), in addition to saving some footprints. Development of such PCB-embedded current sensors is thus the main research concern of this project.

2. RESEARCH METHODOLOGY

The project consists of a number of tasks to be investigated by a postdoctoral fellow. Its core task is to find solutions that can enormously reduce volume of the conventional PCB Rogowski current sensor (RCS). Despite that, the resulting RCS must simultaneously retain its wide bandwidth and ability to work in a hostile environment, characterized by large voltage transients and high field strength. To achieve these goals, the methodology followed is described as follows.

2.1. Structural Design and Layout of Sensor Head and Coil

Performance of a RCS is closely related to the number of coil turns. On one hand, high number of turns is desirable, since it increases measurement accuracy due to the existence of a high mutual inductance. On the other hand, with increasing number of turns, self-inductance of the coil increases faster than its mutual inductance, which in response, can cause the coil resonance frequency and bandwidth to drop. This problem becomes more challenging with the proposed tiny RCS due to its extremely limited size and volume close to those of a coin. Tradeoff between dynamics and accuracy of the developed sensor must hence be carefully investigated when designing structures of the sensor head and coil.

2.2. Development of Techniques for shielding Electrostatic Interferences

Power converters, such as micro-photovoltaic inverters, are shrinking in size, even though their power ratings are rising. Smaller volumes then create a more hostile environment for the current sensors, because of

the increased electrostatic interferences. The condition worsens with WBG devices operating at much faster switching speeds than conventional devices. Immunity, related to rejection of external fields, of the developed PCB RCS must hence be improved, before different currents flowing within the power converter can be measured accurately. Fitting a shield over the coil windings is a common solution for conventional Rogowski coils, but becomes inappropriate with a power converter, since the shield will substantially reduce bandwidth of the sensor. Therefore, an alternative cost-effective solution for rejecting external fields is investigated.

2.3. Identification of Parametric Design Rules

Accurate design rules for choosing components of the developed RCS is necessary, before commercialization and mass production. An equivalent model of the Rogowski coil must hence be developed for that purpose and its theoretical performance evaluation. A final design procedure can eventually be formulated for sizing parameters of the optimized Rogowski coil.

2.4. Inclusion of DC Current Measurement to Rogowski Current Sensor

The key disadvantage of a Rogowski coil is its inability to detect DC current. This hinders its application to certain power converters, whose DC currents may sometimes be essential for both control and protection. A recent hybrid sensing solution that combines Rogowski and anisotropic magneto resistive (AMR) techniques has thus been developed to address that shortcoming. The idea is to rely on AMR for sensing DC and low-frequency current components and a Rogowski coil for measuring high-frequency current components. This solution however suffers from high cost and design difficulty. An alternative technique that uses multiple Rogowski coils to harness switching characteristics of a power converter for DC current measurement is thus suggested for investigation in the project.

2.5. Experimental Test-Bed and Performance Evaluation

Performances of the developed PCB RCS, in terms of its external field rejection, DC current measurement and other characteristics, will be evaluated sequentially using a double-pulse testbed throughout the course of investigation. To demonstrate even more realistically, overall performances of the final sensor prototype will also be tested with a high-power-density power converter to be built in the laboratory. More precisely, the developed current sensor will be integrated within the power converter for short-circuit protection and current control. Its performance accuracy will then be compared with other existing current sensors.

3. RESULTS ACHIEVED SO FAR

A four-layer screen-returned printed-circuit-board (PCB) Rogowski current sensor (RCS) has been developed for measuring fast-changing current of a WBG device with virtually no interference from ambient noises. It uses lesser PCB layers than existing sensors to save costs and much fewer turns for its Rogowski coil to retain its high bandwidth and small size. The latter is however at the expense of more leakage between turns. This causes its self-inductance, needed for designing its bandwidth, to be even more difficult to compute accurately using traditional techniques. Errors as high as 45% have, in fact, been reported in the literature. A piecewise PCB technique has hence been proposed, whose error has been found to be smaller than 5%, if the coil pitch is ten times larger than its track width. For cascading with the Rogowski coil, an appropriate non-inverting integrator has also been implemented for accurately regenerating the measured switch current without being burdened by excessive shortcomings of a traditional integrator. Overall effectiveness of the proposed RCS has eventually been verified experimentally using a double-pulse test setup and a coil with twenty turns. A photograph showing the designed RCS can be viewed from Fig. 1, together with an illustration of how close its measured current i_{SC} tracks the actual current i'_{SC}.

For demonstrating next that self-inductance determination for the Rogowski coil is indeed accurate, Table I can be referred to. The table clearly shows that with the proposed piecewise technique, calculation error is very small, and in fact, becomes smaller as the number of turns decreases. This trend can be explained by recapping that the piecewise technique is proposed to better manage leakage fluxes between adjacent turns of

the coil. Leakage fluxes, in turn, worsen as the number of turns decreases. In other words, the proposed technique will become more accurate as the number of turns drops. In contrast, the compared existing technique relies on a toroidal model, whose leakage flux accountability is very poor. Its calculation error is thus big and will become bigger as the number of turns decreases.

To lastly demonstrate the existence and severity of leakage fluxes, Fig. 2 shows two longitudinal PCB coils with thirty and five turns, respectively. Their finite-element flux distributions analyzed with JMAG are also shown in the same figure. Clearly, with more turns in Fig. 2(a), a vast amount of mutual fluxes links many turns of the coil, even though some leakage fluxes closer to the coil still exist. The distribution however becomes very different in Fig. 2(b), where fewer turns produce mostly leakage fluxes. In other words, the neat mutual flux linking pattern in Fig. 2(a) can no longer be seen. Existing toroidal method for computing self-inductance will hence work fine with Fig. 2(a), while the proposed piecewise method will give more accurate results with Fig. 2(b).

Table I. Measured and Computed Self-Inductances

Turn Number	Pitch (mm)	Measurement (nH) at 1MHz	Existing Method		Proposed Method	
			Theory (nH)	**Error (%)**	Theory (nH)	**Error (%)**
N = 30	1.3	281.19	187.00	**33.50**	230.22	**18.13**
N = 20	2.0	168.53	83.11	**50.68**	160.14	**4.97**
N = 10	3.9	93.85	20.78	**77.86**	92.97	**0.95**

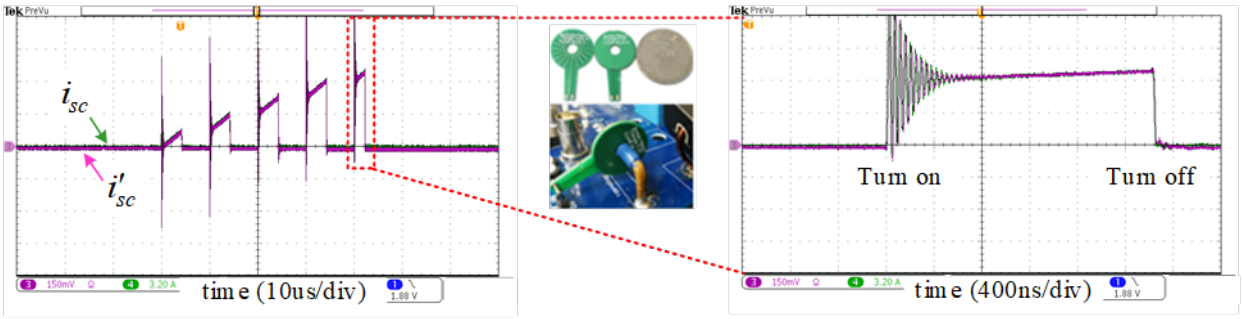

Fig. 1. Illustration of measured current following actual current accurately (actual current measured with Tektronix TCP0030A current probe with a bandwidth of 120MHz).

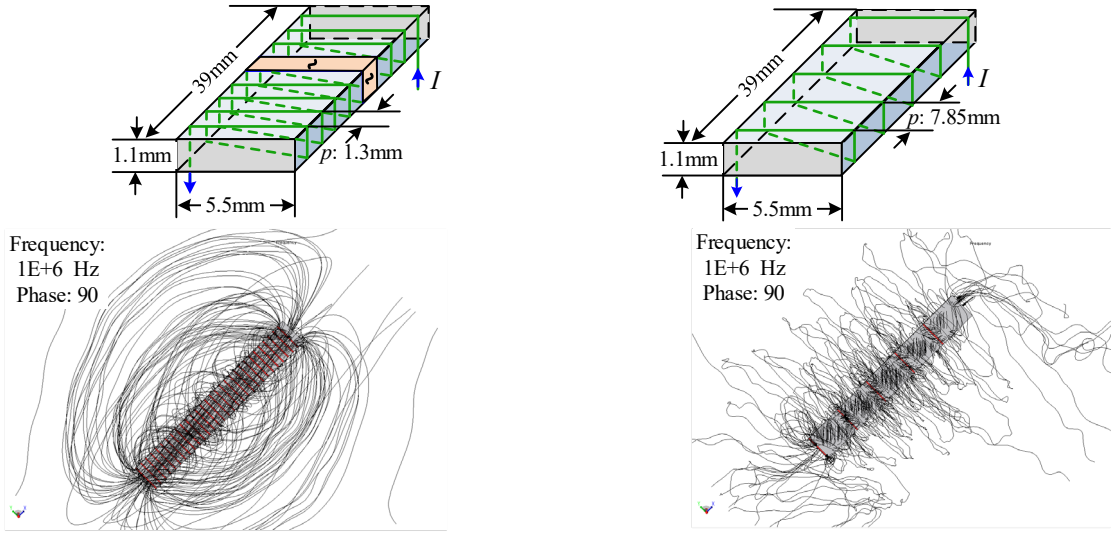

(a)
(b)

Fig. 2. Structures and longitudinal magnetic field distributions of (a) thirty-turn and (b) five-turn PCB coils.

4. PUBLICATION AND AWARDS

C[1] L. Ming, C.Q. Yin, Z. Xin, P.C. Loh, and Y. Liu, “Screen-Returned PCB Rogowski Coil for Switch Current Measurement of SiC Devices,” *IEEE Applied Power Electronics Conference and Exposition (APEC)*, IEEE, Anaheim, California, USA, pp. 958-964, March 17-21, 2019

WORK IN PROGRESS

DEVELOPMENT OF HIGH-PERFORMANCE TRIBOELECTRIC NANOGENERATORS FOR RENEWABLE BLUE ENERGY HARVESTING

Principal Investigator: Professor ZI Yunlong
Department of Mechanical & Automation Engineering
CUHK

Research Team Members:
Ms. Jingjing Fu[(1)], Dr. Yubiao Sun[(1)], Dr. Xiaoyi Li[(1)], Dr. Jiaqi Wang[(1)]

[(1)] Department of Mechanical and Automation Engineering, CUHK

Reporting Period: 01 July 2018– 30 April 2019

INNOVATION AND PRACTICAL SIGNIFICANCE:

Innovation: *The innovation of the proposed research lies in the development of high-performance TENGs for blue energy harvesting. Traditional water energy harvesting uses electromagnetic generators (EMG), which are usually huge, heavy, expensive, and technically difficult for construction in deep water. Further, studies have demonstrated that EMG are extremely inefficient in harvesting the low-frequency mechanical energy that is generated by ocean waves. TENG possess several advantages over EMG technology as they are lightweight and able to float, cost-effective and easy to produce, and efficient in harvesting low-frequency energy. Our research will focus on maximizing TENG output through addressing two crucial fundamental issues: the air-breakdown effect inside TENG and the parasitic capacitances brought by seawater, which have never been systematically studied before. For the first time, we propose to develop TENGs with novel designs to address these issues. It is expected that the output performance of TENG could increase 10-100 times through our proposed research.*

Practical significance: *Considering the challenges of energy security and environmental protection, developing renewable energy sources is of critical importance for Hong Kong. With Hong Kong's extensive coastline and water area percentage of 59.8%, Hong Kong is strategically placed to take advantage of a convenient, clean and renewable power source. Especially for areas with complex coastlines that are not suitable for water shipping, electrical generation is the best option to utilize them. Additionally, the ocean currents and tropical storms that are common in Hong Kong, provide an abundant amount of mechanical energy that could potentially be converted to electrical energy. Lastly, developing the blue energy harvesting technology to replace the fossil fuels will also decrease the emissions of pollutants and greenhouse gases, which is critical for environmental protection. Therefore, developing blue energy harvesting through TENG is beneficial to Honk Kong on many levels including the mediating the energy crisis, promoting environmental protection, and advancing both economic and social development in Hong Kong.*

ABSTRACT:

Electricity is the world's fastest growing form of end-use energy consumption. Between 2015 and 2040, world net electricity generation will increase by 45%. Non-renewable fossil fuels still account for >60% of electricity generation. However, 70% of the earth's surface is covered by ocean, which represents a huge untapped clean and renewable energy source. Estimated to provide power of over 75 TW, ocean energy could satisfy energy demands around the world. To effectively harvest this "blue energy" especially the low-frequency mechanical energy generated by ocean waves, three-dimensional networks of triboelectric

nanogenerators (TENG) have been proposed. To test this concept, however, TENG units first need to be refined to optimize their output performance. To date, factors that limit the performance include the challenge that achievable charge density is limited by the phenomenon of air breakdown; additionally, the parasitic capacitances brought by the conductive seawater may suppress the performance of TENG. We propose experimental and theoretical studies that will focus on mitigating these limiting factors by developing novel structural and material designs, greatly enhancing the output performance of TENG. The proposed research will lay the cornerstone for further technologic advancement in large-scale harvesting of kinetic water energy using TENG units.

1. OBJECTIVES AND SIGNIFICANCE

1.1 Objectives: (1) To simulate and experimentally demonstrate a TENG design that will minimize the air-breakdown effect using controlled high pressure and inert gas environments; (2) To simulate and experimentally develop optimized structural/material designs to minimize the influences of the parasitic capacitances brought by the conductive seawater; (3) To determine the optimized designs and produce a TENG that provides maximal available output, and to compare with other technologies used in blue energy harvesting.

1.2 Significance: Considering the challenges of energy security and environmental protection, developing renewable energy sources is of critical importance for Hong Kong. With Hong Kong's extensive coastline and water area percentage of 59.8%, Hong Kong is strategically placed to take advantage of a convenient, clean and renewable power source. Especially for areas with complex coastlines that are not suitable for water shipping, electrical generation is the best option to utilize them. Additionally, the ocean currents and tropical storms that are common in Hong Kong, provide an abundant amount of mechanical energy that could potentially be converted to electrical energy. Lastly, developing the blue energy harvesting technology to replace the fossil fuels will also decrease the emissions of pollutants and greenhouse gases, which is critical for environmental protection. Therefore, developing blue energy harvesting through TENG is beneficial to Honk Kong on many levels including the mediating the energy crisis, promoting environmental protection, and advancing both economic and social development in Hong Kong.

2. RESEARCH METHODOLOGY

2.1 Theoretical modeling and simulation of water-wave TENG: The basic model of the water-wave TENG is built and simulated by COSMOL Multiphysics, a cross-platform finite element analysis simulation software. It can provide the potential and electric field distribution which can be used to determine the breakdown status and the voltage output. It can also simulate the balanced charge status so that the available charge output can be given.

2.2 Experimental studies on the breakdown and parasitic-capacitance effects: In the measurement circuit as shown in **Fig. 2a**, the charging TENG is used to provide the high voltage required to approach the breakdown conditions in the test TENG. The charge transfer was measured by the electrometer with mark of "Q", and the voltage was calculated by the measured current through the electrometer with mark of "A" multiplying the shunt resistance R. The voltage at the turning points is recorded as the breakdown voltage, and then it was mapped into the V-Q diagram of TENG to outline the breakdown region. A high-speed camera is used to record the sparks during breakdown. In the non-breakdown part of the V-Q plot, the capacitance can be estimated by the slope.

2.2 Fabrication and electrical measurement of water-wave TENG output: A hollow plastic ball was used as the shell. Two copper films were attached to the inner side of the shell. A silicone rubber solid ball was put into the plastic ball to act as the moving part. Water-wave energy was simulated by a linear motor to supply a periodical external force with specified frequency. A pressure sensor was simultaneously placed under the TENG to calibrate the applied force. And the electrical properties of TENGs including output voltage, power, reliability and consistency were investigated by using a digital oscilloscope with a 100 MΩ probe, or a Keithley 6514 electrometer.

2.3 Fabrication of the optimized water-wave TENG design: To fill in the high-pressure CO_2, we designed and fabricated a ball-shell TENG with a screw cap, in which the high-pressure CO_2 gas can be filled and packaged inside (**Fig. 3a**). Silicone sealing layer is applied after tightening the cap to maintain the high-pressure environment inside. To reduce the parasitic capacitance from the water, we fabricated an additional layer made from packaging foams, with thickness of ~0.5 cm.

2.4 Development of the pressure vessel for quantitative analysis of the environmental factors: A chemical reaction chamber (from Gongyi Yuhua) was modified as a pressure vessel for testing TENG in controlled environments. A low-speed bidirectional motor was installed to provide the driven motion for TENG, and a framework was built inside to support the TENG. The electrodes were connected to the electrometers outside of the vessel through copper wires.

3. RESULTS ACHIEVED SO FAR

3.1 The modeling and simulations of the water-wave TENG

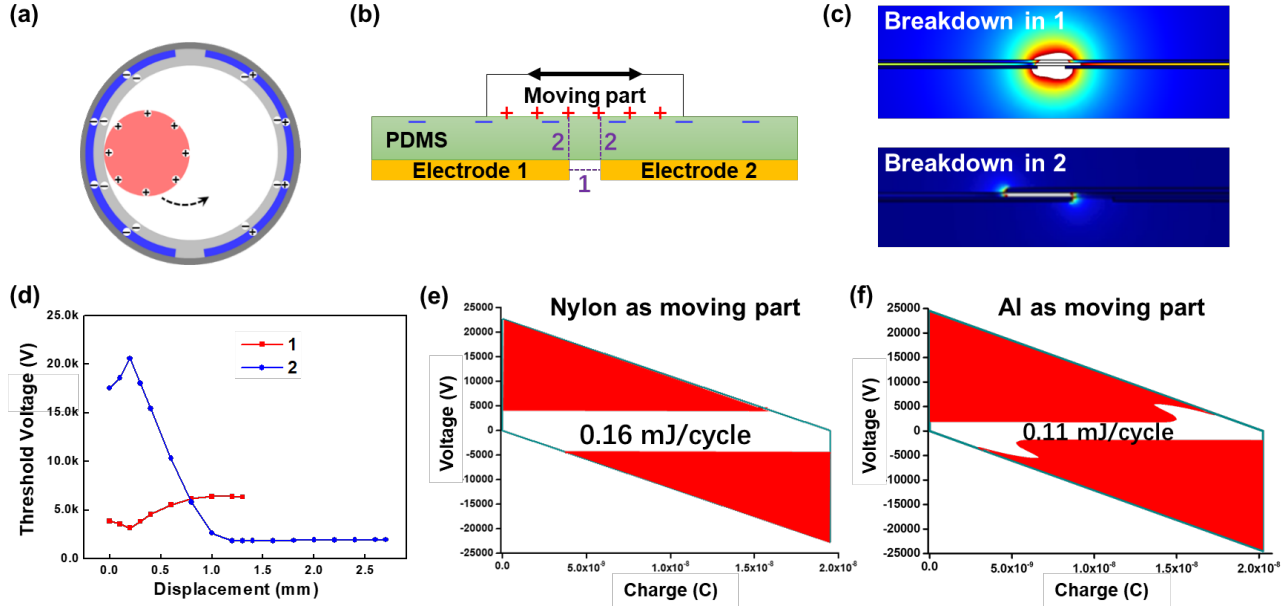

Figure 1: The modeling and simulation of water-wave TENG.

The original ball-shell structured TENG to harvest wave energy used in this project is schematically shown in **Fig. 1a**. Due to the triboelectrification, the electrons will be transferred from the electrodes to the ball. With the oscillations provided by the water waves, the inner moving ball can rotate from one electrode to the other one, which can electrostatically induce the potential difference between two electrodes, as the driven force of the current in the external circuits. To understand the breakdown effect in this water-wave TENG, the sliding-freestanding (SF) mode can be used to model this TENG. The schematic diagram of the SF-mode TENG is shown as **Fig. 1b**. There are two types of potential breakdown simulated, including horizontal air breakdown (type 1), and vertical dielectric breakdown (type 2). The model and simulations on the parasitic-capacitance effect have already been demonstrated and shown in the proposal previously.

The device breakdown criterion is set as below: if the minimum electric field along any line between electrodes or triboelectric surfaces is larger than the air-breakdown threshold electric field (3×10^6 V/m), then the breakdown happens, and there will be electron transfer between electrodes or triboelectric surfaces which can greatly impact the performance. The simulation of the electric field distribution is conducted in COMSOL Multiphysics software package, as shown in **Fig. 1c**. The simulated threshold voltages corresponding to different types of breakdown are plotted versus the displacement, as shown in **Fig. 1d**. And then we plotted the V-Q diagrams showing the breakdown regions in red, as shown in **Fig. 1e-f**. We notice that even though Al-PDMS friction can provide a little higher charge density, the TENG with insulating nylon as the moving layer can allow much more effective energy output (0.16 mJ/cycle) than that with conductive Al as the moving layer (0.11 mJ/cycle), due to the suppressed type-2 breakdown. Therefore, to avoid type-2 breakdown, we can choose insulating materials for the moving ball.

3.2 Experimental studies on the breakdown and parasitic-capacitance effects

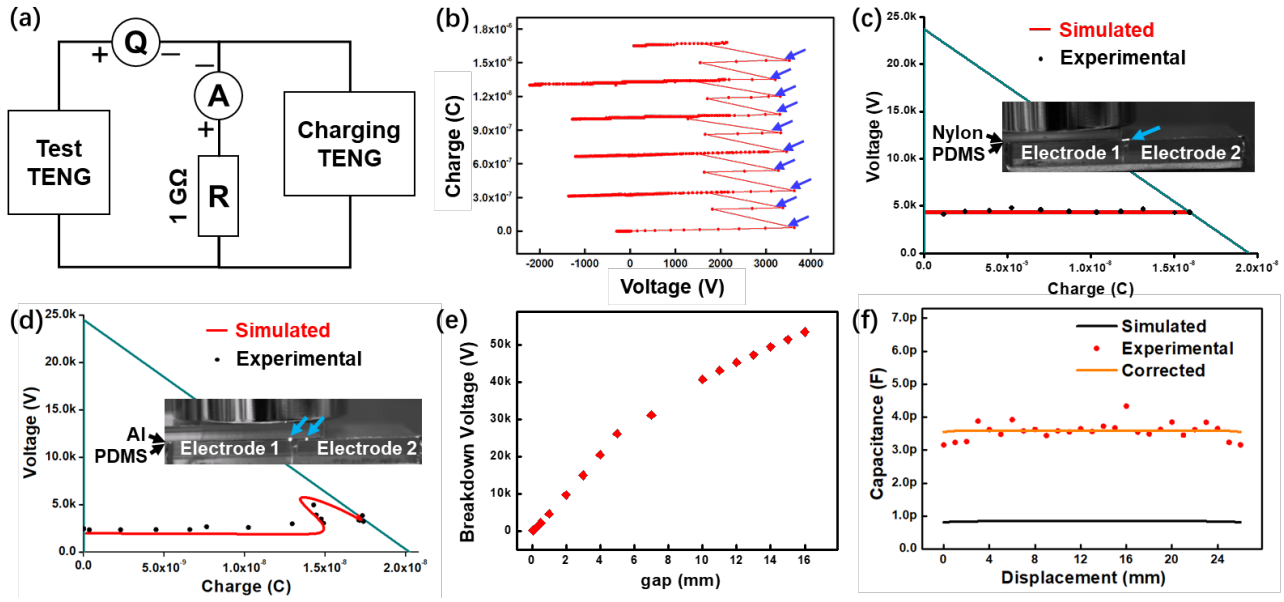

Figure 2: Experimental studies on the breakdown and parasitic-capacitance effects.

To directly observe the air-breakdown effect, we developed a measurement circuit to evaluate the breakdown effect, as shown in **Fig. 2a**. The hypothesis is, if there is breakdown happening, the measured V-Q plot will show clear turning points. The typically measured Q-V plots are shown in **Fig. 2b**, with the arrows indicating the breakdown points. As plotted in the V-Q diagram of the TENG, the experimental measured breakdown points are very consistent with the simulated results (**Fig. 2c-d**). The breakdown sparks are clearly observed through a high-speed camera, as indicated by arrows in the **insets of Fig. 2c-d**. We also experimentally demonstrated that the type-1 breakdown voltage can increase with the gap distance between electrodes (**Fig. 2e**), as a method to decrease the breakdown effect. This effect can be suppressed further within high-pressure inert environment.

We also revealed the parasitic-capacitance effect. Due to this effect, the measured capacitance values are much larger than the simulated results, as shown in **Fig. 2f**. After several repeated test, we can consider the average value of the difference between the simulated and the experimental capacitances as the parasitic capacitance. And then the corrected theoretical capacitance is calculated and plotted as the orange line, which is consistent with experimental results.

3.3 Optimized design of the water-wave TENG

In order to suppress the breakdown effect through the high pressure and inert gas environment, we modified the TENG structure design, as shown in **Fig. 3a inset**. To compare the output electric performances under different environment, the 1 atm air and 1.5 atm CO_2 were filled inside, respectively, and the results are shown in **Fig. 3a-b**. From these plots, we can conclude that the 1.5 atm CO_2 can greatly enhance the open-circuit voltage and short-circuit charge by both around 1.6 times, by suppressing the air-breakdown effect.

When the TENG is operated in water, the tested voltage and charge outputs are reduced to ~80 V and ~22 nC, respectively, as shown in **Fig. 3c-d**, due to the parasitic-capacitance effect from the water. To reduce that, we fabricated an additional packaging layer outside, as shown in **Fig. 3c inset**. With that, the voltage and charge outputs are recovered to be ~190 V and ~40 nC, respectively (**Fig. 3c-d**). The overall capacitance is reduced from ~0.28 nF to be ~0.21 nF. These results are well consistent with our theoretical simulations.

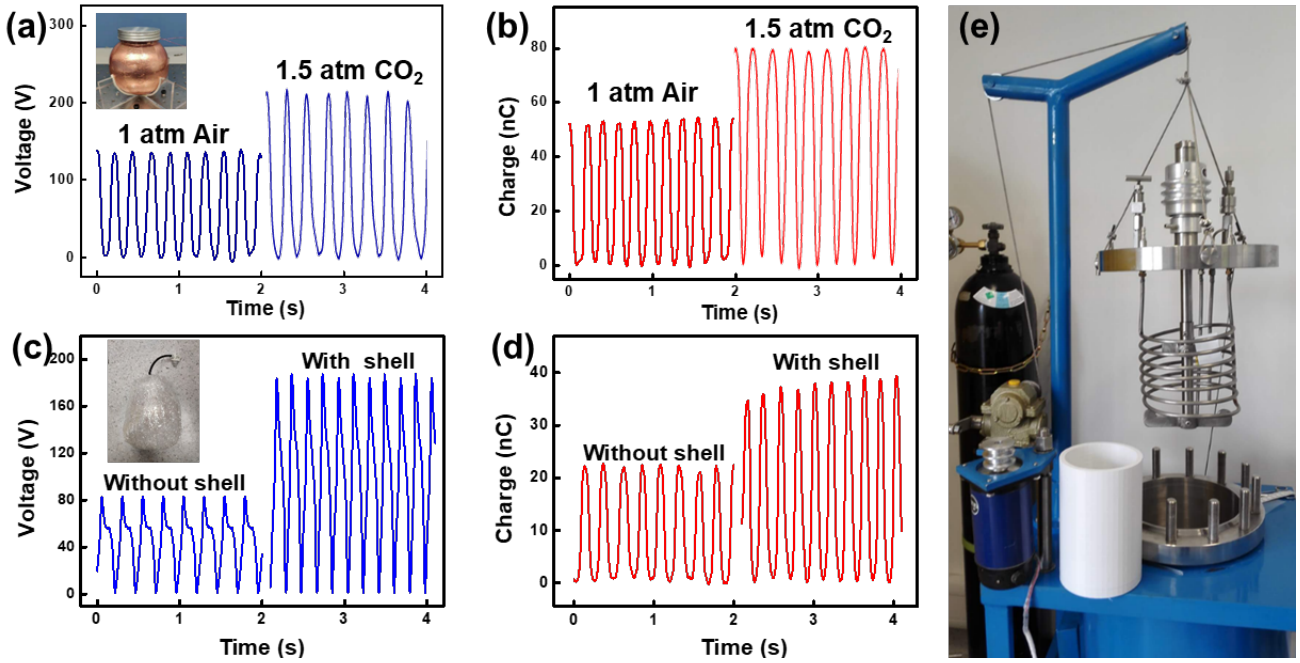

Figure 3: Optimized design of water-wave TENG and the high-pressure vessel

3.4 Development of the high-pressure vessel for quantitative analysis of the environmental factors

Even though we have demonstrated the optimized design, we still cannot evaluate and optimize the performance quantitatively, since it is impossible to control and maintain the internal environments very precisely. To address this issue and to test the device performance under even higher pressures, we have modified a steel-made chemical reactor (**Fig. 3e**) to provide the desired environment for the output performance evaluation of TENG. This reactor can withstand high pressure up to 15 MPa (148 atm). This reactor can provide quantitative controls on environmental factors, including pressure, gas concentration, temperature, *etc*. The stirring blades can provide the mechanical motions to mimic the water waves with various frequency and magnitude. When TENG is placed inside the vessel and floating on the water surface, the electrical measurement can be conducted under precisely-controlled environmental parameters. More results will be produced from this system in the future.

4. PUBLICATION AND AWARDS

J[1] G. Xu, X. Li, X. Xia, J. Fu, W. Ding, **Y. Zi**, "On the force and energy conversion in triboelectric nanogenerators," *Nano Energy*, Elsevier, Netherlands, 59, 154-161 (2019).

J[2] H. Wang, Q. Zhu, Z. Ding, Z. Li, H. Zheng, J. Fu, C. Diao, X. Zhang, J. Tian, **Y. Zi**, "A fully-packaged ship-shaped hybrid nanogenerator for blue energy harvesting toward seawater self-desalination and self-powered positioning," *Nano Energy*, Elsevier, Netherlands, 57, 616-624 (2019).

J[3] F. Chen, Y. Wu, Z. Ding, X. Xia, S. Li, H. Zheng, C. Diao, G. Yue, **Y. Zi**, "A Novel Triboelectric Nanogenerator Based on Electrospun Polyvinylidene Fluoride Nanofibers for Effective Acoustic Energy Harvesting and Self-powered Multifunctional Sensing," *Nano Energy*, Elsevier, Netherlands, 56, 241-251 (2019).

J[4] X. Li, G. Xu, X. Xia, J. Fu, L. Huang, **Y. Zi**, "Standardization of Triboelectric Nanogenerators: Progress and Perspectives," *Nano Energy*, Elsevier, Netherlands, 56, 40-55 (2019).

*J[5] Z. Wen, J. Fu, L. Han, Y. Liu, M. Peng, L. Zheng, Y. Zhu, X. Sun, **Y. Zi**, "Toward Self-powered Photodetection Enabled by Triboelectric Nanogenerators," Journal of Materials Chemistry C, The Royal Society of Chemistry, United Kingdoms, 6, 11893-11902 (2018).*

WORK IN PROGRESS

TUNABLE SPINDLE USING SELF-EXCITED VIBRATION FOR HIGH EFFICIENCY RENEWABLE ELECTRIC GENERATORS

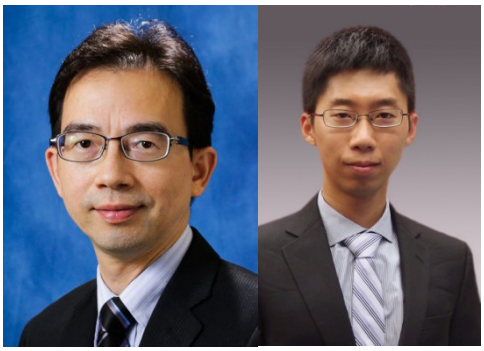

Principal Investigator: Professor Wei-Hsin LIAO
Department of Mechanical & Automation Engineering
CUHK

Co-Investigator: Professor Ping GUO [(1)]

Research Team Members:
Han Gao, Research assistant [(1)]
Jianjian Wang, Postdoc fellow [(1)]
Jing Huang, PhD student [(1)]
Ru Yang, PhD student [(1)]

[(1)] Dept. of Mechanical and Automation Engineering, CUHK

Reporting Period: 01 July 2017 – 31 May 2018
(to be completed in June 2019)

INNOVATION AND PRACTICAL SIGNIFICANCE:

This project proposes a novel spindle design for renewable electric generators, which utilizes high frequency vibration for improved tribological performance, higher energy efficiency, and reduced wear. The proposed design is supported by three major innovations: **(1)** vibration-induced friction reduction; **(2)** self-excited vibration without any extra power supply; and **(3)** a tunable spindle structure for a wide operation range. This project, if successful, will significantly improve the performance of traditional renewable electric generators in terms of efficiency and lifetime, which have play an ever increasing role in the era of clean energy.

ABSTRACT

Considering the world population growth, diminishing of fossil fuel sources, and environmental pollution, the use of renewable resources, such as hydroelectric, nuclear, and wind energy, has been emerging as an important form of clean energy. The core functional part in these renewal energy technologies is an electric generator. One critical issue determining the efficiency and reliability of renewable electric generators lies in the interaction between the spindle shaft and bearing surfaces. The friction coefficient largely influences the power generation efficiency while the contact condition determines the wear rate of the shaft and bearings. This project proposes a novel spindle design for renewable electric generators, which utilizes high frequency vibration for improved tribological performance, higher energy efficiency, and reduced wear. The proposed design is supported by three major innovations: (1) vibration-induced friction reduction; (2) self-excited vibration without any extra power supply; and (3) a tunable spindle structure for a wide operation range. The proposed design has a high potential for commercialization due to its much improved performance without major increase in cost and design complexity. This project, if successful, will not only help the development of fundamental research but also the application of renewable electric generators.

1. OBJECTIVES AND SIGNIFICANCE

This project proposes a novel spindle design for renewable electric generators, which utilizes high frequency vibration for improved tribological performance, higher energy efficiency, and reduced wear. The proposed design is supported by three major innovations: (1) vibration-induced friction reduction; (2) self-excited vibration without any extra power supply; and (3) a tunable spindle structure for a wide operation range. This project, if successful, will significantly improve the performance of traditional renewable electric generators in terms of efficiency and lifetime, which have play an ever increasing role in the era of clean energy.

2. RESEARCH METHODOLOGY

This research project will be carried out to accomplish a prolonged bearing lifetime for the rotating-spindle-type electric generators together with a higher energy efficiency. There are three main research tasks in this project:

1. Propose a low friction bearing technology by the principle of vibration-induced friction reduction to prolong the lifetime of high-load bearings and increase the power efficiency in rotating-spindle-type electric generators.
2. Establish a self-tunable vibration generating device without extra electric power supply or piezoelectric elements, which reduces the extra cost for vibration system and simplifies the overall structure.
3. Realize a self-excited vibration spindle system accommodated with position-adjustable-bearings, which is capable of changing the resonant frequency of the spindle. Therefore an optimized vibration-induced friction reduction effect will be accessible when the self-excited vibration frequency is in accordance with the resonant one.

3. RESULTS ACHIEVED SO FAR

3.1. Research Progress

We have developed a non-contact journal bearing with bi-directional driving capability utilizing the coupled resonant mode. It combines the functions of an axis positioner, non-contact journal bearing, and rotary motor. The shaft levitation is achieved by creating a stable air film using near-field acoustic force; while the non-contact rotation is realized by controlling the pressure distribution within the air film using coupled resonant mode. The mechanism of non-contact rotation can be explained by the schematics shown in Fig. 1. Unlike previous designs utilizing a traveling wave and viscous shear force, the rotational driving force is mainly contributed by the tangential component of the levitation pressure. During the compression stage of the air film, due to the slope angle of the bearing upper surface, the net reaction force from the air produces a circumferential force acting in the counter clockwise direction of the shaft. During the release stage, both the bearing surface slope angle and the pressure force change the direction, so the net reaction force still produces a counter clockwise torque on the shaft. For both the compression and expansion stages, the reaction force applied on the shaft has a circumferential component in the same direction.

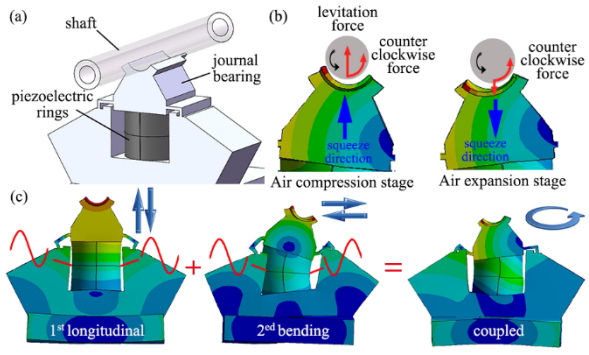

Figure 1. (a) Design of a single driving unit; (b) operation principle for shaft levitation and rotation; and (c) coupled mode shapes.

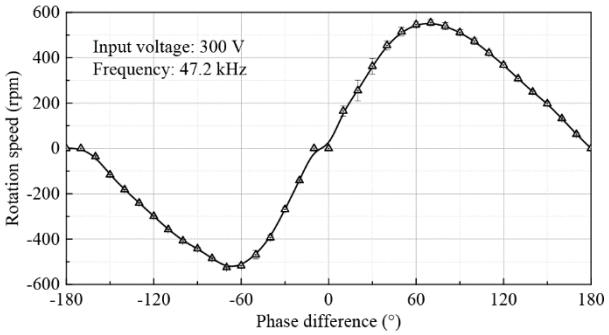

Figure 2. The relationship between rotation speed and phase angle.

The non-contact shaft rotation can be achieved and controlled by exciting the structure at a frequency between the two modes and adjusting the input phase angle or input voltage amplitude. The bearing was excited at 47.2 kHz with a voltage amplitude of 300 V, while the phase angle was adjusted from -180° to +180°. The relationship between the rotation direction as well as speed and the input phase angle is plotted in Fig. 2. The bearing demonstrated identical performance when rotated in the clockwise and counter clockwise directions. The rotation speed reached a peak value of ±555 rpm at a phase angle of 70°. The bearing could be switched to a pure levitation state by setting the phase angle to 0° or 180°.

Based on the design principle proposed in this project, an advanced functional prototype with six driving units was fabricated for two-dimensional radial position control. The 3D model and functional prototype are shown in Fig. 3. The main body of a U-shaped bearing frame was fabricated from a single aluminum alloy workpiece using electrical discharge machining (EDM) to ensure the coaxiality between the two sets of driving units. On each side, three identical driving units are placed 120° apart. Each driving unit functions similarly as the single unit described in the previous sections. The overall operating frequency of this design would be higher than that in a single unit due to the increased stiffness from the unibody design.

In additional to the levitation and rotation control, the radial position control capability is demonstrated. The driving units were grouped by their angular position and controlled by the signals #1 – #3, as shown in Fig. 3. In the vertical direction, the shaft position could be controlled in a range of 18.3 μm, when the signals #1 and #2 were simultaneously varied from 100 V to 350 V. The minimal stable increment could reach 200 nm when the voltage increment was 5 V, as shown in Fig. 4(a). In the lateral direction, the radial position could be controlled in a range of 2.1 μm, when we adjusted the amplitudes of signals #1 and #2 in the opposite direction. The minimal stable increment could also reach 200 nm when the voltage increment was 10 V, as shown in Fig. 4(b). Finally, the radial runout was measured at a rotation speed of 512 rpm, when the driving frequency was 64.9 kHz with a 75° phase shift angle. The total indicator runout was within 6 μm as indicated in Fig. 4(c), which is a combination from the shaft form inaccuracy and spindle runout.

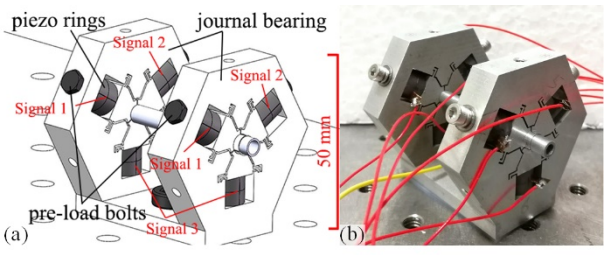

Figure 3. Design of the active non-contact journal bearing with six driving units: (a) 3D model and (b) functional prototype.

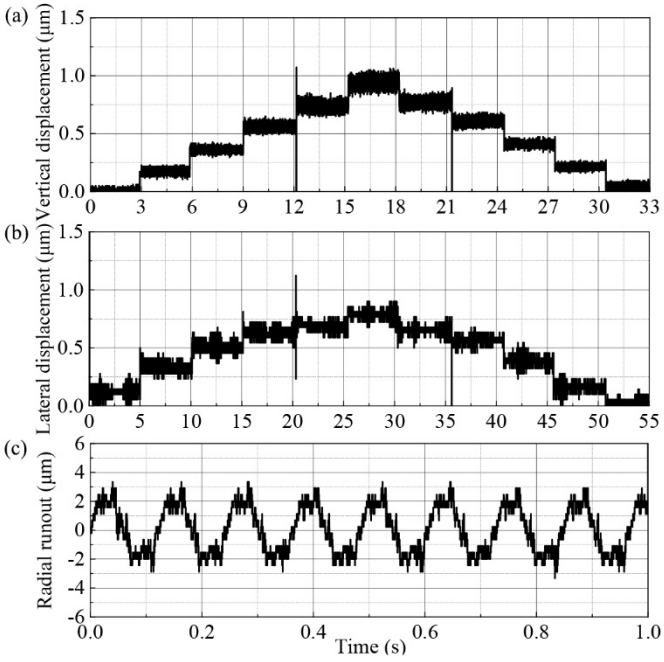

Figure 4. Active axis position control in the (a) vertical and (b) lateral directions; and (c) shaft runout during rotation.

3.2. Commercialization Efforts

1. Press Conference
We have made a press conference at CUHK on Oct 9, 2017 about our research outputs, which was reported by a number of local media, including Sing Tao Daily, Ming Pao, Oriental Daily News, Hong Kong Economic Journal, Apple Daily, Wen Wei Po, Ta Kung Pao, Metro Daily, Headling Daily, Sky Post, Hong Kong Commercial Daily, Sing Pao, South China Morning Post, etc. One of the press released photo is attached for reference (shown in Fig. 5).

2. Exhibition at InnoCarnival 2017
We have demoed our work, levitating actuator using near-field acoustic, at the Inno Carnival at the science park during Oct 21 – 29. It attracted some attention from different investors. The highlight includes the presentation of our project to Secretary for Innovation and Technology of Hong Kong, as shown in the attached figure (Fig. 6).

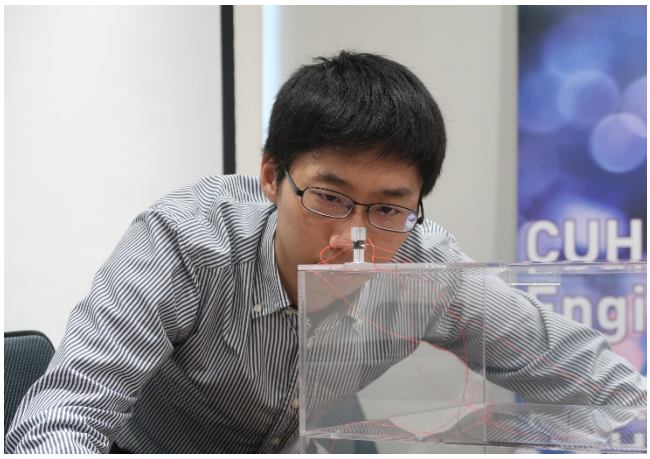

Figure 5. Press conference photo

Figure 6. Presentation at InnoCarnival 2017

3. Hasbro Presentation

We have presented our research results at the Tech Summit of Hasbro, Hong Kong on October 18. Hasbro is an American-based multinational toy and board game company (which makes the board game, Monopoly). The company showed some interest in our technology.

4. Academic Presentation

We have also presented our work in various academic settings and invited presentations, including Northwestern University (Jan 29, 2018, USA), Technical University of Denmark (May 22, 2018, Denmark), and KTH Royal Institute of Technology in Stockholm (May 25, 2018, Sweden).

4. PUBLICATION AND AWARDS

J[1] J. Wang, P. Feng, J. Zhang, and P. Guo, "Experimental study on vibration stability in rotary ultrasonic machining of ceramic matrix composites: Cutting force variation at hole entrance," *Ceramics International*, 2018.
J[2] P. Guo and H. Gao, "An active non-contact journal bearing with bi-directional driving capability utilizing coupled resonant mode," *CIRP Annals Manufacturing Technology*, 2018.
C[3] S. Gao and P. Guo, "Modeling and tool trajectory monitoring of an ultrasonic elliptical vibration tool," *International Symposium on Flexible Automation*, Kanazawa, Japan, 15-19 July, 2018.
C[4] R. Yang, J. Huang and P. Guo, "Frequency dependence of levitation force in near-field acoustic levitation," *International Symposium on Flexible Automation*, Kanazawa, Japan, 15-19 July, 2018.
*C[5] J. Wang, Y. Yang, and P. Guo, "Effects of vibration trajectory on ductile-to-brittle transition in vibration cutting of single c*rystal silicon using a non-resonant tool," CIRP Conference on Surface Integrity, Tianjin, 11-13 July, China

COMPLETED

ROBUST NICKEL-MOLYBDENUM–YTTRIA STABILIZED ZIRCONIA (NIMO–YSZ) ANODE MATERIALS FOR SOLID OXIDE FUEL CELLS

Principal Investigator: Professor Yongsheng CHEN
Department of Mechanical & Automation Engineering
CUHK

Research Team Members:
Jiazheng Ren[(1)], Ming Li[(1)], Alex Chinghuan Lee[(1,2)], Kai Cheng[(1)]

(1) Dept. of Mechanical and Automation Engineering, CUHK
(2) Shun Hing Institute of Advanced Engineering

Project Start Date: 1 July 2016
Completion Date: 30 June 2018

ABSTRACT

This proposal aims to develop new anode materials to improve durability of the state-of-the-art solid oxide fuel cells (SOFCs). SOFCs are electrochemical devices that convert chemical energy of a fuel (commonly hydrogen, more importantly, fuels derived from renewable sources, such as biomass and municipal wastes) and oxidant directly into electrical energy. They are energy efficient and environmentally benign, and their large scale applications in electricity production may address the environmental, climate change, and water concerns that we are facing today.

There are major technical barriers that have to be overcome before SOFCs can be commercialized and widely used for power generation. Among them is anode degradation. For the state-of-the-art Ni–YSZ anodes, carbon deposition (or coking) on and sulfur poisoning of the anode are responsible for the performance loss due to the presence of impurities in carbonaceous fuels, a price that comes with the SOFC's fuel flexibility. These problems are usually dealt with separately. We will design new NiMo-YSZ anode materials to mitigate carbon deposition and sulfur poisoning simultaneously with the years' experience of the PI in studying these phenomena in steam reforming reactions. If successful, this project will promote the final commercialization of SOFC technology for power generation.

1. OBJECTIVES AND SIGNIFICANCE

(a) Objectives
1. Find the optimal composition of NiMo-YZS anode materials for minimal degradation.
2. Determine the proper formation of NiMo, i.e., physical mixture or alloy as materials structure influences their performance.
3. Determine the optimal H2S content and other reaction conditions for minimal coking and sulfur poisoning.
4. Perform multiple characterization techniques to determine the degradation mechanism in NiMo-YSZ anode materials.

(b) Significance
This proposal aims to develop a new catalytic approach for stable hydrogen production from steam reforming of transportation fuels, such as gasoline and diesel, which can be produced from petroleum or bio-oil. If successful, this project will pave the way for on board hydrogen

production for fuel cell applications, and distributed hydrogen refilling stations using current gas station infrastructure. The high energy efficiency associated with fuel cells and using bio-oil as a hydrogen source will result in much lower carbon dioxide emissions, and contribute to the mitigation of anthropogenic climate change. This new approach will promote new research activities in catalysis in general if it becomes possible to combine two or even more catalytic reactions to produce desirable outcomes. It is foreseeable that it will boost fundamental research in heterogeneous catalysis in terms of surface reaction mechanisms, which in turn will promote the development of new catalysts for real-world applications.

Hydrogen is a promising energy carrier for emerging energy technologies such as fuel cells. Currently the most widely used technology for hydrogen production is steam reforming of natural gas over a Ni catalyst. To supply hydrogen for future onboard fuel cell applications or hydrogen refill stations, steam reforming of transportation fuels is desirable since (1) these fuels have much higher volumetric energy densities than methane; and (2) these fuels are readily available in the existing gas station infrastructure. The steam reforming reaction uses a metal oxide supported metal catalyst, and a major technical barrier for this technology is catalyst deactivation due to sulphur poisoning and carbon deposition. "Sulphur poisoning" refers to a phenomenon in which steam reforming catalysts deactivate much faster because of the organic sulphur impurities in transportation fuels. The popular theory is that the sulphur impurities react with the metal catalyst and form metal sulphides, which makes the catalysts lose their functions. Carbon deposition results from the decomposition of hydrocarbons (a necessary step for hydrogen production). When carbon atoms from the decomposition do not react with oxygen efficiently, they will accumulate and cover the catalyst surface, leading to the loss of catalyst performance. The state-of-the-art approach is to address the two problems separately. For sulphur poisoning noble metals and metal alloys have been employed; and for carbon deposition, promoters are added to expedite carbon gasification – a reaction that removes carbon. Our approach in this proposal is to address them simultaneously. This is inspired by our recent discovery on the sulphur poisoning mechanism.

We have found that initially the formation of metal sulphides causes a fast but minor deactivation of the catalysts, and subsequently there is a clear correlation between carbon deposition and catalyst deactivation. Thus, carbon deposition is a more severe problem for long-term system operation. A subsequent investigation into the carbon formation mechanism reveals certain effects of hydrocarbon structure on catalyst deactivation. Our preliminary data shows that steam reforming of benzene produced slower catalyst deactivation than that of hexane. This is surprising: one would expect the opposite as benzene has a ring structure similar to carbon deposition. A probable reason is the competitive adsorption between sulphur and hydrocarbon on the catalyst surface. Benzene has a higher affinity with the metal catalyst than hexane. Since both sulphur impurities and hydrocarbon molecules compete for the same catalyst surface sites, benzene competes better with the sulphur than hexane and thus slows down sulphur adsorption more. Another beneficial effect is that the metal catalyst also catalyzes carbon gasification; less sulphur adsorption means more catalytic sites are available for gasification thus improving the rates of carbon removal. Therefore, we propose a new approach by introducing a second catalytic function to the system, which will in situ convert structurally undesirable hydrocarbons in transportation fuels to more desirable hydrocarbons.

2. RESEARCH METHODOLOGY

We will develop nickel-molybdenum–yttria stabilized zirconia (NiMo–YSZ) anode materials. In our design, Ni and Mo will be metal particles, either in separate phases or in alloy form. The Mo oxide layers on Mo surface are active for aromatization reaction (producing benzene from CH_4 or CO and H_2). The proposed research includes two tasks:

Task 1. Catalyst synthesis and steam reforming. Nickel and molybdenum powders will

be purchased and used in the experiments. One purpose of the proposed research is to determine the optimal ratio between Ni and Mo, and the best configuration of these two metals in the anode – physical mixture or alloy. The synthesis of Ni-Mo alloy will be carried out using a method reported in the literature.[13] The metal or alloy particles will then be dispersed on YSZ support using proper binders.

The NiMo-YSZ anode materials will then be tested in steam reforming reactions using SOFC operation conditions. The fuel used in the reaction will be CH_4, a surrogate for biogas. The reaction temperatures will be 750 – 850 ºC. All catalysts will be reduced in situ with H_2 prior to the reaction. CH_4 and H_2O together with ppm levels of H_2S will be fed into the reactor at a steam/carbon ratio of 2:1, and the gaseous products will be analyzed with an online gas chromatography (GC).

Task 2. Anode deactivation mechanisms. To investigate sulfur poisoning and carbon deposition on the catalyst, a suite of materials characterization techniques will be employed to probe the physical and chemical properties of the catalysts before and after reforming reaction. These techniques include XPS, XRD, TPO, and SEM-EDX.

1. XPS – X-ray photoelectron spectroscopy. XPS is a surface technique, which detects about the top 10 nm of a catalyst for its surface chemical composition and chemical states of its constituents. The information provided by XPS is essential to understand catalyst performance and possible deactivation mechanisms. For example, when there is formation of carbon deposition, the proportion of carbon in the surface will increase and those of Ni and Mo will decrease.
2. XRD – X-ray diffraction. XRD is a bulk technique and measures the crystalline phases in the anode materials. The bulk structure affects its surface properties, and more importantly, it determines the mechanical stability of the catalyst, which is one reason that an SOFC anode fails. XRD is also used to estimate the particle size of a phase when it's crystalline and has a size in a range of a few to a few hundred nm. We will use XRD to monitor Ni and Mo particles and their sintering and the formation of Ni-Mo alloy.
3. TPO – temperature programmed oxidation. TPO is a process in which a catalyst, usually used, is burned under oxidation condition (e.g., pure oxygen) with increasing temperature (reaching about 1000 ºC). With IR quantifying the amount of CO_2 evolved in the process, the information of carbon deposition including carbon species and carbon location can be obtained. We will use TPO to characterize carbon deposition on the anode materials.
4. SEM-EDX – scanning electron microscopy – energy dispersive X-ray analysis. The techniques mentioned above are averaging techniques in nature, meaning they measure an average property of a catalyst. SEM-EDX provides a means to directly visualize a catalyst surface and its chemical composition. It serves as a reminder when we study catalyst structure-performance relationship that the surface is different from an ideal surface with various features.

The fundamental understanding of the anode deactivation mechanisms obtained in Task 2 will be fed back to Task 1 to guide the development of robust NiMo-YSZ anode materials.

3. RESULTS ACHIEVED

We performed experiments that confirmed that addition of Mo increases the adsorption of CH4, leading to increase of carbon deposition when there is no presence of sulfur impurities. It is determined that the current approach may not be able to solve the catalyst deactivation problem for all fuels. In light of the fact that in the anode, there is substantial amount of CO_2 present, the research proceeds to study CO_2 reforming of methane, a reaction that is significant but overlooked in anode reactions.

We developed a new IR-based technique for catalyst evaluation for dry reforming of methane. Gas chromatography (GC) is almost exclusively used to evaluate catalyst performance. In order to measure the catalyst activity with GC, an inert gas with a constant flow rate is usually fed into the system as an internal standard. Our IR-based method is used to achieve the same technical goal with much higher time resolution and much smaller measurement errors. IR is applied to measure the molar fractions of CH_4, CO_2, CO, and H_2O in the reaction effluent. By applying general mass

balance principle and the relevant reaction stoichiometries, catalyst performance is successfully measured without an internal standard. The results are quite close to those obtained by GC with much higher time resolution, making it possible to observe fast reaction kinetics. As a result, first successful measurements of carbon deposition kinetics were made under real reaction conditions. Carbon deposition is a major catalyst deactivation mechanism. Although numerous kinetic modelling works have been done on carbon formation, there were only scarce attempts to measure carbon deposition kinetics under relevant (but not real) conditions due to technical difficulties.
We also developed a technique that allows us to well control the reduction of Ni catalyst that activates the catalyst. This important step is usually performed, however, based on individual preference or "gut feeling" rather than scientific evidence. We started with an ordinary Ni/Al_2O_3 catalyst prepared by incipient wetness impregnation method. With our novel control technique assisted by IR spectroscopy, we were able to well control the reduction extent in full range for the Ni catalyst. Four reduction extents (41%, 75%, 89%, and 100%) were tested for its effects on catalyst performance. It was found that 41% reduced catalyst suffered from rapid deactivation while the others performed very well with no clear sign of deactivation within 24 h of reaction time. Catalyst tests show that the 75% reduced catalyst was a super performer with CH_4 and CO_2 conversions close to the thermodynamic limits and meets if not overperforms the best catalysts reported in the literature. This work would open up great opportunities for tuning catalyst performance without incurring exotic catalyst formulation and complex synthesis methods.

4. PUBLICATION AND AWARDS

J[1] J. Ren, A.C. Lee, K. Cheng, M. Li, Y. Chen, "Measure the unmeasurable by IR spectroscopy: carbon deposition kinetics in dry reforming of methane". *ChemPhysChem*, 2018, 19, 1814-1819.

J[2] M. Li, K. Cheng, J. Ren, A.C. Lee, Y. Chen, "Turning an ordinary Ni/Al_2O_3 catalyst into a super performer for dry reforming of methane by controlled reduction", submitted to *Energy and Environmental Science*.

C[1] J. Ren, M. Li, A.C. Lee, K. Cheng, Y. Chen,, "IR SPECTROSCOPIC MEASUREMENT OF HYDROGEN PRODUCTION KINETICS IN METHANE DRY REFORMING", *9th International Conference on Hydrogen Production, submitted to a special issue in International Journal of Hydrogen Energy.*

Biomedical Engineering Track

Research Reports In Biomedical Engineering

Newly Funded Projects (2019-2021)	* Development of a Folded bilayer Scaffold for Intestinal Tissue Engineering
	* Optogenetic Regulation of Hormone Production for Glucose Homeostasis Maintenance
Continuing Projects (2018-2020)	* Development of Highly Sensitive Quantitative Phase Microscopy for Label-free Imaging of Neuronal Network Activities
(2017-2019)	* Development of a Novel Robotic Manipulator for Confined Space Surgery
	* Development of an Inertial Microfluidics Based Approach for the Isolation of Mitochondria from Biological Samples
Completed Projects (2016-2018)	* An MRI-guided Robotic System for Breast Biopsy
	* Intention-driven Shoulder Rehabilitation for Targeted Meuro-muscular Training using an Exo-musculoskeletal Robot
	* Engineering Antimicrobial Surfaces Based on Micro-topography Using a Novel Ultrasonic Machining Method

The following reports are enclosed in "Research Highlights" printed in July 2018

Completed Projects (2015-2017)	* Development of a Novel flexible Surgical Robot with Haptic Sensation * Development of Injectable Supramolecular Hydrogels for Regenerative Medicine * Developing Optomechanical Devices based on Layered Nanomaterials for Single-Biomolecule Mass Spectrometry

The following reports are enclosed in "Research Highlights" printed in August 2017

Completed Projects (2014-2016)	* Development of High-speed Laser Scanning Microscope for In Vivo Deep Brain Imaging * Mechanism for the Transcytosis of Targeted Nanoparticles Across the Blood-brain barrier
(2013-2015)	* Development of the Next Generation Neurosurgical Assistant System Based on Functional Brain Mapping * Biomimetic Scaffold for Stem Cell Based Cartilage Regeneration and Drug Delivery

The following reports are enclosed in "Research Highlights" printed in June 2015

Completed Projects (2012)	* Dielectrophoresis Nano-separator for Precision Manufacturing of Polymeric Nanoparticles for Tumor-Targeted Drug Delivery

The following reports are enclosed in "Research Highlights" printed in June 2014

Completed Projects (2011)	* Viewing Biomolecules at the Right Site by Plasmonic Tweezers and Surface Enhanced Raman Scattering

The following reports are enclosed in "Research Highlights" printed in 2013

Completed Projects (2010)	* An inexpensive functional finger prosthesis with rebounded type progressive hinge lock * Diffusion Tensor MRI Predictors of Cognitive Impairment in Confluent White Matter Lesion

	* Lanthanide-impregnated Molecularly Imprinted Polymer Microspheres as Antibody Mimics on an Optofluidic Platform for the detection of Disease Biomarkers
Completed Projects (2009)	* Terahertz Probe for in Vivo Imaging
	* Signal Processing Strategies on Cochlear Implant Devices for Effective Speech Perception of Tonal Languages
	* Development of A Robotic Endoscope Holder for Nasal Surgery

The following reports are enclosed in "General Report and Research Highlights 2009-2011" printed in October 2011.

Completed Projects (2008)	* Development of Highly Sensitive and Large Throughput Surface Enhanced Raman Scattering (SERS) Substrates for Molecular Diagnosis
Completed Projects (2008)	* Research on Language and Brain Waves
	* Development of an Efficient Locomotion Mechanism for Wireless Active Capsule Endoscope
(2007)	* Bio-electromagnetic Modeling and Experiment Setup for Medical Electronics RF Safety Assessment
	* Medical Applications of Terahertz Imaging
	* Hybrid Assistive Knee Braces with Smart Actuators
(2006)	* RF Radiation Effect and Efficiency of Wireless Medical Devices on Human Body
	* Photonic Biosensor Micro-arrays for Screening of Common Cancers

The following reports are enclosed in "Research Highlights 2005-2007" printed in January 2008.

Completed Projects (2005)	* Cochlear Implants
	* Virtual Anatomy and Dexterous Simulators for Minimal Access Cardiothoracic and Neuro-endoscopic Surgeries
	* Systematic Synthesis of Nano-informatics Chips by Nano-Robotics Manipulation

(Funded Year)

DEVELOPMENT OF A FOLDED BILAYER SCAFFOLD FOR INTESTINAL TISSUE ENGINEERING

Principal Investigator: Professor Hon Fai CHAN
Institute for Tissue Engineering and Regenerative Medicine, Department of Biomedical Engineering, CUHK

Project Start Date: 1 July 2019

ABSTRACT

Short bowel syndrome can be caused by birth defect or surgical removal of part of the intestine resulting from a number of diseases. It is associated with high morbidity and mortality. Current therapies are mostly ineffective, ultimately requiring an intestinal transplant but complications arise. Construction of tissue-engineered small intestine (TESI) in vitro, in which patient cells are cultured on a biomaterial scaffold, offers a therapeutic alternative. However, the current scaffold designs do not take into consideration the distinct properties of different layers of the native intestine wall. In addition, the dense mucosal folds, which are present along the inner surface of intestine and assume an important functional role, have not been reproduced. Recently, we have engineered a folded bilayer hydrogel scaffold with tunable mechanical properties via a theory- and simulation-guided approach for the first time. A soft and stretchable hydrogel is stretched before a relatively stiff hydrogel is layered on top. Subsequent relaxation induces controlled folding of the top layer, and the process is reversible. To further develop the strategy for clinical translation, we propose to 1) optimize the properties of the bilayer hydrogel scaffold including porosity, stiffness, and adhesion between two layers; 2) direct the differentiation of primary intestinal organoid in the bilayer scaffold. The successful completion of the project will improve the current design of TESI and advance the field of intestinal tissue engineering.

INNOVATION AND PRACTICAL SIGNIFICANCE:

To include a paragraph to highlight specifically the innovation and practical significance of your work. Both VC and the door would like to see more research endeavors be directed to innovation and technology transfer for the betterment of mankind.

The major innovation of the current work lies in the design of the folded bilayer hydrogel scaffold. All scaffold materials reported previously for the production of TESI consist of single-phase materials such as polylactic-co-glycolic acid (PLGA), poly-ε-caprolactone, chitosan etc, without taking into consideration the distinct properties of different layers of the intestinal wall. Decellularized tissue is an exception but its application is limited by human tissue source. The bilayer hydrogel scaffold is expected to outperform current designs by better recapitulating the multi-layered structure of small intestine. In addition, we are the first group demonstrating the fabrication of a folded scaffold by mechanics-guided folding, which represents a new paradigm in tissue engineering. The technique is novel but at the same time simple for scale-up production. We

will file a patent application on the scaffold materials and fabrication technique after they are optimized, and actively pursue preclinical and clinical trial to bring the potential therapy to patients.

PROJECT OBJECTIVES:

1. Short bowel syndrome (SBS) affects 3-4 individuals per million people[1]. A number of conditions can lead to SBS, such as congenital anomalies and intestinal resection following Crohn's disease. Since SBS can cause malabsorption and malnutrition, it is associated with high morbidity and mortality, especially in children in which the estimated 5-year mortality approaches 40%[2].
2. Current therapies aiming to increase absorption or restore intestinal length are ineffective. Intestinal transplantation is the last resort but is limited by tissue supply and complications such as graft rejection[3].
3. The development of a tissue-engineered small intestine (TESI) by incorporating patient's own intestinal cells (e.g. organoid unit derived from intestine tissue) into a scaffold represents an attractive option for autologous transplantation[3]. However, none of the reported TESI has been applied in clinic so far. Possible reasons include a lack of control of organoid differentiation and complications arising from multiple surgeries required for the in vivo maturation of TESI[4].
4. Generating TESI resembling native intestine in vitro without the need for in vivo maturation would be advantageous.
5. The current scaffold fabrication approaches fail to recapitulate mucosal fold, which increases surface area for absorption and endows the intestine with the flexibility to contract and expand, and mimic the properties of distinct layers of the intestine wall, consisting mainly of mucosa, submucosa, muscle layers and serosa.
6. Our lab has recently demonstrated the fabrication of a folded bilayer hydrogel scaffold based on the concept of surface instability[5]. The scaffold displays folding and unfolding behavior similar to the native mucosal folding-unfolding occurring during peristalsis.
7. To further develop the strategy for clinical translation, we will achieve the following aims (**Figure 1**).
8. Aim 1: Optimize the properties of the bilayer hydrogel scaffold including porosity, stiffness, and adhesion between two layers;
9. Aim 2: Direct the differentiation of primary intestinal organoid (containing intestinal stem cells and the supporting mesenchyme) in the bilayer scaffold by applying mechanical and biochemical cues.
10. We expect to identify a scaffold formulation with optimal porosity, stiffness and adhesion property for organoid culture, and apply cues to direct organoid to differentiate into different intestinal cell types at appropriate location.
11. The successful completion of the project will improve the current design of TESI that should lead to better outcome in preclinical and clinical studies, eventually offering a cure of SBS.

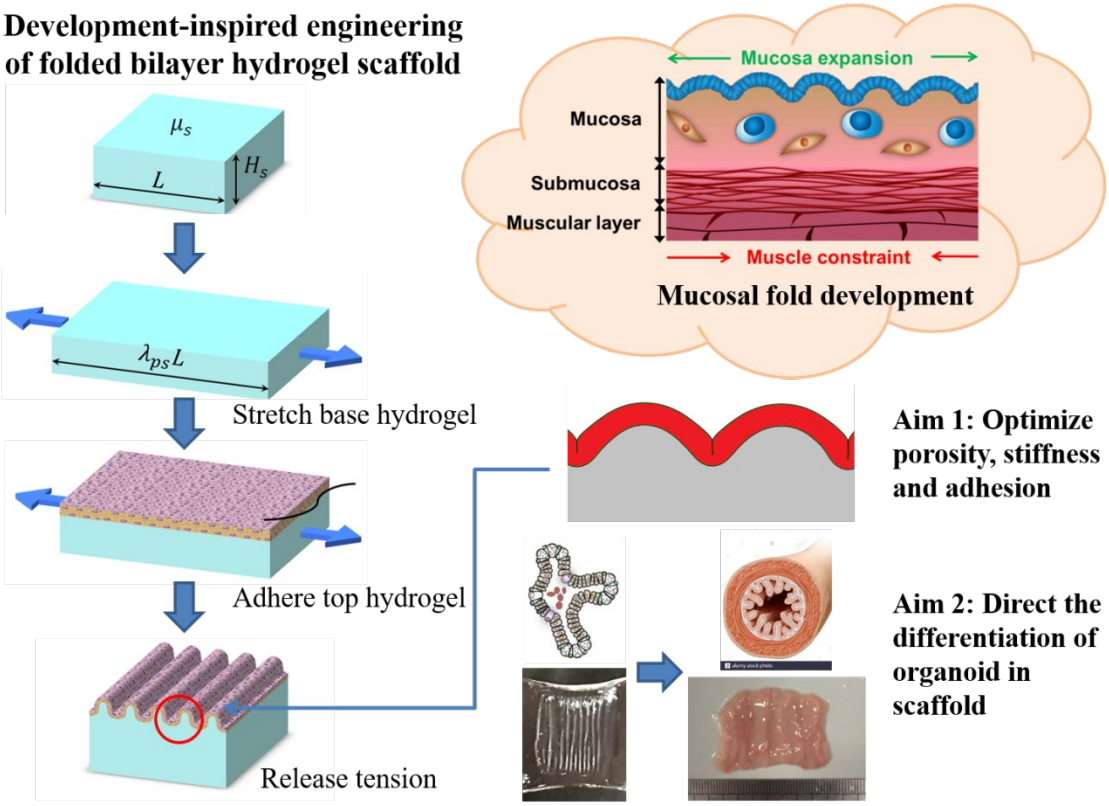

Figure 1. Specific aims of the proposed project. The proposal intends to further develop the folded bilayer hydrogel scaffold we reported and optimize it for intestinal organoid culture and differentiation.

Reference (Papers by our group are highlighted.)

[1] P. Seetharam, G. Rodrigues, Short bowel syndrome: a review of management options, Saudi journal of gastroenterology : official journal of the Saudi Gastroenterology Association, 17 (2011) 229-235.

[2] L.Y. Martin, M.R. Ladd, A. Werts, C.P. Sodhi, J.C. March, D.J. Hackam, Tissue engineering for the treatment of short bowel syndrome in children, Pediatric research, 83 (2018) 249-257.

[3] R.G. Spurrier, T.C. Grikscheit, Tissue engineering the small intestine, Clinical gastroenterology and hepatology : the official clinical practice journal of the American Gastroenterological Association, 11 (2013) 354-358.

[4] M.R. Ladd, L.Y. Martin, A. Werts, C. Costello, C.P. Sodhi, W.B. Fulton, J.C. March, D.J. Hackam, The Development of Newborn Porcine Models for Evaluation of Tissue-Engineered Small Intestine, Tissue engineering. Part C, Methods, 24 (2018) 331-345.

[5] H.F. Chan*, R. Zhao*, G.A. Parada, H. Meng, K.W. Leong, L.G. Griffith, X. Zhao, Folding artificial mucosa with cell-laden hydrogels guided by mechanics models, Proceedings of the National Academy of Sciences of the United States of America, 115 (2018) 7503-7508. (*These authors contributed to this work equally).

OPTOGENETIC REGULATION OF HORMONE PRODUCTION FOR GLUCOSE HOMEOSTASIS MAINTENANCE

Principal Investigator: Professor Liting DUAN
Department of Biomedical Engineering, CUHK

Project Start Date: 1 July 2019

ABSTRACT

Diabetes is a progressive and complex disease featured by chronically deregulated blood glucose levels affecting more than 422 million people in the world. In Hong Kong, one in ten people suffer from diabetes, and the prevalence will continue to increase due to the rapid growth of the aging population. Aberrant insulin production is a hallmark of both type 1 and type 2 diabetes. Since no cure is available yet, current treatment strategies include strict food control along with lifelong regular injections of insulin. Many research efforts are devoted to developing alternative methods to increase the insulin concentration for diabetic patients. Novel methods than enable precisely controlled and rapid production of hormones regulating blood glucose levels hold great promise to provide effective treatments. Here we propose to design and construct optogenetic systems that use light to control the production of blood glucose regulating hormones. We expect light-inducible production of insulin or glucagon-like peptide can offer a promising approach to treat diabetes. Besides, we plan to establish an orthogonal optogenetic system to express different hormones under the light stimulation of different wavelengths. We expect the proposed orthogonal system will be able to balance blood glucose level bidirectionally, thus presenting a great tool to study the glucose homeostasis and the mechanisms underlying diabetes.

INNOVATION AND PRACTICAL SIGNIFICANCE:

The generation of cells producing insulin or other related hormones would provide an unprecedented cell source for drug discovery and cell transplantation therapy targeting diabetes. To this end, presented here is a previously unavailable strategy that uses LIGHT to precisely and rapidly control the production of one or two hormones in engineered cells for glucose homeostasis. The novel optical strategy offers many key advantageous over the currently available cell-based methods to balance the blood glucose level (e.g. transplantation of healthy islet cells or stem cell-derived pancreatic cells), including:

1. *Precise control over the production of the related hormones with high spatial and temporal resolution*
2. *Fast on-and-off switch of the hormone production*
3. *The capacity to bidirectional influence glucose homeostasis by orthogonally inducing the production of two hormones with opposite effects on the blood glucose concentration*
4. *Good scalability*

Therefore, the proposed strategy will have a broad appeal to the pharmaceutical and clinical sectors targeting diabetes.

PROJECT OBJECTIVES:

1. To develop optical control of insulin production in living cells as a potential treatment for type 1 diabetes

2. To develop optical control of glucagon-like peptide (GLP) production in living cells as a potential treatment for type 2 diabetes

3. To develop an orthogonal optogenetic system to independently produce insulin (or GLP) and glucagon for bidirectional maintenance of blood glucose level

WORK IN PROGRESS

DEVELOPMENT OF HIGHLY SENSITIVE QUANTITATIVE PHASE MICROSCOPY FOR LABEL-FREE IMAGING OF NEURONAL NETWORK ACTIVITIES

Principal Investigator: Professor Renjie ZHOU
Department of Biomedical Engineering, CUHK

Co-Investigator: Prof. Vincent Chi Kwan Cheung [(2)]

Research Team Members:
Yujie Nie, PhD student [(1)],
Mengxuan Niu, Junior Research Assistant [(1)],
Peiyuan Huang, Junior Research Assistant [(1)], and
Kam Pang So, Junior Research Assistant [(2)]

[(1)] Dept. of Biomedical Engineering, the Chinese University of Hong Kong
[(2)] Dept. of Biomedical Science, the Chinese University of Hong Kong

Reporting Period: 1 July 2018 – 30 April 2019

INNOVATION AND PRACTICAL SIGNIFICANCE:

The development of optical recording techniques for mapping action potentials is important as it offers many key advantageous over the traditional electrophysiology techniques (e.g., patch clamping), such as:

a. Noninvasiveness without physical contacts,
b. Spatial and temporal resolvability,
c. High-throughput measurement capability.

However, label-free optical imaging techniques (i.e., without using fluorescent tags), that do not suffer from photobleaching and slow kinetics of fluorescent proteins, still have not been developed for long term and high speed recording of action potential signals on excitable mammalian cells. Among possible label-free techniques, interferometric microscopy, particularly the quantitative phase microscopy (QPM), is promising in satisfying the sensitivity and speed requirements needed for imaging action potentials. The PI, Prof. Renjie Zhou who is an expert on QPM, has recently implemented MEMS-based mirrors and highly sensitive cameras into QPM systems. He recently co-developed a theory for understanding the phase noise limit in such systems, which has led to achieve 10-4 temporal sensitivity with 10 ms temporal resolution in a QPM system. In order to image neuronal action potentials as proposed in this project, we need to further achieve 10-5 temporal sensitivity and 1 ms temporal resolution. Therefore, we will develop a QPM system that integrates the following technical innovations:

a. A high stable interferometric microscopy design,
b. A better usage of the dynamic range of a high well-depth camera,
c. Capability of operating in the reflection-mode QPM system to inheritably provide 10x better sensitivity.

Our system will enable us to image, for the first time, the electrical activities of cultured neurons, such as those from induced pluripotent stem cells, without fluorescence labeling. This work will promote strong collaborations with the School of Biomedical Sciences at CUHK through the Co-I Prof. Vincent Cheung who is a neurobiologist. By mapping the neural network activities of multicellular organisms, e.g., Caenorhabditis elegans, it will establish our technique as an

important neural imaging tool for revealing functional maps of complex nervous systems in the future.

ABSTRACT

The challenge in neuroscience lies in the ability to monitor neuronal network activities to study mechanisms of increasingly complex behaviors under normal and disease conditions. These demands of neuroscience can only be met by developing novel microscopy technologies that can image at single neuron levels. Neuronal network activities are characterized by electrical impulses called the action potentials, which has been mapped with fluorescence-based imaging techniques using bright voltage-sensitive dyes. However, such methods suffer from photobleaching of the fluorescent proteins, preventing them for long-term neuronal network functional studies. Therefore, the development of a label-free optical imaging technique (i.e., without using fluorescent tags) is critical in solving this issue. During this project, we propose to develop a highly sensitive interference microscopic technique for imaging the action potential signals in neuronal networks. In the first phase, we have developed a quantitative phase microscope (QPM) and tested its imaging performance. To demonstrate the feasibility in using our QPM system for neural imaging, we have tested its sensitivity with different types of cameras. We have also worked on achieving phase cancellation which can be further used to improve the sensitivity of our system. For the next stage, we plan to use our system for imaging primary neurons, as well as those induced from pluripotent stem cells. If we can successfully image the action potentials in a label-free setting (no one has succeeded so far), this will be a major milestone that will enable many important discoveries in neuroscience.

1. OBJECTIVES AND SIGNIFICANCE

We aim to develop a QPM system that integrates the following technical innovations:

a. A highly stable interferometric microscopy design,
b. A better usage of the dynamic range of a high sensitivity camera.
c. A further improvement of sensitivity by wave-front shaping and phase cancellation.

With this QPM system, we will image the electrical activities of neurons, such as those from induced pluripotent stem cells or primary neurons, without fluorescence labeling.

2. RESEARCH METHODOLOGY

As a foundational step, we will build a QPM that is mechanically stable. Diffraction phase microscopy (DPM) system has been well proven to be one of the most stable QPM systems. There will be several modifications to a regular DPM system (as illustrated in Fig.1) to allow for breaking the hardware limit on temporal sensitivity. At first, a spatial light modulation (SLM) based wavefront shaping system will be built before sample illumination for phase cancellation. MEMS mirror based SLMs in general have higher mechanical stability (~ 10^{-6}) compared with liquid crystal-based SLMs (~10^{-3}), thus can be a better choice for canceling the phase of the sample without adding substantial noise. In order to do that, a flat wave-front will be first projected on the SLM and then the phase of the sample will be measured with a camera. After that, the inverse phase of the sample will be projected on the SLM before its phase is measured again. At the end, we expect to measure a relatively flat phase that indicates the sample is "concealed". Preliminary results in Fig. 2 have demonstrated this principle, where the phase of a 10 μm polystyrene bead has been cancelled. During the initial test, a liquid crystal based SLM is used, but the same procedure can be directly applied to MEMS mirror based SLM for high mechanical stability. The second modification is that we applied a super-high well depth camera with an electron well depth of more than 2 million to achieve sub-nano sensitivity.

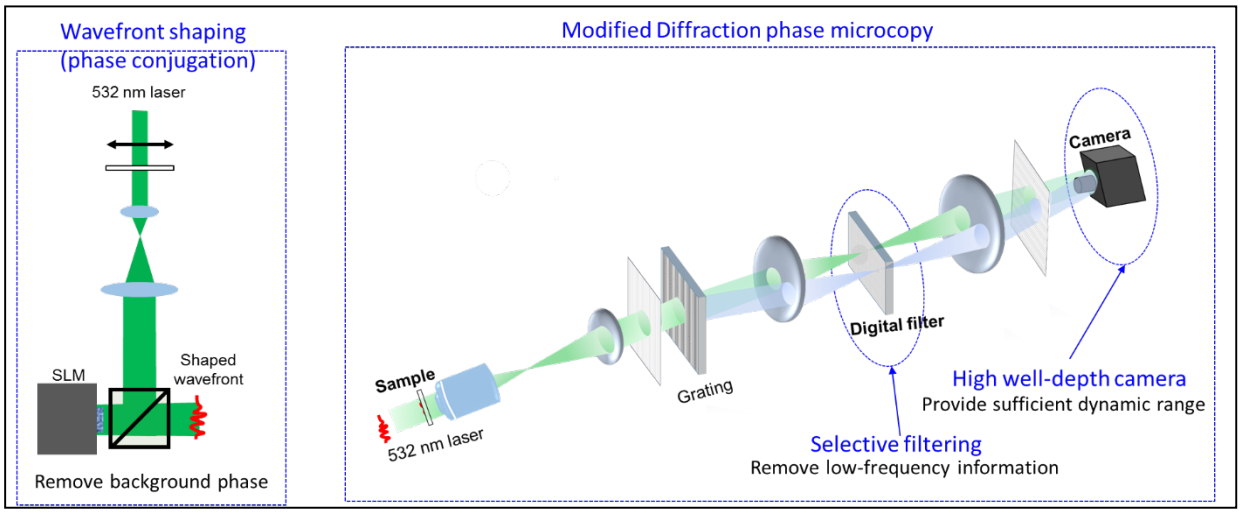

Fig. 1. Proposed design of the highly sensitive QPM system.

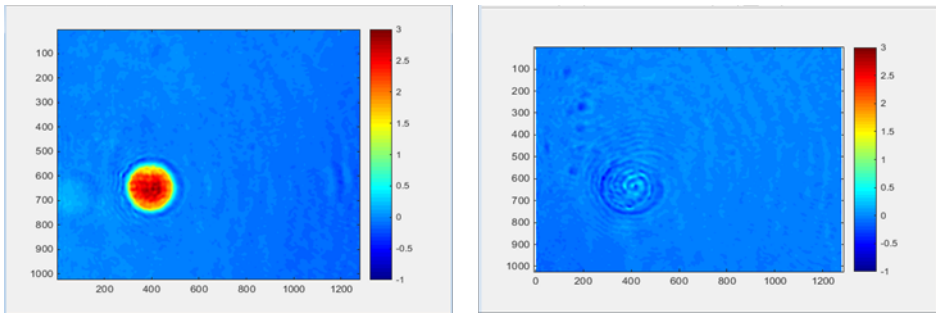

Fig. 2. Cancellation of the phase of a 10 μm bead.

3. RESULTS ACHIEVED SO FAR

3.1 Design and build a versatile common-path quantitative phase microscopy system

Figure 3(a) shows the schematic design, where a fiber-coupled 532nm CW laser with power stability less than 1% is used as the illumination source. Light from the fiber was collimated and focused to a 20× objective and then collimated by the 150 mm focal tube lens. The sample image was projected onto a transmission grating. The first diffraction order was passed unobstructed, while the 0th order was filtered with a 10μm pinhole mask placed in the Fourier plane of a 4-f optical system, consisting of a 35 mm lens and a 150 mm lens. Interferogram were formed on the camera. The actual system that has been constructed is shown in Fig. 3(b).

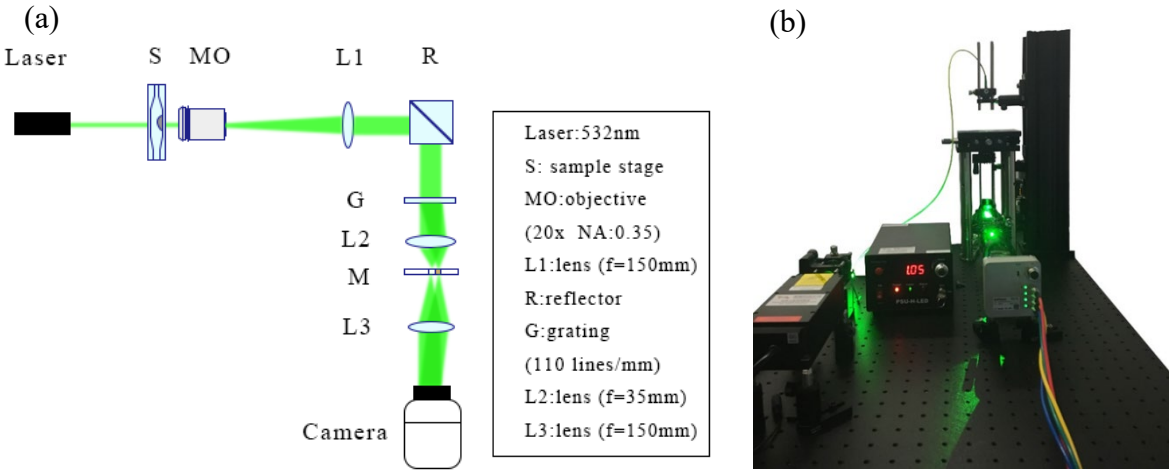

Fig. 3. (a) Schematic design of the QPM system; (b) the photo of the actual QPM system.

3.2 Comparison of sensitivity of different cameras

Table 1. Comparison of camera sensitivity

Camera model	Interferogram	Noise distribution (mrad)	Temporal noise (nm)	Spatial noise (nm)
SMN-B 012-U	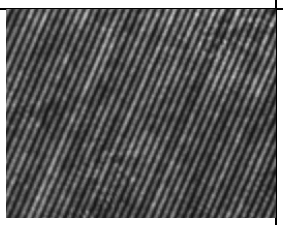	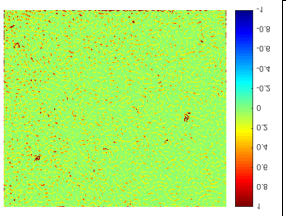	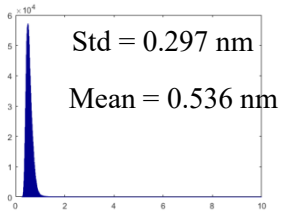	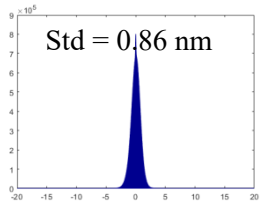
Flea3 FL3-U 3-32S2 M	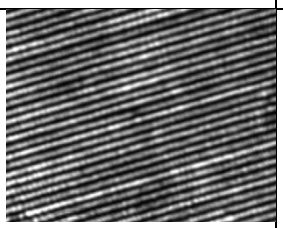	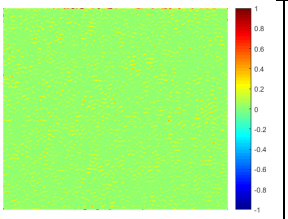	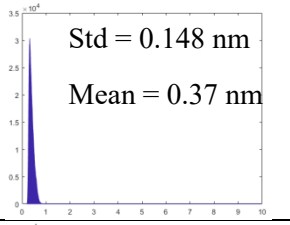	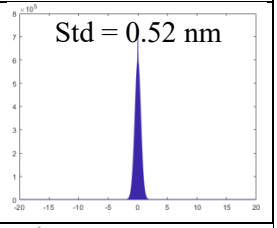
C1285 R12M	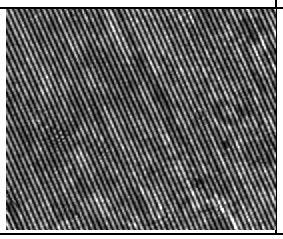	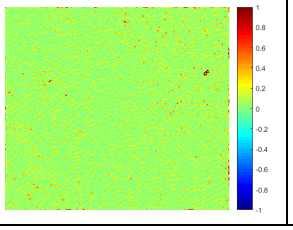	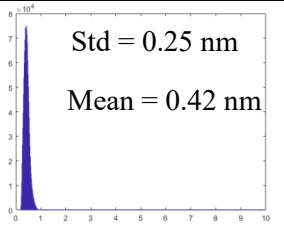	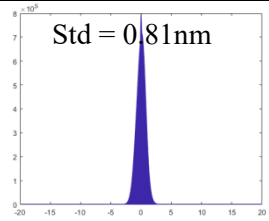

We have tested our system temporal and spatial noise with different types of cameras, and the results are summarized in Table 1. The noise is characterized through mean and standard deviation (Std) values. As shown, the values of temporal noise are less than 1 nm which indicates a high sensitivity has been achieved by our setup. We are also trying high well depth camera and high-speed camera with spatial and temporal average algorithms to further reduce the noise level.

3.3 Sample Testing

In order to validate the feasibility of our setup, we used standard 5um polystyrene beads for testing. We first capture a calibration image which does not contain the sample to subtract the background from the sample

image. Then we conduct phase retrieval procedure to obtain the phase map as shown in Fig. 4(a). During the procedure, a Fourier transform of the interferogram is obtained as shown in Figure 4(c). For both sample region and background image, a bandpass filter is used to extract the modulated signal, which is then brought back to the baseline. Figure 4(b) indicates the region of interest from Figure 4(a), and a line profile showing the height of sample is drawn in Figure 4(d). The results show that our system can quantitative measure the thickness of sample.

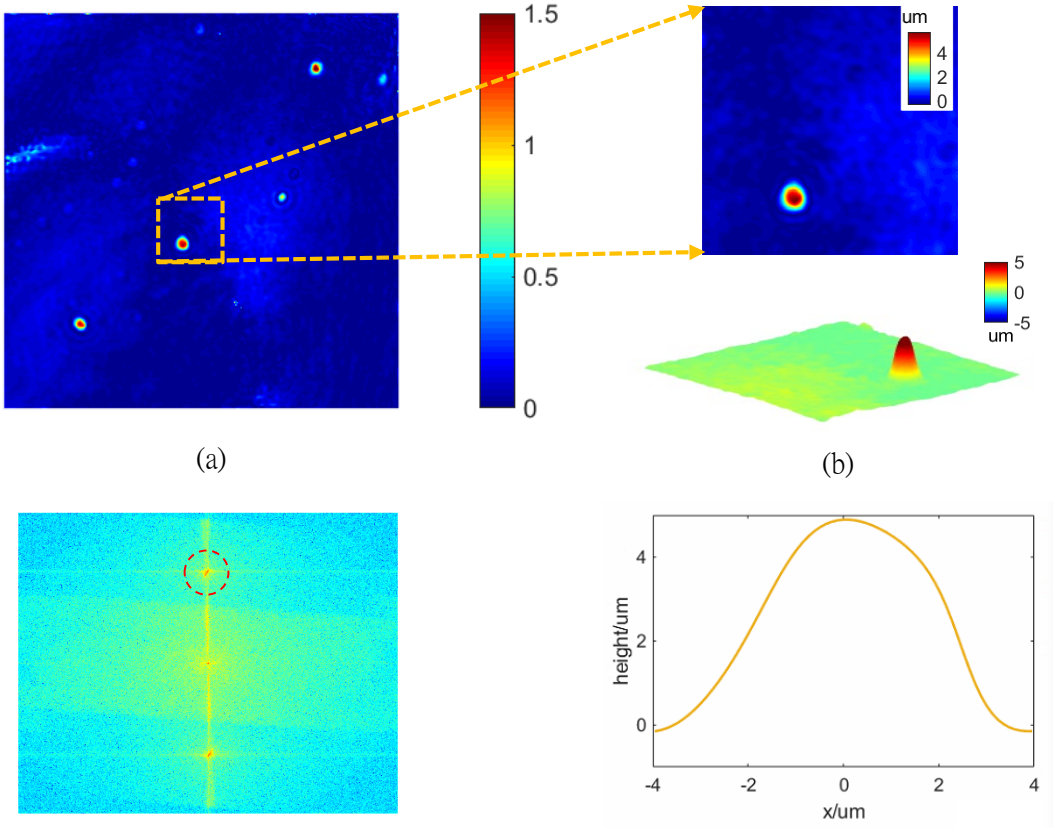

Fig. 4. DPM system validation. (a) Phase map of a captured interferogram; (b) a zoom-in height map of (a); (c) the Fourier spectrum modulus of the interferogram; (d) a line profile of the 5 μ m bead.

3.4 Wave-front shaping and phase cancellation

There are several modifications to a regular DPM system to allow for breaking the hardware limit on temporal sensitivity. Here we used an SLM in a digital optical phase conjugation (DOPC) system, which was then integrated with our DPM system for sample phase cancellation (as shown in Fig. 5). This integrated system was developed through a collaboration with Prof. Puxiang Lai's lab (Department of Biomedical Engineering at PolyU).

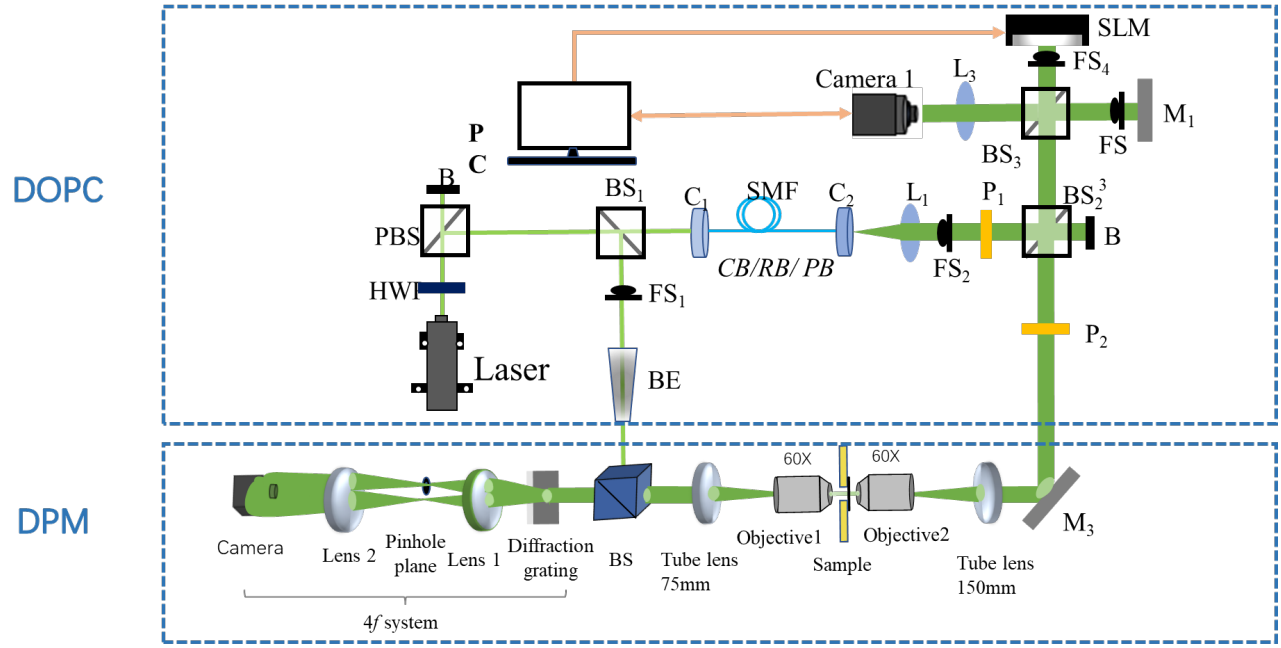

Fig. 5. The integrated system that contains digital optical phase conjugation (DOPC) and DPM.

First, a flat wave-front was first projected on the SLM, and then the phase of the sample is measured by the DPM system. We tested our system by measuring the phase and height map of the 5μm bead (as shown in Fig.6), and the result validated the performance of this integrated system.

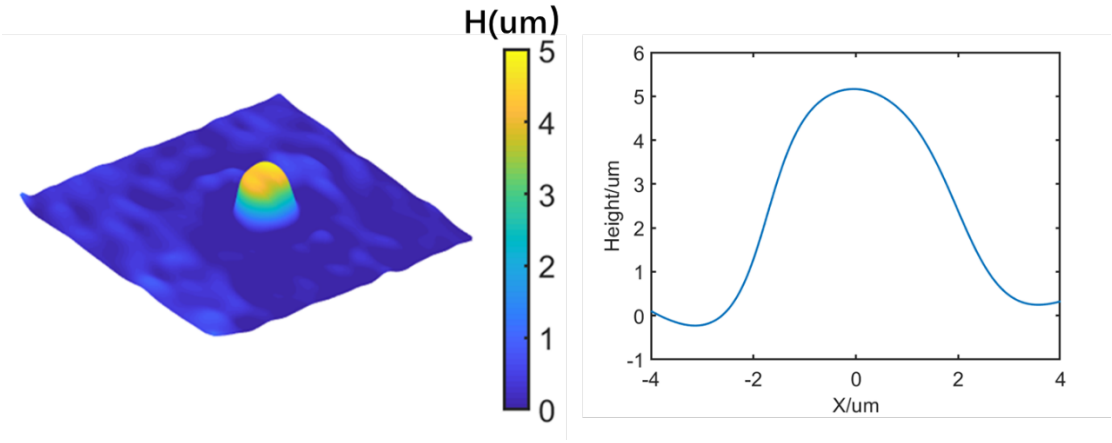

Fig. 6. The height map and line profile images of the 5um beads.

After that, the inverse phase of the sample was projected on the SLM before its phase was measured again with DPM. Finally, a relatively flat phase was measured that indicated the sample is “cancelled”. Figure 7 shows the validation results of achieving phase cancellation of a 5μm bead. We are currently working on implementing this system for imaging biological cells and then neurons.

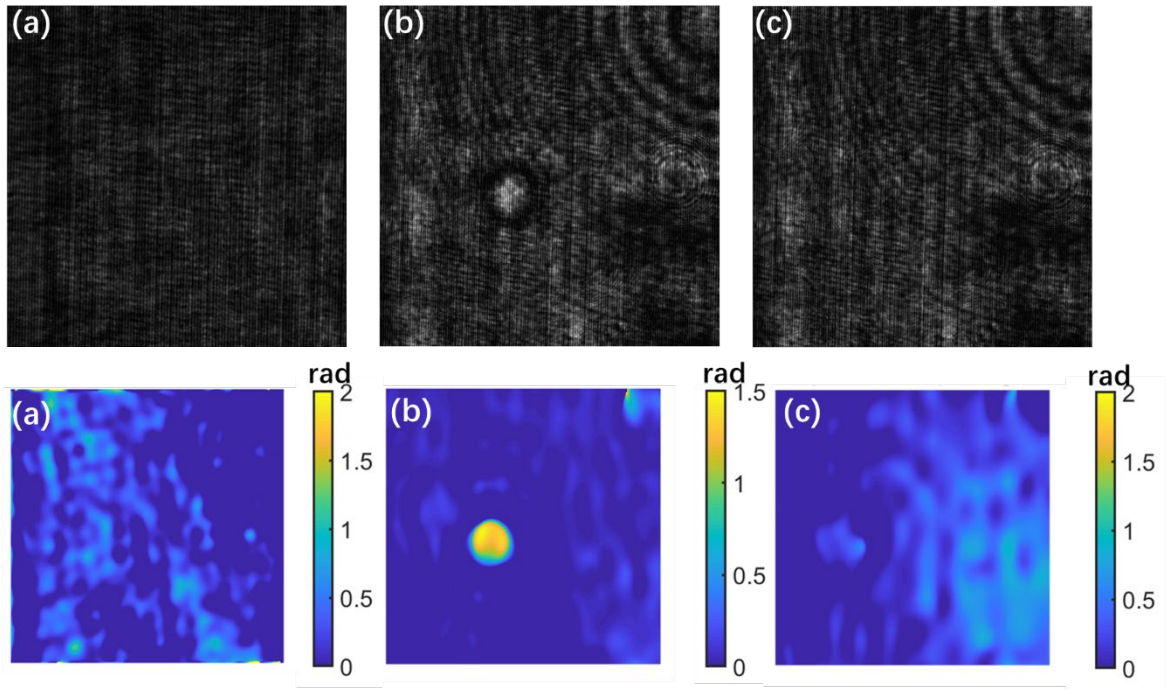

Fig. 7. Validation of using phase conjugation for cancellation the phase of a 5 μ m bead. (a) Background interferogram without sample; (b) interferogram with the sample moved to the field of view; (c) interferogram after conducting the phase conjugation experiment. (d), (e), and (f) correspond to the retrieved phase maps of (a), (b), and (c), respectively.

4. PUBLICATION AND AWARDS

[1] R. Pandey*, R. Zhou*, R. Bordett, C. Hunter, K. Glunde, I. Barman, T. Valdez, and C. Fincke, "Integration of Diffraction Phase Microscopy and Raman Imaging for Label-free Morpho-molecular Assessment of Live Cells," Journal of Biophotonics 12, e201800291 (2019). link * denotes the corresponding authors

WORK IN PROGRESS

DEVELOPMENT OF A NOVEL ROBOTIC MANIPULATOR FOR CONFINED SPACE SURGERY

Principal Investigator: Professor AU, Kwok Wai Samuel
Department of Mechanical & Automation Engineering, CUHK

Co-Investigator (if any): Prof. Philip Chiu[(2)]

Research Team Members:
Yuanpei Choi, PhD Student, Research Assistant [(1)]
H. Y. Yip, MPhil Student, Research Assistant [(1)]
Vincent Hui, Research Associate [(1)]

[(1)]Dept. of Mechanical and Automation Engineering, CUHK
[(2)]Dept. of Surgery, CUHK

Reporting Period: 1 July 2017 – 31 May 2018
(to be completed in June 2019)

INNOVATION AND PRACTICAL SIGNIFICANCE:

Although substantial progress has been made, existing flexible instruments still lack synergy among the core surgical enablers including the instrument accessibility, size, and surgical functionalities. The success of this project will provide a new mechanical and control framework for the development of robotic instrument that is capable of overcoming these limitations. This innovative robotic system enables surgeons to provide more accurate, effective, and less invasive procedure even for the complex cases such as skull base surgery, which are currently difficult to treat even with the state-of-the-art robotically assisted surgery. The proposed technology can also allow more patients suitable for and can benefit from MIS in these anatomical regions, ultimately, improving the quality of life of patients

ABSTRACT

Minimally Invasive Surgery (MIS) has been widely adopted in many surgical specialties. Still, for some hardly accessible anatomical regions, only limited options of MIS can be offered by physicians. Accessing these regions often require surgical tools passing through tortuous natural orifices. Yet, existing surgical instruments are predominantly straight and rigid with limited surgical capabilities.

Inspired by nature, a robot with dexterous flexible structure will allow us to address the aforementioned clinical challenges. Here, we focus on the development of the hardware design and intelligent kinematic-based control algorithms for dexterous flexible manipulator. These enabling technologies will be integrated together to set out a robotic platform for accessing and navigating tortuous, narrow spaces in the human that is not possible before. The platform should be versatile for the use in many minimally invasive procedures demanding for flexible access to confined anatomical areas, such as sinuses, base of skull, esophagus, bronchi, ureter, kidney, urinary bladder. To demonstrate the clinical efficacy and general practicality, we will perform the mock surgical procedures with the platform on phantom. The success of the development can offer significant benefits to the patients and open up a great opportunity for future technology transfer and commercialization.

1. OBJECTIVES AND SIGNIFICANCE

Robotic Minimally Invasive Surgery (MIS) has been widely adopted in many surgical specialties [1][2]. In 2016 alone, over 750,000 surgical procedures were performed world-wide using the da Vinci Surgical Robotic System [3]. Nevertheless, existing surgical robotic platforms are bulky in size, while their instruments are predominantly straight and rigid with a large diameter (dia.~8mm). These system limitations prevent the physicians to provide less invasive diagnostics and treatment to patients who have diseases in the hardly accessible anatomical regions (e.g. paranasal sinuses, base of skull, larynx, bronchi, and etc.) [4-7]. For example, in endonasal sinuses and skull base surgery (Fig. 1), physicians normally use straight and rigid tools to reach the target site through the nostril. Due to the limitations of the instrument dexterity, only a small fraction of patients (below 20%) are suitable for this surgery [4-7]. Patients with this disease opt to receive more invasive treatment that requires creation of surgical accesses through the patients' forehead or cheek such as lateral rhinotomy. These large, traumatic openings can create serious complications including double vision, retention of mucus that can lead to infectious complications, brain swelling, seizures and cheek disfigurement.

Inspired by nature, we know that dexterous flexible robot will be the technological pathway to address this fundamental clinical and robotic problem. There is a need to have a tiny flexible robotic manipulator that can navigate through the tortuous natural orifices and also offer superior dexterity and surgical capabilities to perform surgical tasks in a confined space. To achieve this goal, we focus on the development of the hardware design and intelligent kinematic-based control algorithms for dexterous flexible manipulator. These enabling technologies will be integrated together to set out a robotic platform for accessing and navigating tortuous, narrow spaces that are not accessible using existing methods. The platform should be versatile for the use in many minimally invasive procedures demanding for flexible access to confined anatomical areas, such as sinuses, base of skull, esophagus, bronchi, ureter, kidney, urinary bladder.

This success of the project will enable surgeons to provide more accurate, effective, and less invasive procedure even for the complex cases in the anatomical regions, which are currently difficult to treat even with the state-of-the-art robotically assisted surgery. The proposed technology can allow more patients suitable for and can benefit from MIS in these regions, ultimately, improving the quality of life of patients.

1. D. B. Camarillo, T. M. Krummel, and J. K. Salisbury, "Robotic technology in surgery: past, present, and future," The American Journal of Surgery, 188, pp. 2S-15S, 2004.
2. G. D. Hager et al., "Surgical and interventional robotics: Part III [Tutorial]," IEEE Robotics and Automation Magazine, vol. 15, issue 4, pp. 84-93, 2008.
3. Intuitive Surgical Annual Report 2016 (http://www.annualreports.com/HostedData/AnnualReports/PDF/NASDAQ_ISRG_2016.pdf)
4. P. Castelnuovo, I. Dallan, P. Battaglia, and M. Bignami, "Endoscopic endonasal skull base surgery: Past, present and future," Eur. Arch. Otorhinolaryngol., vol. 267, no. 5, pp. 649–663, 2010.
5. L. M. Cavallo, F. Esposito, and P. Cappabianca, "Surgical limits in transnasal approach to opticocarotid region and planum sphenoidale: An anatomic cadaveric study," World Neurosurg., vol. 73, no. 4, pp. 301–303, 2010.
6. J. Burgner et al. "A telerobotic system for transnasal surgery," IEEE Trans. Mechatron., vol. 19, no. 3, pp. 996–1006, Jun. 2014.

7. J. S. Chneider, J. Burgner, J. R. Webster, and P. T. Russell, “Robotic surgery for the sinuses and skull base: What are the possibilities and what are the obstacles?,” Curr. Opin. Otolaryngol. Head Neck Surg., vol. 21, no. 1, pp. 11–16, 2013.

2. RESEARCH METHODOLOGY

The proposed project consists of four main aims:

a. **Aim 1: Modeling of flexible instrument with coupled tendon drive.** In this phase, we will establish a framework of mechanics-based modeling for coupled tendon driven flexible instruments.
   i. ***Task 1.1: Develop Kinematics Models*** We will derive and explore different kinematics model for tendon-driven flexible instruments and investigate pros/cons and practicality for these models
   ii. ***Task 1.2: Analyze the effect of cable friction and compliance.*** We will extend the proposed models to consider the frictional and compliance effect in the cable transmission. We will analyze the corresponding performance degradation and hope to use that information for the design of feedback compensation in the future development.
   iii. ***Task 1.3: Simulation and experimental validation*** We will conduct simulation and experiments to validate our proposed models. We will characterize the instrument and identify the necessary model parameters experimentally.

b. **Aim 2: Design and fabricate complex hybrid-flexible robotic instrument** This aim is to investigate and fabricate different flexible instrument designs. During the design process, the PI and the Co-PI, Dr. Philip Chiu will establish a set of relevant design requirements. The PI will also seek the expert knowledge from collaborator, Dr. Zheng Li for instrument design and fabrication.

c. **Aim 3: Design a closed-loop controller for instrument control**, **based on the fusion of the measurement of the distal sensors, proximal motor encoder, and cable tension**. In this aim, we will develop a control framework that allows us to achieve high performance servo control as well as stable interaction with environment based on the fusion of sensing measurement.

d. **Aim 4. Evaluate the clinical efficacy of the proposed system** This aim is to evaluate the overall instrument system performance. We will integrate the proposed manipulator-instrument system with the da Vinci Research kit (dVRK) robot and setup the software to support the tele-operated instrument control. Co-PI, Dr. Philip Chiu and other physicians will be invited to evaluate the clinical efficacy of the system on a human phantom.
   i. ***Task 4.1: Construct an experimental actuation unit for flexible instrument prototypes.*** We will build and develop a computer-controlled actuation unit for testing the flexible instrument. The system will be capable of handling coupled tendon drive and supporting high bandwidth, output torque experiment and testing.
   ii. ***Task 4.2 Develop a proof-of-concept surgical robot system, integrating with the dVRK robot*** We will integrate the flexible manipulator system to our dVRK robot to offer tele-operated control for clinical evaluation.

3. RESULTS ACHIEVED SO FAR

- For Aim 1: We has been performed and various kinematics models have been developed and verified in both simulations and hardware of our initial flexible instrument. We also developed a novel friction model to explain the performance degradation in the tendon driven flexible instrument and initial experiments were performed to verify the results.
- For Aim 2: We has designed and constructed initial hybrid flexible instrument prototypes for investigation. More design iterations will be required to further improve the instrument performance.
- For Aim 3: Initial closed-loop kinematics control study of flexible instrument was performed. Significant performance was observed. More advanced closed-loop controller will be designed in the next phase of development.
- For Aim 4: We have constructed the experimental actuation unit for flexible instrument prototypes. We also integrated with a basic flexible instrument with dVRK and the corresponding kinematics model was implemented into the same software framework. Basic tele-operated control for the initial flexible instrument was performed.

4. PUBLICATION AND AWARDS

[1] X. Y. Chu, T. Y. Chung, and K. W. Samuel Au., "A Systematic Modelling Approach for Motor-Cable-Joint Kinematics of Coupled Tendon-Driven Surgical Instrument," Hamlyn Symposium on Medical Robotics, June 2018 (Accepted)

[2] K. LU, H. B. Lin, C. W. Vincent Hui, and K. W. Samuel Au "A Case Study of Gravity Compensation for da Vinci Robotic Manipulator: A Practical Perspective," ICRA18 workshop on Supervised Autonomy in Surgical Robotics, May 2018.

[3] K. C. Lau, Yuanpei Cai, Y. Yam, and K. W. Samuel Au, "Comparison Study of Geometric Representation for Continuum Manipulator," ICRA18 workshop on Supervised Autonomy in Surgical Robotics, May 2018.

WORK IN PROGRESS

DEVELOPMENT OF AN INERTIAL MICROFLUIDICS BASED APPROACH FOR THE ISOLATION OF MITOCHONDRIA FROM BIOLOGICAL SAMPLES

Principal Investigator: Professor Megan Yi-Ping HO
Department of Biomedical Engineering, CUHK

Research Team Members:
Shirui Zhao, Shun Hing Fellow[(1)]
Md. Habibur Rahman, PhD Student[(1)]
Qinru Xiao, MSc Student[(1)]
Tinna Stevnsner, Associate Professor[(2)]
An-Chi Wei, Assistant Professor[(3)]
Chen Chang, Master Student[(1)]

[(1)]Department of Biomedical Engineering, CUHK
[(2)]Department of Molecular Biology and Genetics, Aarhus University, Denmark
[(3)]Graduate Institute of Biomedical Electronics and Bioinformatics, National Taiwan University, Taiwan

Reporting Period: 1 July 2017 – 31 May 2018
(to be completed in July 2019)

INNOVATION AND PRACTICAL SIGNIFICANCE:

Defective mitochondria have been linked to several important human diseases, that urgently calls for the fundamental understanding of the disease mechanisms. To this end, presented here is a previously unavailable strategy enabling a fast and cheap isolation of mitochondria from samples of clinically relevant sizes. The proposed technology is revolutionary, yet highly transformable to a commercial product for routine clinical investigations and biological studies. Therefore, the developed platform will have a broad appeal to the pharmaceutical and clinical sectors targeting mitochondrial diseases. Table 1 summarizes the practical cost and expected performance for the isolation of mitochondria using the inertial based approach compared with other commercially available kits.

Table 1. Comparison between the Inertial Based Isolation of Mitochondria and the Commercially Available Kits.

	Inertial Based	Thermofisher	Abcam	Qiagen
Assay Time (Post-Lysis)	10 min	40 min	>30 min	>45 min
Required Cells	100	2×10^7	4×10^7	5×10^6
Bench Top Availability	Yes	Yes	Yes	Yes
Purity	High	High	High	High
Required Reagent Exchange	No	Yes	Yes	Yes
Price Per Isolation (HKD)	20	45	97	296

ABSTRACT

This project aims to develop a novel approach to rapidly isolate mitochondria from samples of clinically relevant sizes. While currently available methods are mostly laborious and not suitable for small-scale analyses in the clinics, the proposed approach is able to handle 200 microliters of sample and process the isolation within 30 minutes. Aside from the possibility for small-scale analysis, the proposed approach offers many distinct features, including the simple procedures, undemanding equipment request, minimal damages to the isolated mitochondria, and continuous batch processing. Possibilities to analyse mitochondria from a limited amount of clinically relevant patient samples are expected to expand our knowledge towards the basic biological mechanisms of mitochondrial function, and to elucidate how mitochondria are involved in the development of diseases such as cancers, premature aging syndromes, diabetes and neurodegenerative disorders. For instance, it becomes practical to obtain mitochondria from the patient samples, and to elucidate how defective mitochondria link to the mitochondria-associated diseases. Furthermore, the isolation principle may be tailored for an array of subcellular fractions, rendering more efficient identifications and characterizations of intracellular organelles of interest and, consequently, advancing the study of biology and medicine continuously.

1. OBJECTIVES AND SIGNIFICANCE

1.1. Objectives

- To optimize and fabricate the inertial microfluidic chip for the isolation of mitochondria
- To demonstrate effective recovery of mitochondria using purified mitochondria as a model
- To develop a series of protocols for the characterization of isolated mitochondria
- To revise the design chip for a rapid isolation of functional mitochondria from crude human cell lysates of a clinically relevant sample size

2. RESEARCH METHODOLOGY

2.1. Task 1: Optimization of the Microfluidic Chip Using Purified Mitochondria

We have designed and fabricated the chip capable of separating polystyrene particles of 1.9 μm and 7.32 μm (Figure 1a). The inertial lift and so-called Dean drag forces collectively render particles of different sizes to migrate differently along the channel width. More specifically, mitochondria of smaller sizes compared to other cytosolic fractions (i.e. nuclei and cell debris) migrate to the outer half of the channel, whereas the larger cellular organelles move to the inner half of the channel. The size-dependent equilibrium position is determined by the inertial forces of the particulates and the Dean vortices generated by the spiral channel geometry. Prior to the start of this project, we have optimized that the design to direct up to 90% of mouse liver mitochondria (provided by Aarhus University) into the targeted outlet. Due to the heterogeneous nature of mitochondria, the microfluidics design (channel geometry) and the operating flow rates have been optimized empirically as shown in Figure 1b.

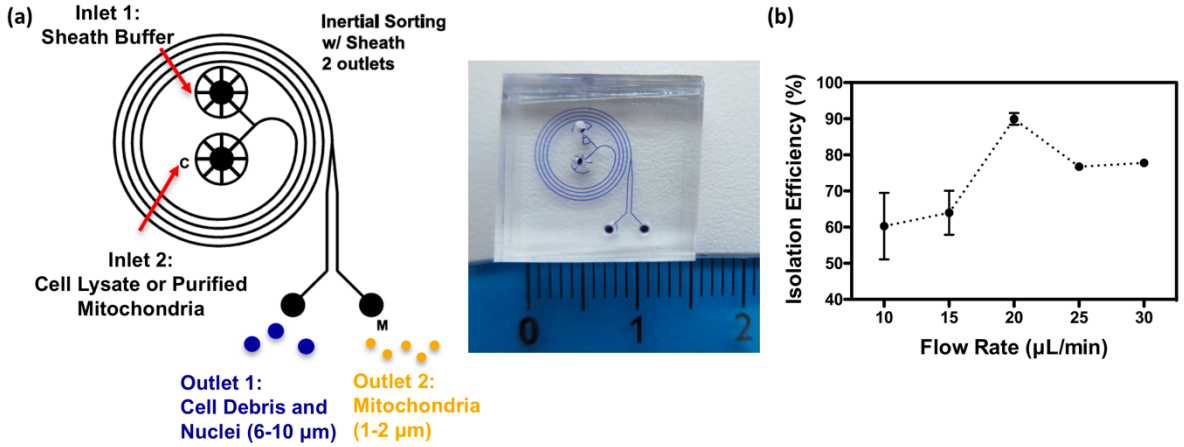

Figure 1. (a) Schematic showing the design of the chip. (b) Optimization of flow rates using purified mitochondria.

2.2. Task 2: Characterization of the Isolation Performance

As a parallel effort of Task 1, we have established relevant characterization techniques to evaluate (1) the isolation efficiency, (2) the isolation purity and (3) the mitochondrial functionality.

(1) The isolation efficiency: As a fast method to quantify the amount of retrieved functional mitochondria isolated by the microfluidic chip, the active mitochondria are stained with a commercially available fluorescent dye, MitoTracker™ Red FM. This red-fluorescent dye accumulates in mitochondria with a membrane potential - a hallmark for functional mitochondria. We have established the protocols by measuring the total fluorescence intensity (ex. by a fluorimeter).

(2) Isolation purity: Western blotting analysis will be performed to check the purity of the isolated mitochondria. The Ku86 protein will be used as the marker for the nuclei, while Tom20 will be used to identify the mitochondrial specific protein. The isolation purity will be determined by comparing the fractions of the two proteins from samples retrieved from the two outlets.

(3) The mitochondrial functionality: To further validate whether the retrieved mitochondria retain their biological functionality, mitochondrial generated reactive oxygen species (ROS) from unsorted and sorted mitochondria will be measured by a fluorescently labelled probe 2',7'-dihydrodichlorofluorescein (DCFH) which emits an intense green fluorescence upon deacylation and subsequent oxidation. ROS, as a typical product of cellular metabolism, are mainly generated by mitochondria. Therefore, the measured fluorescence intensity of DCFH may serve as an indication of the mitochondrial functionality after isolation.

2.3. Task 3: Optimization of the Chip Design for Crude Biological Samples

Due to its large diversity, isolation of mitochondria presents a tangible challenge when it comes to separating this organelle from other cellular components. The subsequent task is to optimize and validate the chip design for handling biological crude sample. Human embryonic kidney cells (HEK293) are used as a model cell line. Crude cell lysate will be prepared following standard protocols. Briefly, the cells will be homogenized by lysing the cell membranes in a hypotonic buffer followed by mechanical disruption with a Dounce glass homogenizer. Samples from the two individual outlets are collected without further post-processing and then analysed by the characterization techniques developed in Task 2. Based on the MitoTracker™ Red FM staining, current isolation efficiency is around 75% from crude cell lysates. Further investigation will be conducted using other cell lines of high metabolic requirements, such as mouse muscle cells (C2C12).

3. RESULTS ACHIEVED SO FAR

3.1. Isolation of mitochondria from crude cell lysates

Through pre-processing, namely cell lysis by Dounce homogenization, current chip design is able to isolate 75% of functional mitochondria with 200 microliters of crude cell lysates in 20 minutes (Figure 2a). In the second year, this project will focus on the characterization of isolated mitochondria by validating the isolation purity and further investigation of the functionality of isolated mitochondria as discussed in Task 2.

As observed in Figure 2b, the isolation efficiency decreases as the cell concentration increases. This is not surprising because the excessive cellular contents may affect the flow profile, rendering less optimal sorting (i.e. 3540 cells/μL). Therefore, further emphasis will also be placed on improving the isolation yield (i.e. the total amount of isolated mitochondria) by enabling the processing of higher concentration of samples.

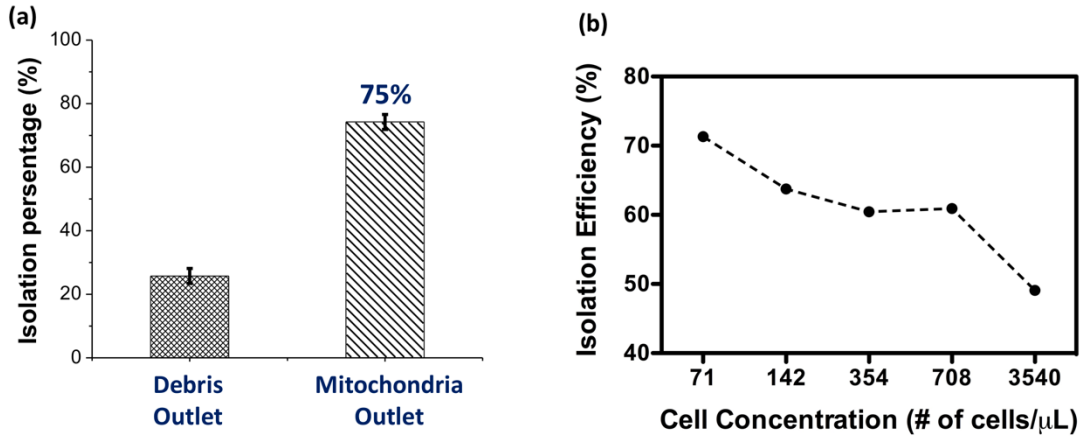

Figure 2. (a) Mitochondrial isolation efficiency of the current design. (b) Negative correlation of the cell concentration and isolation efficiency.

3.2. Optimization from the perspective of cell pre-processing

Dounce homogenization has been the most widely used method for breaking up the cell membrane, however, the level of shear is largely determined by the clearance between the pestle and the mortar, as well as the number of strokes and grinding speed. The poor reproducibility due to the operational variation poses a significant challenge for the continuous optimization of our device's isolation efficiency. To fundamentally resolve the limitation, we have moved forward and designed a microfluidic device to extract mitochondria directly on-chip. Preliminary results have shown promise in processing small amount of sample with high retrieval efficiency (Manuscript in Preparation). We plan to integrate both the extraction and isolation modules on-chip as an all-in-one processing strategy for mitochondrial extraction. Furthermore, similar strategy is also expected to adopt for the isolation of other subcellular organelles, such as autophagosomes.

3.3. Future Perspectives

Preliminary data obtained under the support of this project has served as the foundation of the following submitted grant proposals:

- RGC General Research Fund (GRF): "On-Chip Extraction and Isolation of Mitochondria and the Subsequent Characterization of Mitochondrial Subtypes" (Ref. no.: 14201518), PI: Megan Yi-Ping Ho (Result pending)
- Columbus Program, Ministry of Science and Technology (MOST), Taiwan: "Integrative Platform of Mitochondrial Toxicity Screening" (Ref. no.: 107WFA0110185), PI: An-Chi Wei, Co-I: Megan Yi-Ping Ho (Funded)

4. PUBLICATION AND AWARDS

C[1] C. Chang, Y. P. Ho and A. C. Wei, "Computational Modeling of Mitochondrial Metabolism and Dynamics in Ageing, " *The 1st International Mitochondria Meeting for Young Scientists*, Kyoto, Japan, 2018.

Note: Chen Chang has been awarded a Young Investigator Scholarships by the YongMito Program: http://www.fbs.osaka-u.ac.jp/YoungMito2018/YoungMito2018/Scholarships_%26_Awards.html

COMPLETED

AN MRI-GUIDED ROBOTIC SYSTEM FOR BREAST BIOPSY

Principal Investigator: Professor Yun-Hui LIU
Department of Mechanical and Automation Engineering, CUHK

Co-Investigator:
David Navarro-Alarcon[2], Defeng Wang[3], Hayley Louise Chung[4], Terrance Chan[5]

[1] Dept. of Mechanical and Automation Engineering, CUHK
[2] Hong Kong Polytechnic University
[3] Dept. of Imaging and Interventional Radiology, CUHK
[4] Time Medical Systems Ltd.,
[5] North District Hospital

Project Start Date: 1 July 2016
Completion Date: 30 June 2018

ABSTRACT

In the United States, breast cancer is the second most common cause of cancer mortality in women. In China alone, around fifty-five thousand women die from breast cancer each year. To determine whether a growth of breast tissue is cancerous or not, a biopsy is conducted to extract and analyse sample cells from the suspicious area. In this research project we aim to develop a new robotic manipulator which can accurately insert the biopsy needle into the target lesion. The trajectory of the robot will be guided with real-time visual feedback from a magnetic resonance imaging (MRI) scanner. To operate the robot inside the scanning room, the mechanical structure of the robot will be fabricated with MRI-compatible materials such as titanium and nylon, and a combination of pneumatic and piezoelectric actuators (which comply with the non-magnetic requirement) will be used to drive the motion of the mechanism. Compared to the traditional manual biopsy, the proposed image-guided biopsy system will considerably improve the accuracy of the needle insertion, shorten the overall procedure's time and reduce the trauma inflicted to the tissues. This research project has clear potential for future commercialisation of the obtained outputs.

1. OBJECTIVES AND SIGNIFICANCE

Motivation. Breast cancer is the most common type of invasive cancer among women in the world (Jemal 2011). High incidence rates are traditionally associated with economically developed countries, however, in the past decades many developing nations have experienced an increasing incidence rate of this form of cancer. In 2012, 187,000 cases were diagnosed in the mainland China (Zeng 2014; Wang 2015), which accounted for almost 12% of the world's total new cases. The incidence in urban areas in China currently shows an annual increase of 3.7%, an alarming trend that threatens with enormous economic impact to the Chinese society. To improve the disease's survival rate, it is essential to accurately detect cancerous tissue growths in early stages by performing a breast biopsy (which extracts sample tissues from the suspicious area for later analysis). This procedure is typically conducted in a minimally invasive manner by introducing a biopsy needle into the tissues and guiding it with some medical imaging system such as MRI. Compared to ultrasound and mammogram, MRI has a better detection rate and tissue contrast (Saslow 2007), and does not exposes the patient to harmful radiation, e.g. from x-rays.

Current practice and its complications. In traditional MRI-guided breast biopsy, the patient is

first placed in a prone position with her breast tightly immobilised with a fixation mechanism (commonly referred to as the grid). Next, the patient is introduced into the MRI bore and a first diagnosis scan is performed to locate the lesion and to calculate the needle's insertion coordinates. Then, the patient is removed from the bore and a coaxial needle is introduced into the tissues to reach the target. The patient is once again placed inside the bore and a second MRI scan is performed to corroborate the needle's location (Liberman 2005). If this scan reveals that needle is deviated from the target, further needle adjustments and scans must be performed. Note that the insertion of biopsy needles remains up to this day a manual procedure that requires several iterations to properly position it inside the tissues. This manual procedure is time-consuming as multiple scans and "in/out" from the bore are required, and potentially increases the trauma inflicted to the tissues since the needle's position needs to be adjusted.

Original contribution. As an innovative solution to the above stated problems, in this project we propose to develop a new computer-controlled robotic system which automates the complex needle insertion task. Compared to the current practice of MRI-guided breast biopsy, the proposed robot will improve the procedure by:

1. Eliminating the need to move the patient in and out of the magnetic bore multiple times (this will result in faster, therefore, more economical procedures),
2. Guiding the needle's insertion trajectory with computer controls and real-time MR images (this will result in a more accurate needle positioning compared to a hand-held manual insertion),
3. Reducing the number of needle re-insertions and adjustments needed to reach the target (this will result in a reduced stress and discomfort to the patient), and
4. Enabling the real-time confirmation and visualisation of the needle's tip location.

Project challenges. There are several challenges in developing this type of robotic system. First, the high magnetic field used by MRI scanners imposes strict requirements to the types of materials that can be used in a robot operating inside the magnetic bore. This imaging technology strictly prohibits the use of ferromagnetic metals such as stainless steel (which is the most commonly used material in robot mechanisms). Second, the intense magnetic field also restricts the types of actuators and sensors that can be used to control the motion of the robot. Note that traditional electrical motors cannot be used since their working principle is based in the electromagnetic effect, which produces significant visual artifacts. Also, conventional sensors tend to include ferrous materials which will also affect the imaging process. Third, closed bore (cylindrical) MRI scanners have very limited in-bore space to laterally accommodate a needle manipulator alongside the patient. Note that the robot must to be able to perform needle insertions from a lateral direction since most breast lesions (around 62%) are located in the breast's outer-upper quadrant zone (Lee 2005).

Significance: The novelty of the robot that we propose is its capability to automatically drive the needle into the target lesion without the need to remove the patient from the magnetic bore. This innovative feature will allow radiologists to considerably reduce the procedure's time and cost. This objective can be achieved through the collaboration of the CUHK team (which has extensive experience in the design, development and image-based control of medical robots) and Time Medical Systems (which develops MRI scanners and therefore can customise a machine for robotic applications).

References

- Jemal A et al (2011), "Global cancer statistics", CA Cancer J, 61(2): 69-90, 2011
- Zeng H et al (2014), "Female breast cancer statistics of 2010 in China: Estimates based on data from 145 population-based cancer registries", J. Thoracic Disease 6.5: 466–470, 2014

- Wang F and Yu Z (2015), "Current status of breast cancer prevention in China", J. Chronic Diseases and Translational Medicine, vol. 1, issue 1, 2-8, 2015
- Saslow D et al (2007), "American cancer society guidelines for breast screening with MRI as an adjunct to mammography", CA Cancer J Clin, vol. 57, pp. 75–89, 2007
- Liberman L et al (2005), "MRI-guided 9-gauge vacuum-assisted breast biopsy: Initial clinical experience" Am. J. Roentgenol, vol. 185, no. 1, pp. 183–193, 2005
- Lee AH (2005), "Why is carcinoma of the breast more frequent in the upper outer quadrant? a case series based on needle core biopsy diagnoses", The Breast, vol. 14, no. 2, pp. 151–152, 2005

2. RESEARCH METHODOLOGY

Design of MRI-compatible robots. Our aim in this project is to build a robotic system which can perform needle insertions within the magnetic bore. To guarantee the MRI compatibility of the system, we will develop a non-magnetic mechanism that is entirely driven by pneumatic actuators and whose configuration is measured by optical signals only. This innovative design will allow us to control the robot without sending any electrical signals in/out of the MRI shield room.

Based on our pilot study, we will first optimise the preliminary design and then build the first prototype. To perform the needle insertion task, the system must have the following functional requirements: (a) The robot must be able to insert a biopsy needle into the breast tissues from a lateral configuration inside the scanner's magnetic bore. (b) The robot must be able to control the 3D position of the needle with an [x,y,z] motion range of [75,130,100] mm. (c) The structure of the robot, its actuation mechanisms, and its feedback sensors must all be MRI compatible, that is, they must not affect the image quality.

To fulfil the above functional requirements, we propose to build a new robot specifically customised for breast interventions which has the following key features:

- Structure. To accommodate the robotic needle driver alongside the patient, we will develop a mechanism with a compact size that distributes the main structure and its actuators horizontally, effectively optimising limited space within the scanner's bore. The proposed mechanism will have a Cartesian-like configuration composed of 3 linear DOF that independently control the x-y-z displacements of the needle. For the x-axis, a combination of a non-magnetic slides, an aluminium power screw and a nylon nuts mechanism are used to distantly transmit the motion from the actuators; we plan to use the power screw because it can provide a slow and accurate motion.
- Actuation. In this project, we plan to use pneumatic motor because they present the best SNR properties amongst all MRI-compatible actuation systems. To drive the motion of the robot, we will develop a new type of pneumatic actuator which is based on the Tesla turbine. A Tesla turbine is a bladeless turbine, consisting a set of smooth disks inside. When the compressed air flows in through the inlet nozzle, it spirals into the centre exhaust and creates a vortex. Inside the vortex, the viscosity of air will create a drag force on the disks surface, which in turn results in the expected rotary motion of the shaft. Double-acting pneumatic cylinders (made of plastic to guarantee the magnetic compatibility) will also be used in the robot to drive the insertion motion of the needle.
- Procedure. The proposed robotic system will be specifically designed to manipulate the "coaxial introducer sheath with the stylet". In breast biopsies, this needle device is used for two main purposes: (i) to perform the initial puncture to the tissues that drives the needle to the target lesion, and (ii) once this desired location has been reached, this coaxial sheath is used to support the biopsy gun which removes the tissues.

Development of the MRI-guided motion controller.
The controller of the robot will be composed of two main parts: a (low-level) motion control system which regulates the actuation mechanisms, and a (high-level) trajectory tracking controller which guides the needle with MRI feedback. The former part represents control hardware such as pneumatic servo-valves and motion controllers that is needed to drive the actuators. The latter part represents numerical control algorithms such as filters and adaptive estimators that are needed to plan/guide the needle's trajectories. In the robotic system that we propose, the insertion displacement of the biopsy needle will be servo-controlled with continuous MRI feedback. To accomplish this task we will use a double-acting cylinder, which has two air transmission lines to command the motion of the rod in both forward and backward directions; single-acting cylinders cannot be used in MRI applications since they rely on metallic springs to retract the rod to the backward position. For precise positioning, we will also install a position sensor to this linear joint which will also be used to estimate the joint's velocity. We plan to use a 5/3 pressure-proportional valve to accurately servo-control the needle in intermediate positions. To prevent degrading the image quality, the circuitry and sensors must be shielded and located at a safe distance from the scanning bore. To control the x-y motions, we will use two rotational piezoelectric motors.

3. RESULTS ACHIEVED

With the funding provided by SHIAE, we have achieve the following two main outputs:

1 Robotic prototype. We developed a new robotic prototype which can insert the biopsy needle into breast tissues while operating inside the scanner's bore. The magnetic compatibility of the developed pneumatic insertion mechanism allows it to be used even during continuous imaging. The robot has a compact mechanical structure that allows it to perform both frontal and lateral insertions inside an open bore scanner (to the best of our knowledge, the proposed robot is amongst the first to address this crucial dimensional issue by using a Cartesian mechanism). To command the robot's motion, we developed a robust control method which combines the feedback from multiple sensor modalities; the controller's stability has been rigorously analysed using energy-based theory.

To fulfil the above given design requirements, we propose to develop a robot consisting of three active linear joints for needle positioning and insertion motions (note that the proposed system is only suitable for open bore configurations). This 3-DOF design in intended to replicate the linear motions of a manual biopsy using the grid method. Fig. X conceptually depicts the details of proposed 3-DOF mechanism. To achieve stable motion, Del-Tron non-magnetic slides (made of aluminium, silicon nitride, graphite) are installed on each active axis. An aluminium power screw (Abssac) with a nylon nut is used in the x-axis to transmit motion from actuator to the joint. Two parallel slides are installed on the y-axis to provide stable support to the biopsy gun from both sides; this vertical axis uses a brass rack and pinion to transmit the motion from the actuator to the joint.

The first two DOF of this system serve to align the needle's axis with the target lesion. To command the motion of these joints, two non-magnetic piezo motors (GTUSM60, Jiangsu Glittering Orient Ultrasonic Motor Co.) are installed; these actuators provide a torque output of up-to 1 Nm. The z needle insertion axis is attached between the parallel slides. To measure the robot's configuration, Spectra Symbol position (resistive) sensors are installed in all three joints, whose signals are measured using shielded cables. Most of the structure is 3D printed with some transmission and support components made of aluminium and brass.
The mechanism that drives the needle into the tissues is actuated by a double-acting pneumatic cylinder (an Airpel from Airpot). This linear actuator is fully non-magnetic, since its housing, piston

rod, and all of its components are fabricated using plastic and/or brass. The insertion mechanism is attached to the parallel slides of the vertical axis (i.e. the y direction). This structure provides support to the biopsy gun from both sides (in our model we consider a 230 mm ATEC biopsy system from Hologic), which results in an increased stability of the system. The axis' slide has a linear travel range of 75 mm, which is used for providing smooth pushing/pulling motions to the piston rod. The width of the mechanism is small enough to accommodate the biopsy gun and pneumatic cylinder side by side.

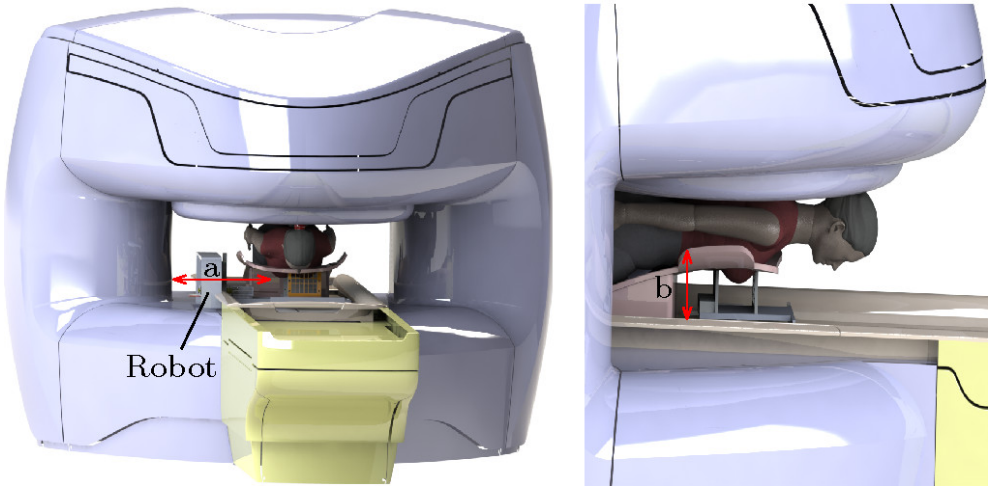

Figure 1 Conceptual model of the robotic system

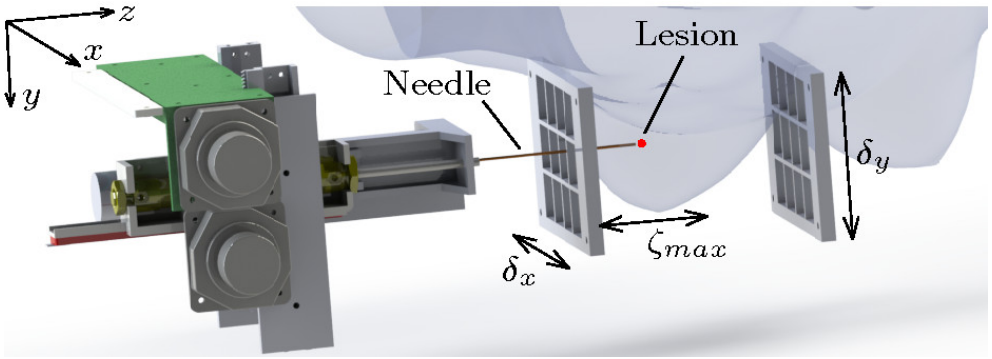

Figure 2 Details of the needle driving mechanism

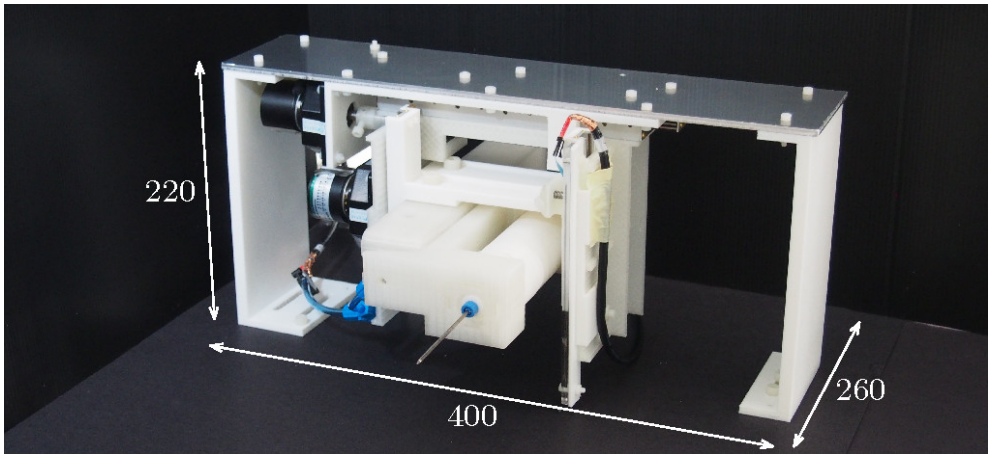

Figure 3 The developed 3 axis robotic prototype

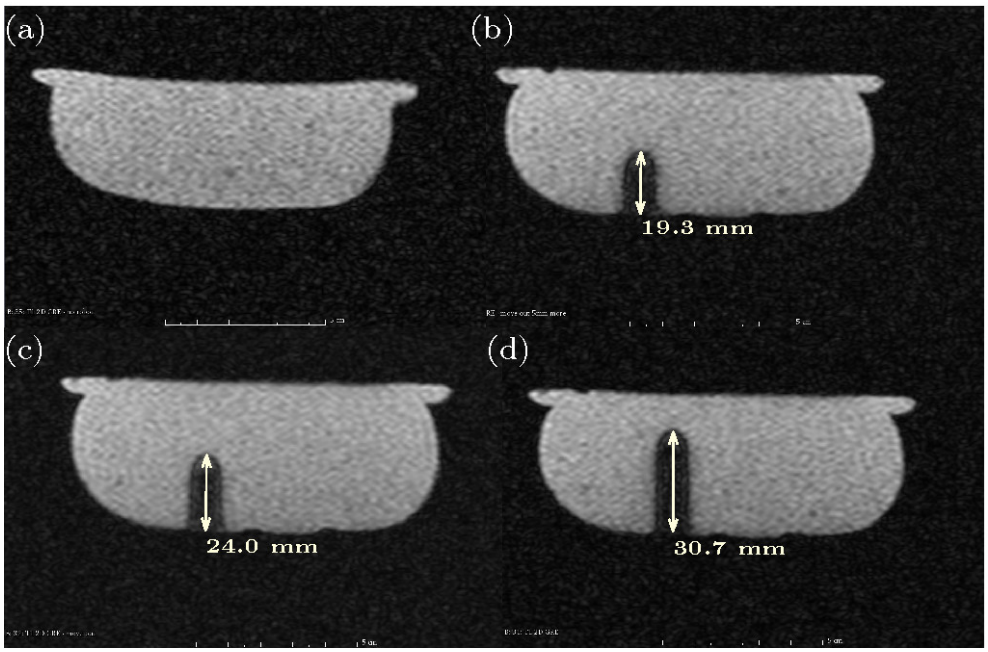

Figure 4 Experiments with phantom tissues under continuous MRI scans

2 MRI-compatible pneumatic actuator. We have developed a new MRI-compatible pneumatic actuator that allows to effectively generate continuous smooth rotary motions. The basic mechanical structure of this new system is based on the Tesla turbine. To guarantee that it can operate under continuous MR imaging, it is fabricated using 3D printing technology, and its angular position is measured using fibre optics. Experiments are conducted to verify the motor's MRI-compatibility and performance.

The actuator's motion principle is based on the Tesla turbine, which was developed by Nicola Tesla in 1905 as a hydroelectric power generator. The proposed motor is a blade-less turbine that operates based on the boundary layer effect of the driving fluid. It consists of a set of several smooth disks separated by a small gap, and that are fixed together to central rotating shaft. Each disk is provided with four exhaust holes that are placed near to the disk's centre. When compressed air flows into the motor through the inlet nozzle, it spirals around the shaft and moves towards the exhaust ports creating a vortex. The fluid vortex induces a drag force over the disks' surface, that results in rotational motion of the motor shaft.

Our objective is to develop an MRI-compatible actuator that can operate within the magnetic bore. Therefore, in the design and fabrication of the motor it is important to select non-magnetic materials for its components. The motor's structure was 3D printed with PLA (polylactic acid) using a standard 3-axis printer in our laboratory; only the disks and spacers were printed by resin using SLA (stereo-lithography) printing. The disks were fabricated with this latter method since it produces a much smoother surface that helps to create stable airflow for driving the motor. The disks printed with PLA have a much rougher surface, even when using the smallest layer achievable by our 3D printer (0.06 mm in our case); if this method used to build the motor, the rough finishing causes unsteady airflow that affects the motor's performance. It is important to remark that since the disks are fabricated with plastics, they have less rigidity and strength compared to metal-based disks (they may be susceptible to bending when the compressed air first strikes the disk next the inlet port). For our MRI robotics application, we use non-magnetic metals (viz. brass and aluminium) only for a few essential support and driving components. By using this type of metals, we aim to reduce the overall magnetic susceptibility of the actuator.

The basic design of a Tesla motor is characterised for generating a high rotational speed with a low driving torque. In laboratory tests, sensor feedback shows that the developed motor can achieve a rotational speed of around 13000 RPM when driven by compressed air of 4 Bar. To use this motor in a robotic mechanism, we must first modify its speed and torque properties. For that, we developed an custom-made MRI-compatible gearbox with a 1:60 gear reduction (some of the components of this gearbox are fabricated with brass and not plastics so as to improve its strength). The gearbox is built with worm gears for the following reasons: (1) it provides high gear ratio that effectively increases torque and reduces the output speed; (2) it provides a self-locking feature (i.e. it is non back-drivable) that improves stiffness and prevents undesired motions when disturbances arise; (3) it has a simpler structure with fewer components than e.g. planetary gears with the same reduction ratio.

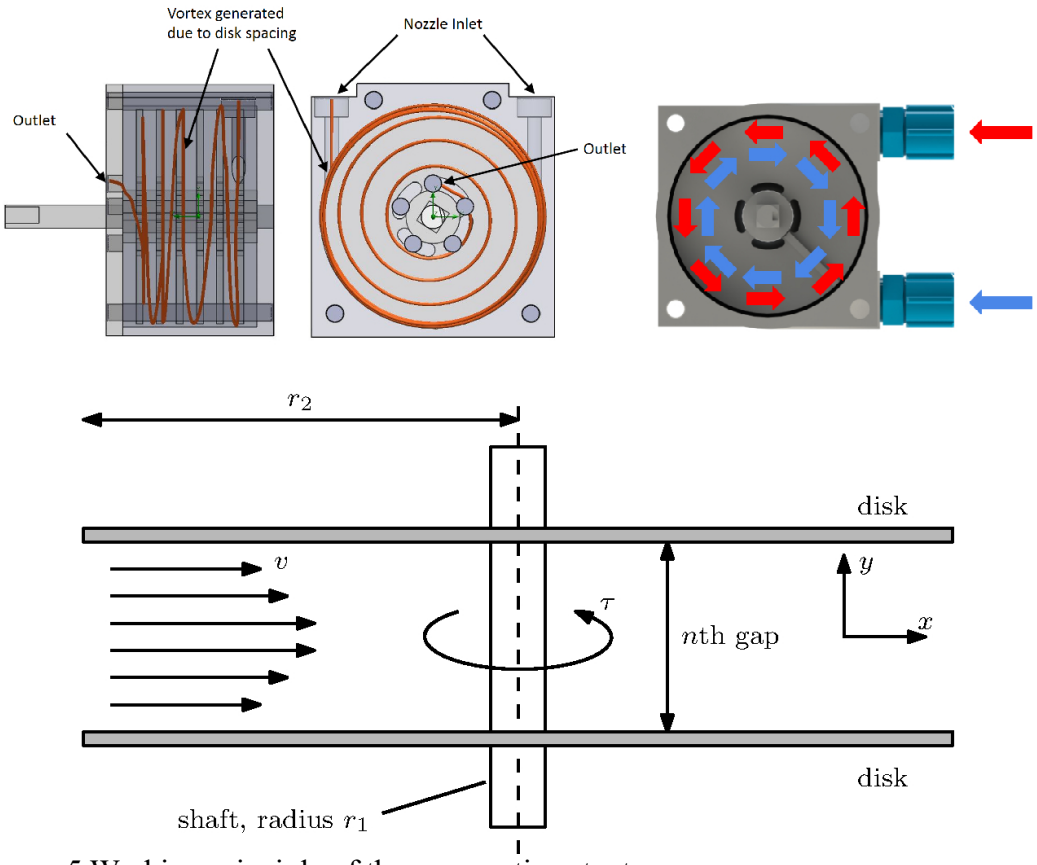

Figure 5 Working principle of the pneumatic actuator

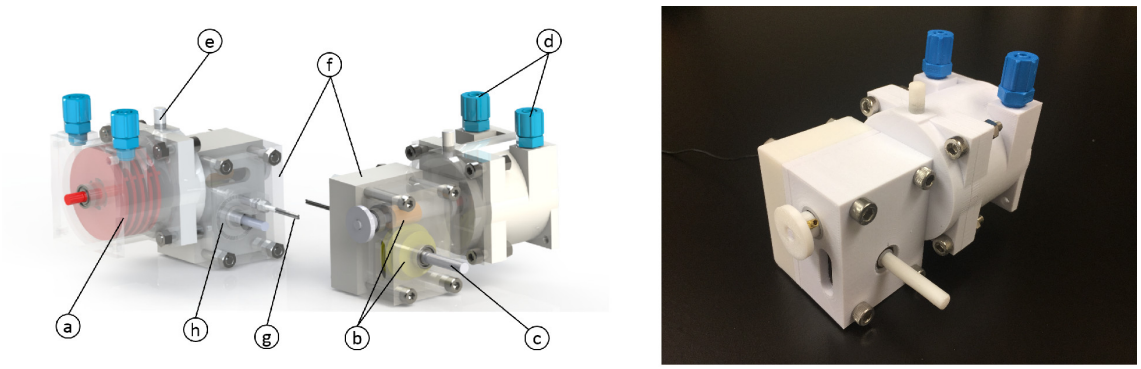

Figure 6 (Left) Schematic drawing of Tesla motor: (a) disks assembly, (b) worm gears, (c) output shaft, (d) inlets ports, (e) silencer, (f) optical fibre, (g) rotary encoder (h) encoder disc. (Right) Prototype of Tesla motor

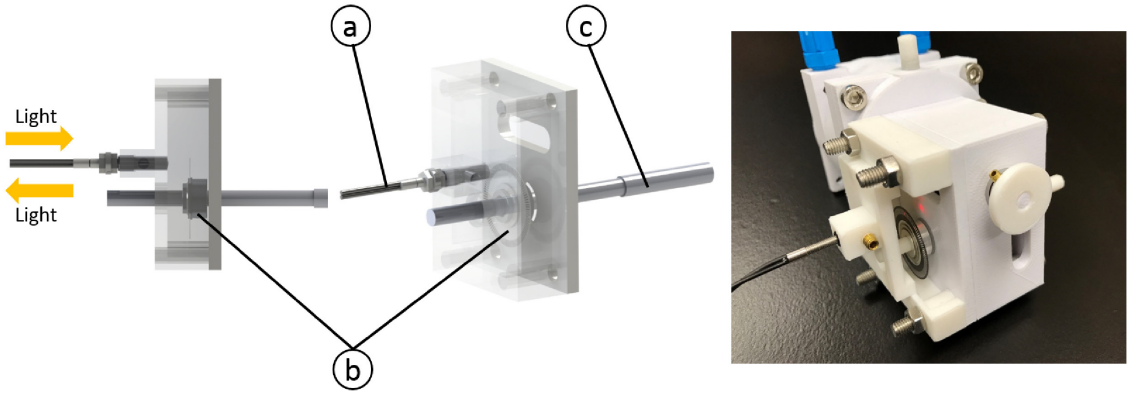

Figure 7 (Left) Details of the proposed rotary encoder, where: (a) optical fibre; (b) encoder disk; (c) output shaft. (Right) The developed prototype for the MRI-compatible sensor.

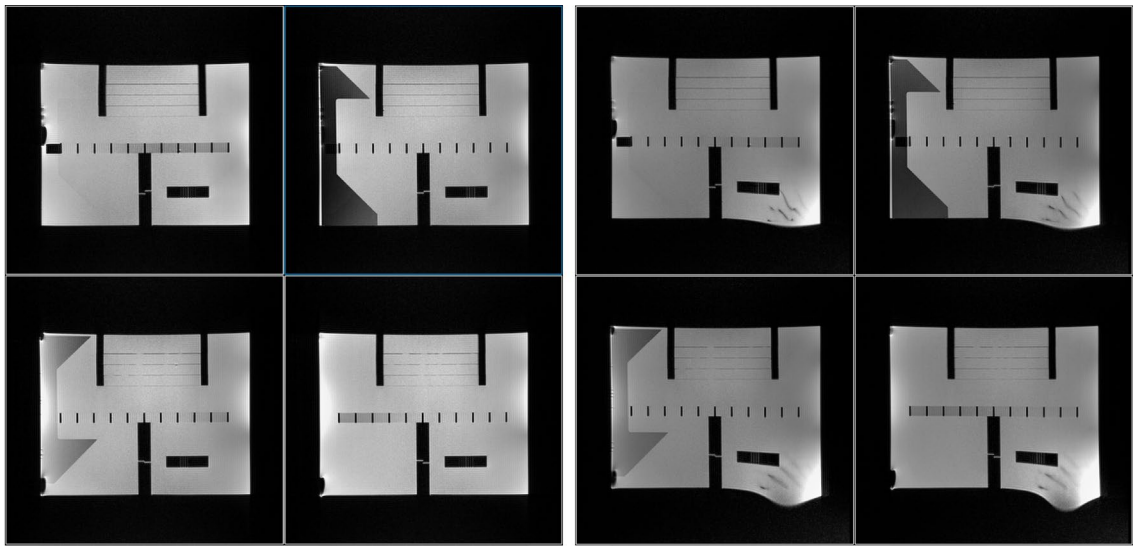

Figure 8 MRI scans to compare the compatibility of our actuator. (left) Scan with the Tesla motor, and (right) scan with a commercial piezo-electric motor.

4. PUBLICATION AND AWARDS

J[1] D. Navarro-Alarcon and Y.-H. Liu, “Fourier-Based Shape Servoing: A New Feedback Method to Actively Deform Soft Objects into Desired 2-D Image Contours”, IEEE Transactions on Robotics, vol. 34, no. 1, 272–1279, 2018
J[2] D. Navarro-Alarcon, S. Saini, T. Zhang, H. Chung, K. W. Ng, M. K. Chow, Y.-H. Liu, “Developing a Compact Robotic Needle Driver for MRI-Guided Breast Biopsy in Tight Environments”, IEEE Robotics and Automation Letters, vol. 2, no. 3, 1648–1655, 2017

C[1] H. M. Yip, D. Navarro-Alarcon, Y.-H. Liu. An Image-Based Uterus Positioning Interface Using ADALINE Networks for Robot-Assisted Hysterectomy. IEEE Int. Conf. Real-time Computing and Robotics, pp. 182–187, 2017
C[2] T. Zhang, D. Navarro-Alarcon, K. W. Ng, M. K. Chow, Y. Liu and H. L. Chung, "A novel palm-shape breast deformation robot for MRI-guided biopsy," 2016 IEEE Int. Conf. on Robotics and Biomimetics, pp. 527-532, 2016
C[3] F. Zhong, D. Navarro-Alarcon, Z. Wang, Y.-H. Liu, T. Zhang, and H.M. Yip. Adaptive 3D Pose Computation of Suturing Needle Using Constraints From Static Monocular Image Feedback. IEEE/RSJ Int. Conf. Intelligent Robots and Systems, 5521–5526, 2016.
C[4] H. M. Yip, D. Navarro-Alarcon and Y. Liu, "Development of an eye-gaze controlled interface for surgical manipulators using eye-tracking glasses," 2016 IEEE Int. Conf. on Robotics and Biomimetics, 2016, pp. 1900-1905

Best student paper award: C[1]

COMPLETED

INTENTION-DRIVEN SHOULDER REHABILITATION FOR TARGETED NEURO-MUSCULAR TRAINING USING AN EXO-MUSCULOSKELETAL ROBOT

Principal Investigator: Professor Darwin Tat Ming LAU
Department of Mechanical and Automation Engineering, CUHK

Co-Investigator (if any):
Prof. Raymond Kai Yu Tong [(2)]

Research Team Members:
- Dr. Ghasem Abbasnejad
- Miss Hiu Yee Cheng
- Mr. Wing Cheong Leung
- Mr. Hung Hon Cheng
- Mr. Yin Pok Chan

[(1)]Dept. of Mechanical and Automation Engineering, CUHK
[(2)]Dept. of Biomedical Engineering, CUHK

Project Start Date: 1 July 2016
Completion Date: 30 June 2018

ABSTRACT

This project aims to develop an exo-musculoskeletal robot for muscle-specific training of the human shoulder. By designing a cable-actuated exoskeleton where the cables are arranged to match the wearer's anatomy, the developed robot aims to improve the effectiveness of targeted neuromuscular training of the shoulder muscles. The robot allows two different modes of operation for the wearer depending on the required situation: 1) an assistive intention-driven mode; and 2) a resistive training mode. The cable actuation is commanded by the position of the upper arm and also from the Electromyography (EMG) signals from the shoulder muscles.

Through this project, the exo-musculoskeletal robot prototype was designed and developed. The software and control system was implemented such that the actuator control, sensor feedback (motion capture and EMG) and the training exercise software are integrated into a complete system. Preliminary tests with human subjects demonstrates the capability of the system to be used in both the assistive and resistive modes, with ability to record required data for further analysis. In addition to the robot development, fundamental research was also conducted relating to the functional analysis of cable/muscle-driven systems and the development of a software/hardware cable-driven platform. From the project, one journal publication (in IEEE Transactions on Robotics, one of the leading journals in robotics) and two conference publications were produced.

1. OBJECTIVES AND SIGNIFICANCE

1. Develop a prototype of a wearable exo-musculoskeletal rehabilitation robot actuated by cables:
   a) Arrange the robot cables anatomically to actuate in parallel six of the major shoulder muscle groups: *pectoralis major*, *deltoid*, *teres major*, *teres minor*, *infraspinatus* and *supraspinatus*.
   b) Allow the system to be attached to the person's upper arm conveniently, to be worn comfortably and the attachment locations of the cable to be easily rearranged.
   c) Capable of providing assistance to a healthy person to carry an extra load in addition to the

weight of their arm.

d) Implement intention-driven control of the exo-muscles through electromyography (EMG) signals that are attached onto the surface of the arm (non-invasively).

2. Demonstrate the potential of intention-driven muscle-specific training in both assistive and resistive modes:
   a) Test the actuation system to provide both assistance and resistance muscle forces.
   b) Demonstrate the sensor feedback systems, both muscle EMG and shoulder position.
   c) Development of different shoulder exercises for human subjects to interact with the system.
   d) Finally, a pilot study of the system will also be performed on a single subject.

Shoulder pain and impairment is a severe problem that affects the quality of life of the impaired subject and inhibits the motion of the arm even in performing even simple daily tasks, such as reaching for objects and feeding one self. Causes of such impairments include stroke, muscle weakness and shoulder subluxation (instability of the shoulder). Furthermore, shoulder subluxation is a common cause of pain for post-stroke patients (between 16-72% of stroke patients). The treatment of such impairments places significant burden on the health system. Successful completion of this project is expected to provide a new approach for performing effective shoulder training to patients with shoulder pain and impairment. Effective treatments would not only improve the quality of life of the patient and also decrease the burden on the Hong Kong health system.

2. RESEARCH METHODOLOGY

In the proposed project, an exo-musculoskeletal IDR robot in assistive and resistive modalities for the shoulder was developed. The cables will be arranged in parallel to the subject's muscles and provided assistance to a particular muscle group. Using EMG feedback, an intention-driven scheme was employed to perform muscle-specific training. In addition to the practical development of the robot, the fundamental analysis of the workspace of muscle-driven systems was performed.

The research methodology consisted of the following main tasks:

1) Design and prototype of the exo-musculoskeletal robot;
2) Integration of sensors to obtain kinematic feedback (IMU and motion capture) and dynamic feedback (muscle activation through EMG);
3) Software development for system to enable intention-driven control and "game" exercises; and
4) Efficient workspace analysis and representation of muscle-driven systems.

I. Design and prototype of the exo-musculoskeletal robot

In this project, the PI proposed to develop a new type of exo-musculoskeletal robot that has cables arranged in an anthropomorphic manner. Six muscle groups identified as the major contributors to shoulder motion and are also situated closer to the surface was used to design the arrangement of cables for the robot: the *pectoralis major*, *deltoid*, *teres major*, *teres minor*, *infraspinatus* and *supraspinatus*.

The cable actuators that were be used in the proposed prototype are the *Myomuscle* units developed by the Myorobotics project consortium who the PI collaborates with. In the design and development of the system, the robot possesses the following features: be easy to attach onto the patient and wear, allow for reconfiguration of the pulley locations on the frame such that cables can be arranged to be in parallel with the muscles, and be safe for the subject to use given the high maximum cable force of the myomuscles.

The arrangement of cables in an anthropomorphic manner is one of the keys to allow the system to provide targeted muscle-specific training. By arranging cables in parallel to specific muscles, the force applied to a particular cable can be controlled to promote strengthening of the corresponding muscle. This is a key difference between the proposed system and existing rehabilitation robots that only assist in producing the

gross motion.

In addition to the mechanical system design, a software system in the Robot Operating System (ROS) was developed in order to control the actuating cables. The software was developed also on top of the CASPR software platform, an open-source software developed for cable-driven robots, such that the control for different number of cables and different attachment locations can be easily performed.

II. Integration of sensors for kinematics and dynamics feedbacks

To provide the kinematics and dynamics feedback for both the control of the robot and also measurement of the human subject data, several sensors were implemented and integrated into the system. For the kinematic feedback of the orientation of the shoulder, two types of sensors (an inertial measurement unit and motion capture system) were used. The motion capture system used was a Polaris tracking system, a medical grade tracking system with high precision and accuracy. Both these sensors provide the 3D orientation of the shoulder in real-time for the robot.

In addition to the shoulder kinematic data, electromyography (EMG) sensors were also used to detect the muscle activation levels. To achieve reliable EMG data, surface EMG electrode sensors (non-invasive), National Instruments DAQ and in-house developed EMG signal processing software was used. The EMG signal must be filtered within the LabView software environment and is then passed into ROS and CASPR. In this robot setup, up to 8 EMG signals can be detected simultaneously, allowing one EMG signal to be detected per muscle to be actuated. This EMG reading, representing the muscle effort of the human wearer of the robot, can be used in two ways: 1) to generate the desired intention-driven command for the actuators; and 2) to observe the efforts and hence behavior of the wearer.

The challenges to overcome in this task is to enable to system to be capable of obtaining stable and accurate physiological feedback data of the wearer.

III. Software development for intention-driven control and "game" exercises

Task 1 and 2 aim to develop the hardware system of the robot such that it has the required actuation and sensing capabilities, and also a basic software system to operate the robot. In this task, the goal is to develop: 1) the software system to achieve intention-driven control in both assistive and resistive modes; and 2) a set of exercises (or games) for the subject to achieve.

The intention-driven control (IDC) refers to the scheme where instead of assisting the user to complete tasks (assist-as-needed or AAN), the actuators only provide assistance in positive relationship to the detected users effort. The advantage of the IDC approach is that it is expected to promote user effort while during the exercise and training, as opposed to the "lazy effect" phenomena observed in the AAN training approach. In the control of the of the cable actuators from the EMG signal using IDC, the following relationship was used:

$$\mathbf{f}(t) = K_p \mathbf{V}_{EMG}(t) \quad (1)$$

The vector $\mathbf{V}_{EMG}$ contains the EMG readings and $\mathbf{f}$ is the forces that the cables should execute. The gains K_p correspond to the amount of assistance after considering the effort from the subject. As observed in [16], it is anticipated that the IDR approach will promote the subject to improve their neurological signal and muscle training in order to complete the set task, for example, the lifting motion of the arm.

Using the IDC scheme, two different exercise modes were developed for the user training: assistive and resistive. The assistive mode refers to the scenario of $K_p > 0$ and when the cable actuators are in parallel with the muscle of interest, such that the cable actuator will provide assistive forces to the robot wearer. In resistive mode, the force should be actuating in opposing direction to provide additional resistance such that the user must provide stronger forces to overcome this. Since cables can only provide pulling but not pushing forces, the resistive cables must therefore be physically arranged to be in the opposite direction.

Another component of the software system, in addition to the IDC and operational modes, is a set of "game

exercises" was developed to guide the user to perform different actions and goals in order to apply the assistive and resistive schemes. The software includes a GUI, instructions and information on the state of the shoulder (such as to achieve the targets of the game) for the user to perform the exercise. In this project, a set of 3 mini-games were developed:

1) Indication of target arm-lifting motion (only reference command)
2) Indication of target arm-lifting motion with feedback of the actual arm position
3) Discrete feedback on performance after arm-lifting motion is complete

IV. Efficient workspace analysis and representation for muscle-driven systems

To supplement the practical development and studies, analysis on the capabilities of the robot and human system is important to gain better understanding on the physiological conditions of the human shoulder and subject. To study this, the generation of workspace provides a useful and global perspective of the capabilities of a robot/human system. Workspace refers to the set of poses in which the shoulder can reach under some prescribed conditions, such as using a set of positive forces in the muscles/cables to produce motion in all directions (*wrench-closure workspace*). This is a challenging fundamental problem due to a range of aspects:

- The generation of the workspace is computationally expensive using existing numerical techniques
- Existing techniques lack information regarding continuity of the workspace
- Existing methods cannot provide visualization for systems with high workspace dimensions

To overcome the aforementioned issues, a new workspace analysis method for cable and muscle-driven systems was developed by extending the PI's previous work on the "ray-based method" of workspace generation. The key idea of this method is that the workspace of the robot can be conveniently generated if only one of the robot's degrees-of-freedom is considered as a decision variable and the remaining as constant values. This simplifies the equations to generate the workspace into univariate polynomial equations that make it efficient to solve. These rays in different generalized coordinate dimensions can then be used to generate a connected lattice providing continuity information about the workspace itself. Finally, a new type of mathematical representation, using an undirected graph, for the workspace visualization and storage. The advantages of this proposed representation include: can represent the workspace of systems of any dimension and provide physical interpretation and meaning of the workspace.

3. RESULTS ACHIEVED

3.1. Prototype Development

The developed prototype possesses four primary muscle groups, the deltoid anterior, deltoid middle, deltoid posterior and pectorial major (as shown in Figure 1).

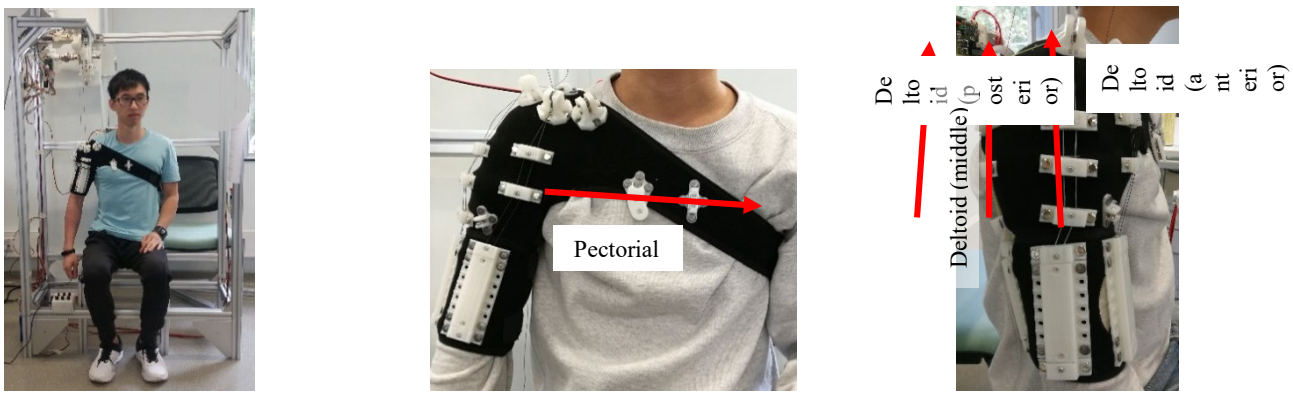

Fig. 1. Exo-muscular robot prototype. Overall view (left), front view (middle) and side view (right).

The three muscles, deltoid anterior, middle and posterior, are involved primary in the shoulder flexion, abduction and extension, respectively. The pectorial muscle is involved in the adduction motion. Figure 2 shows the motion produced by the robot on the subject by providing cable force actuation to each of the

muscles, demonstrating the capability of the exo-muscle robot to motion that is similar to that of the corresponding muscles they are parallel to. Using the Myomuscle cable actuator units, integration with the ROS cable robot software (ROS-CASPR) is completed in order to command the exo-muscles.

Fig. 2. Flexion (left), abduction (middle) and extension (right) motions of the shoulder produced through the robot prototype using the Myomuscle actuator units

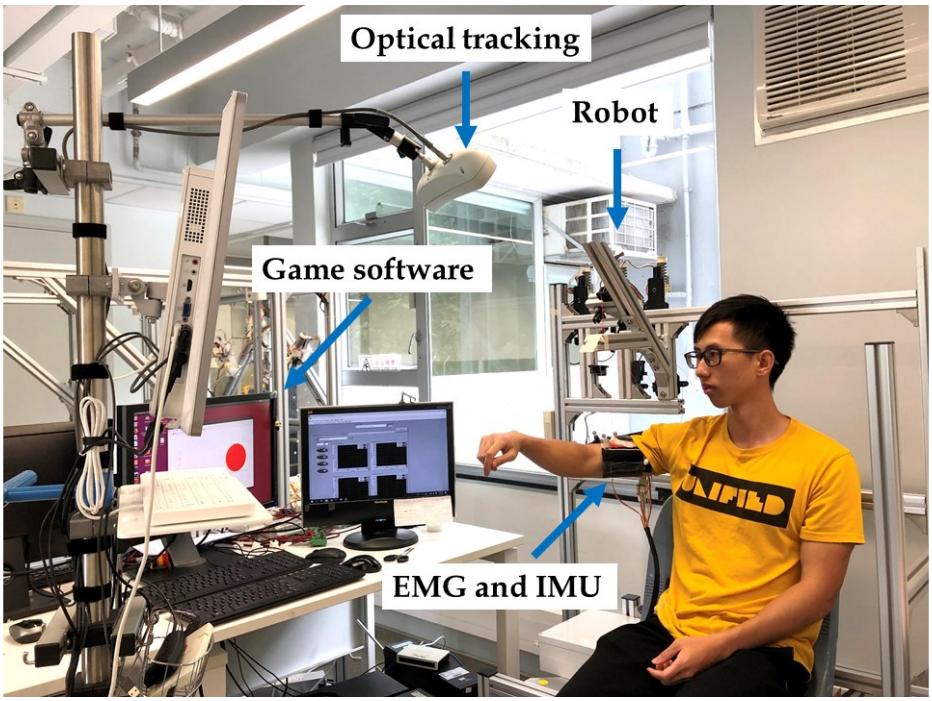

Fig. 3. Complete musculoskeletal robot rehabilitation and exercise system

3.2. Integration of Sensors for Kinematics and Dynamics Feedback

The robot prototype (presented in the above section) can be controlled in two modes: 1) manual command input; and 2) EMG IDR feedback. The manual command input scheme was achieved through potentiometer dials that command each muscle (Figure 4 (left)). This mode is primarily used for testing and calibration. The main mode to be used within the IDR scheme is the EMG sensor feedback from the corresponding muscles that have exo-muscles attached. The EMG sensors, as shown in Figure 4 (right), record the electrical activity of the muscles and then send this information to the ROS software framework. This is then used to provide the actuation command for the corresponding muscle through the proposed scheme in (2). Pre-processing of the signals through a third order Butterworth bandpass filter in National Instruments Labview.

Fig. 4. Command mode of robot: 1) potentiometers dials for each muscle (left); 2) EMG on muscles (right)

Within this task, an appropriate calibration methodology for each muscle was developed. This involves the recording and determination of EMG range and calibrate sensors such that there is no over-saturation and that the required operating EMG range can be measured. The successful EMG integration with the robotic system was demonstrated through a teleoperation experiment. In the experiment, one subject wore the EMG sensors while another wore the robot system, and the detected EMG signals are used to actuate the wearer of the robotic system, while the wearer remains relaxed. Results of the experiment showed that EMG detection in muscle and shoulder motion intention was successful and the produced corresponding motion to the wearer of the exo-muscle robot.

For the motion tracking, a Polaris Vicra motion tracker (Figure 6) and IMU are integrated into the system to capture the orientation/posture of the shoulder during the motion. This is required for both the analysis of the training and in the exercise games for those that use the wearer's current position. This supplements the EMG signals (muscle forces) with kinematics data. The motion of the user at 10 – 20 Hz can be obtained by capturing the motion from the motion tracker and sent to the ROS software.

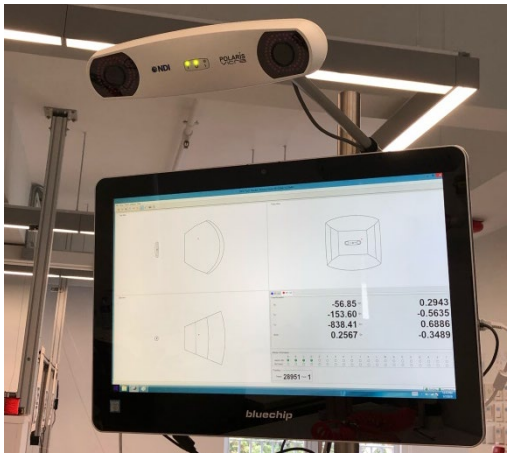

Fig. 5. Polaris Vicra motion tracker

3.3. Software Development for Intention-Driven Control and "Exercise Games"

Preliminary human subject experiments were performed in order to demonstrate the working principles and confirm the potential of the proposed approach. These experiments were performed on three healthy subjects. In this experiment, each subject wore both the EMG sensors and robot, in the same manner as would be expected during the rehabilitation, and the subject were asked to perform shoulder flexion, abduction and extension motion while carrying different amount of weights. The EMG signals on the shoulder muscles were then recorded both with and without the exo-muscle robot assistance for a fixed intention-assistance gain. As shown in Figure 4, it can be clearly observed that the robot assistance using the IDR scheme produced lower measured EMG, indicating that lower muscle forces were required. Consequently, this supports the idea that using the same EMG strength, the wearer would be capable of carrying a heavier load. This validation is important later experiments with impaired subjects as it demonstrates that the robot would be capable of providing additional force during their therapy through the IDR scheme.

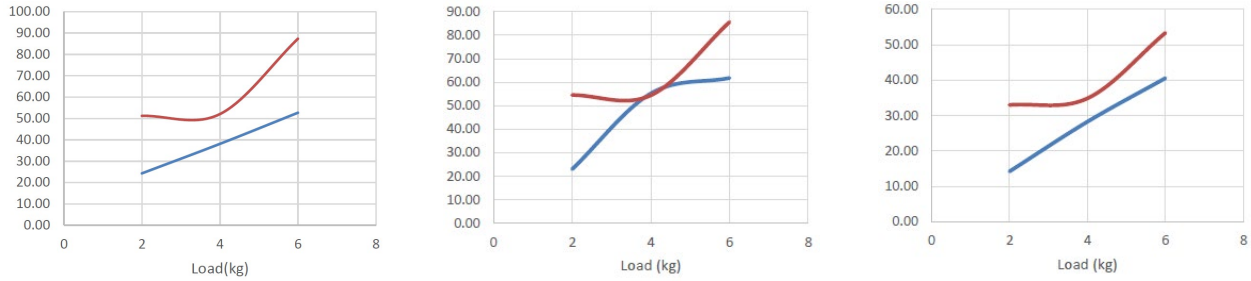

Fig. 6. Summary of human experiments. Load vs EMG reading without robot (red) and with robot (blue). Anterior for flexion motion (left), middle for abduction (middle) and posterior for extension (right).

Within the intention-driven scheme, two modes have been proposed: assistive and resistive. The assistive mode is essentially assigning a positive gain to Eqn. (1). While the resistive mode requires reconfiguration of the cable attachment to act in the opposite direction such that it corresponds to a negative gain to Eqn. (1). In both modes, three different "game exercises" were developed in order to test different hypotheses and interaction modalities between the robot and the wearer. In all three modes, the user subject is required to produce an arm lifting or lowering motion from a beginning to ending pose, and assistance/resistance of different levels (not known by the subject) can be provided.

Game mode 1) This is the most simple game mode, where the required motion of the arm lifting will be shown on the screen (for example from 0 to 90 degrees as in Figure 7) by the solid line and the wearer's current position is also displayed (by the dashed line). Using the feedback obtained by the cable lengths, IMU and optical tracking system, the command and feedback will be displayed both in real-time so that they can adjust their arm movement depending on their performance. The combination of assistance/resistance in this mode would allow: 1) effort to be trained into the user to try to achieve good performance; 2) assistance/resistance level to be adjusted to further help or challenge the subject.

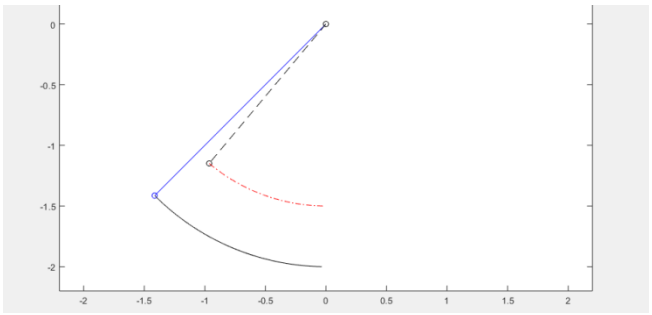

Fig. 7: Visual interface for game 1

Game mode 2) This game mode shows the motion of the desired motion (open loop) *without feedback of the arm's position* (Figure 8). This can be considered as a "partially" blind mode where the subject does not know their performance. The intention of this game mode is to observe the performance of the subject when different assistance/resistance is applied when they are un-aware of the objective impact on them. This tests another aspect of the subject, which is their perception of their own arm posture as they are moving. This sensational skill is also important within the training of human motion.

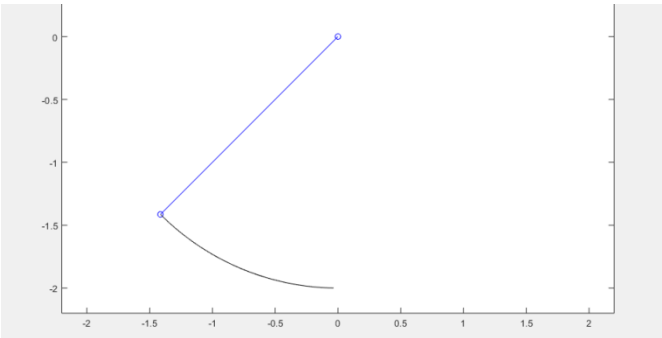

Fig. 8: Visual interface for game 2

Game mode 3) In this mode the user does not know the desired motion in the exercise, unlike in game modes 1 and 2. In this game, the subject will only be provided the results of their motion, such as whether they are slower, matching or faster than the requirements (Figure 9) of the generated motion. Without knowing the requirements, the subject will then need to explore and learn the desired motion through the discrete and course visual feedback for the user. This is anticipated to be a more advanced mode where motor skills have already been more developed and that finer motion with a stronger sense of timing can be further trained, relating the physical and cognitive capabilities training.

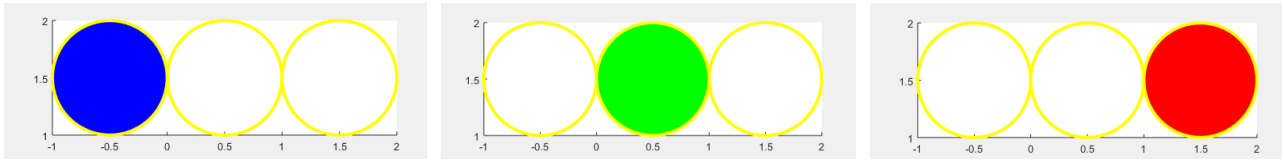

Fig. 9: Visual interface for game 3

With the different games, integration with tasks 1 and 2 allow the games to be both executed and results to be collected. The following are some of the results to show the working case with game 1. Figure 10 shows the EMG data (in % of maximum voluntary contraction) of the deltoid muscles (anterior, middle and posterior/bicep) when performing flexion motion from 0 to 90 degrees with no resistance provided over 10 repeats (baseline). These results show good repetitive patterns for the 10 repeats of the same motion.

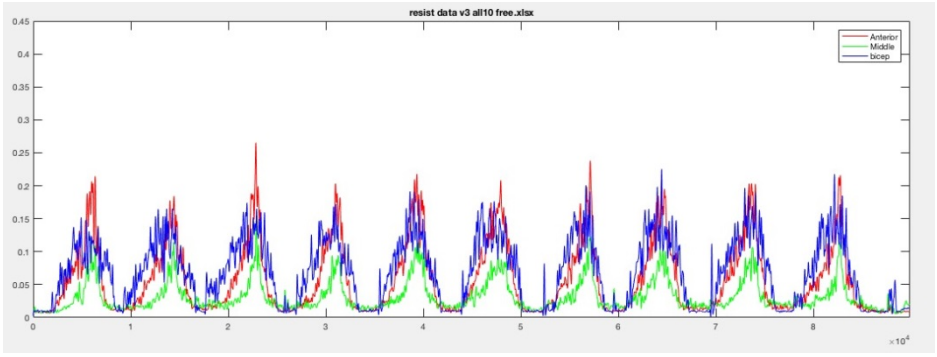

Fig. 10: EMG deltoid muscle data for 0 – 90 degree flexion motion with no resistance over 10 repeats

Figure 11 shows the EMG data of the same muscles for the same flexion motion when a constant resistive force is given to the subject to the anterior muscle (that is, a cable pulling in the opposite direction of the anterior muscle). The results show that there is a consistant increse of anterior deltoid muscle EMG signal compared with the baseline case with no resistance (Figure 10), and hence validating that the subject is increasing deltoid muscle activation to counterbalance the resistance.

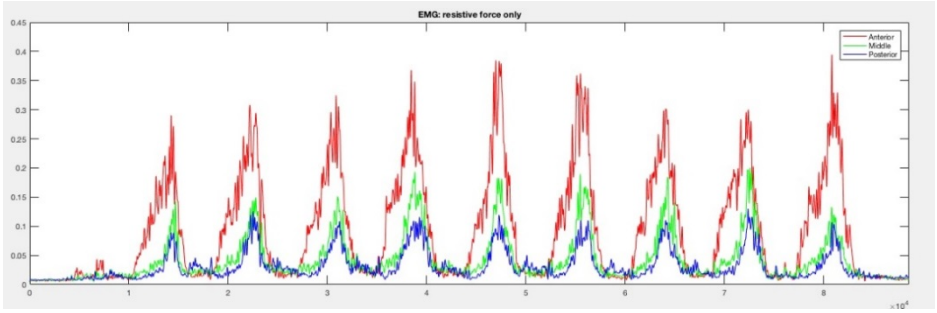

Fig. 10: EMG deltoid muscle data for 0 – 90 degree flexion motion with resistance to the anterior

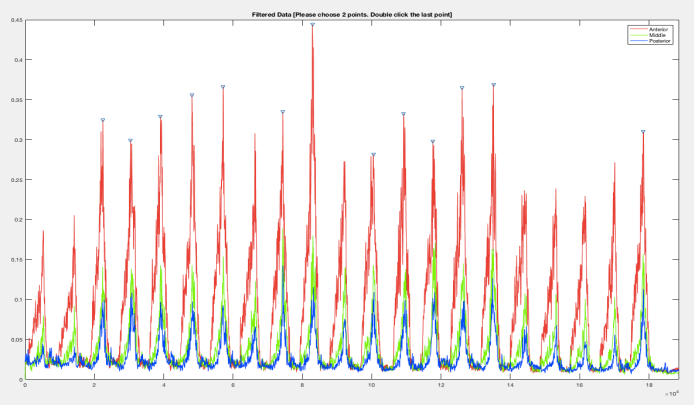

Fig. 11: EMG deltoid muscle data for 0 – 90 degree flexion motion with random resistance to the anterior

Figure 11 shows the EMG data for an experiment where the resistance is provided at different repetitions of the motion at random (over 21 total repeats). The repetitions with resistance applied are marked by blue triangle markers at the top of the EMG signal. It can be seen from the figure that higher EMG signals on the anterior deltoid muscles were detected (as expected) during the repetitions that had resistance applied. This shows the subject's ability to adapt to the presence (and also removal) of resistance.

These simple experiments serve to demonstrate the capability of the system to provide assistance/resistance with the signals collected from the EMG, motion capture and IMU when interacting with the software system and games. Having this system capability would allow a range of different experiments to be designed that can be beneficial for both understanding human learning capabilities and as training/exercises for pathological subjects such as those with stroke or shoulder injury.

3.4. Workspace Analysis

In this work, a generalised ray-based lattice WCW generation approach using a graph workspace representation for CDRs of arbitrary type is proposed. Extending from our previous work [26], this work focuses on the WCW generation for arbitrary types of CDRs (both CDPRs and MCDRs) with any number of cables. For any of the DoFs, it is shown that the WCW ray can be determined by solving a set of univariate polynomial equations. A generalised method to determine the polynomial coefficients without the closed-form analytical workspace boundary is proposed. This can then be used to generate a WCW lattice providing information about the workspace continuity. Subsequently, a graph representation for the WCW is introduced, where the vertices and edges contain the workspace and connectivity information, respectively. Finally, using the CASPR software [31], the WCW for three different CDRs, a 3-DoF planar CDPR, a 4-DoF two-link MCDR and a 6-DoF spatial CDPR, are used to illustrate the benefits of the proposed work.

The proposed method has high computational efficiency, is compact in workspace representation, captures information about workspace continuity and can be applied to any CDR. To the best of the PI's knowledge, this work is unique in two ways: 1) the first ray-based WCW approach that can be generically applied to arbitrary types of CDRs; and 2) the first work to propose a graph-based CDR workspace representation. The graph-based representation brings many benefits, including: ease in representing workspace continuity, the ability to use established graph theory to study the workspace, the ability to incorporate metrics on both the vertices and edges, and the ability to visualise all of the DoFs of the workspace for CDRs of any number of DoFs in 2-D.

Please refer to the published paper journal publication for more details on the methodology and results of the work.

3.5. Summary and Future Plans

In this project, an exomusculoskeletal robot for the purpose of intention-driven rehabilitation and exercising of the shoulder. By using cable actuators that are aligned in parallel to the existing muscles of the subjects, the goal is to provide muscle-specific assistance/resistance conveniently with a lightweight robot. During the project, the development of the robot prototype (both the mechanical and electronic elements), integration of sensory feedback in the form of EMG and shoulder kinematics, and the development of software system with

exercise games that can demonstrate the capabilities of the system were completed. Furthermore, fundamental research was also performed on the robot analysis, such as dynamics and workspace, and resulted in the publication of 1 journal and 2 conference papers. Future work will focus on further development of exercise regimes that are specifically targeted to patient groups, such as stroke and frozen shoulder, so that the system can be useful in clinical practices and also future commercialization opportunities.

4. PUBLICATION AND AWARDS

Through the project, one journal publication has been published in IEEE Transactions on Robotics, one of the leading journals in robotics:

- G. Abbasnejad, J. Eden, D. Lau, "Generalised Ray-Based Lattice Generation and Graph Representation of Wrench-Closure Workspace for Arbitrary Cable-Driven Robots", *IEEE Transactions on Robotics*, *accepted*, 2018

Furthermore, two conference publications were published through the project:

- Y. P. Chan, G. Abbasnejad, J. Eden, and D. Lau, "Improved Computational Speed of System Dynamics for Cable-Driven Robots through Generalised Model Compilation", *in Proc. IEEE International Conference on Real-Time Computing and Robotics*, pp. 230-235, 2018
- Y. P. Chan, J. Eden, D. Lau, and D. Oetomo, "A Survey on Inverse Dynamics Solvers for Cable-Driven Parallel Robots", *Proceedings Australasian Conference on Robotics and Automation*, pp. 1-9, 2017

One conference publication is still currently under preparation to describe the entire robotic system.

The project also allowed one Doctor of Philosophy (Mr. Chen Song), one Master of Philosophy (Mr. Yin Pok Chen) and several final year project students to be involved. Two final year projects from the MAEG programme and the BME programme were involved in this project. They were primarily involved in the system design and their project was awarded the 1st runner up of the CUHK Charles K. Kao Student Creativity Award for the individual entry.

Furthermore, this project was also presented at the 2018 CUHK Shoulder Biomechanics Summit and at the **Shun Hing 65th Anniversary Exhibition event at the Hong Kong Exhibition and Convention Centre.**

(refer to page 15)

COMPLETED

ENGINEERING ANTIMICROBIAL SURFACES BASED ON MICRO-TOPOGRAPHY USING A NOVEL ULTRASONIC MACHINING METHOD

Principal Investigator: Professor Ping GUO
Department of Mechanical and Automation Engineering, CUHK

Research Team Members:
Yang Yang, PhD student [(1)], Chi Shing Yeung, MPhil student [(1)]
Jianjian Wang, Postdoc fellow [(1)]

[(1)]Dept. of Mechanical and Automation Engineering, CUHK

Project Start Date: 1 July 2016
Completion Date: 30 June 2018

ABSTRACT

There are great demands of antimicrobial surfaces, which could prevent the adhesion of micro-organisms and the formation of biofilms. Microbial contamination of surfaces, which are directly exposed to human tissues (surgical equipment) and food (utensils), can cause serious infection and the associated disinfection costs. Biomedical implants, such as prosthetic devices and artificial joints, are subjective to adhesion of pathogenic bacteria and biofilms, which not only significantly reduce the lifespan of the implants but also increase the risks of various infections. Biofouling on marine vessels of barnacles and algae is a great concern in shipping industry due to corrosion to the ship hulls and increased fuel and maintenance costs. The project aims to develop a novel manufacturing process for fast creation of micro-structured surfaces for the antimicrobial surfaces application directly on stainless steel and titanium alloy surfaces which are mostly widely used in the hospitals, food industry, and biomedical market. The outcome from this project will enable the creation of antimicrobial surfaces based on surface micro-topography, which is non-toxic, permanent and chemical free, to be applied to the related applications in hospitals, biomedical implants and devices, food packaging, marine industry, etc.

1. OBJECTIVES AND SIGNIFICANCE

(1) The research project, if carried out successful, will enable the technology to create antimicrobial surfaces, which could prevent the adhesion of bacteria and formation of biofilms, in many critical applications, such as surgical equipment, biomedical devices and implants, and food packaging.

(2) The project aims to develop a novel manufacturing process for fast creation of micro-structured surfaces for the antimicrobial surfaces application directly on stainless steel and titanium alloy surfaces which are mostly widely used in the hospitals, food industry, and biomedical market.

(3) The project aims to systematically study and test the surface micro-topography and its effects on the prevention of microbial adhesion. The surface wettability and an innovative surface roughness engineering index will be utilized as the criteria to categorize different surface micro-features.

(4) The project aims to carry out experiments to produce various micro-patterned stainless steel and titanium surfaces according to the optimized results from our model. These antimicrobial surfaces will then be tested to verify their retention ability of micro-organisms such as S. aureus and

E. coli.

2. RESEARCH METHODOLOGY

The research project, if carried out successful, will enable the technology to create antimicrobial surfaces, which could prevent the adhesion of bacteria and formation of biofilms. There are three main research tasks in this project, namely, (1) development of the ultrasonic texturing system for creating micro-structured surfaces; (2) study of the relationship between surface micro-topography and its effects on microbial retention; (3) to generate various micro-patterned surfaces to test against smooth/polished surfaces using ulva and E. coli as targeted micro-organisms.

We will design and optimize the surface topography based on the surface wettability, engineering roughness index, and the capability of our texturing system. These patterns will be directly machined on stainless steel and titanium surfaces, which are most widely used in hospitals and biomedical related devices. Experiments of their effectiveness on microbial retention will be tested using E. coli as targeted sample micro-organisms to compare with smooth and untreated surfaces.

3. RESULTS ACHIEVED

In this project, in order to satisfy the surface texturing requirements of high-efficiency, high-flexibility and low cost for antibacterial application, we proposed two novel surface texturing process, the modulated elliptical vibration texturing/cutting and quadrate vibration texturing. Two novel ultrafast 2-D non-resonant vibration cutting tools were developed for realizing the proposed novel texturing processes. Finally, biological experiments were performed to evaluate the antibacterial performance of obtained micro/nano structured surfaces.

3.1. Development of ultrafast 2-D non-resonant vibration cutting tools

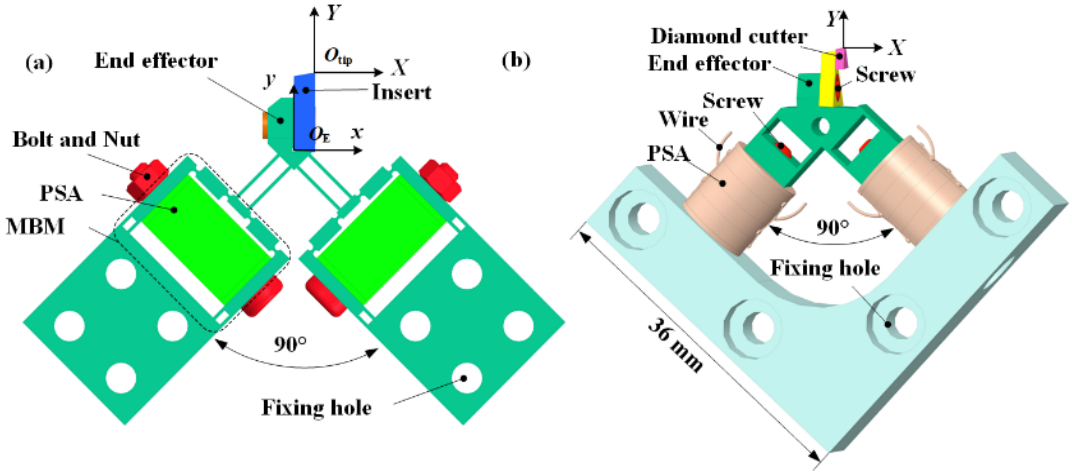

Fig. 1 Illustration of 2-D non-resonant vibration tool. (a) the first tool, (b) the second tool

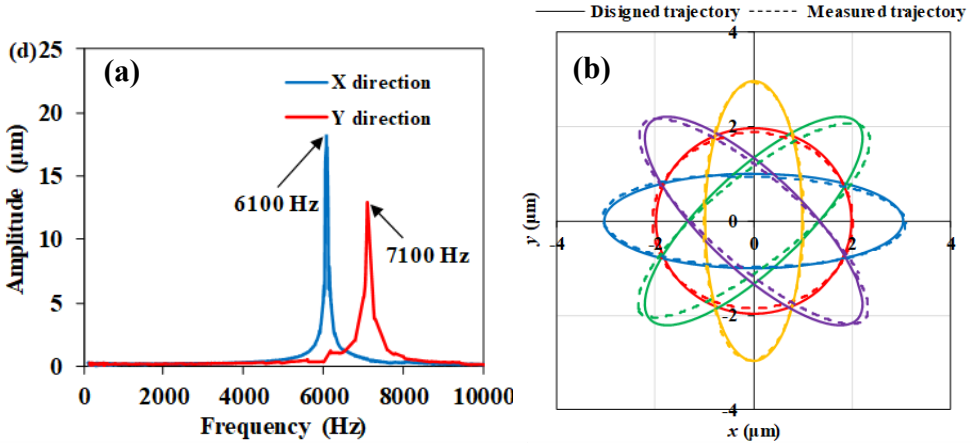

Fig. 2 Performance evaluation of first-generation tool. (a) dynamic tests results, (b) controllability of elliptical vibration trajectory

As shown in **Fig. 1**, two kinds of 2-D non-resonant vibration cutting tools have been developed for the vibration assisted texturing process. Both the two tools have strokes of up to 10 μm, and good controllability of the elliptical vibration trajectory. As shown in **Fig. 2**, the natural frequency of the tool of first generation reaches 6 kHz, which is much larger than that of the existing 2-D non-resonant tools in literatures. In order to realize ultrasonic elliptical vibration, the second tool was developed, which has a natural frequency of 20 kHz, as shown in **Fig. 3.**

The 2-D motion of diamond cutter can be generated by individual two piezo stack actuators (PSAs), according to the following relationship,

$$\begin{bmatrix} u_{\text{out}}^{x} \\ u_{\text{out}}^{y} \end{bmatrix} = \begin{bmatrix} A_x & -A_x \\ A_y & A_y \end{bmatrix} \begin{bmatrix} U_L(t) \\ U_R(t) \end{bmatrix} \tag{1}$$

where u_{out}^{x} and u_{out}^{y} denote the displacement of diamond cutter along the X and Y direction respectively, U_L and U_R are the input voltages of the left PSA and the right PSA respectively, t is time, A_x and A_y are the coefficients that transform input voltages to output displacements, which have be obtained by experimental tests.

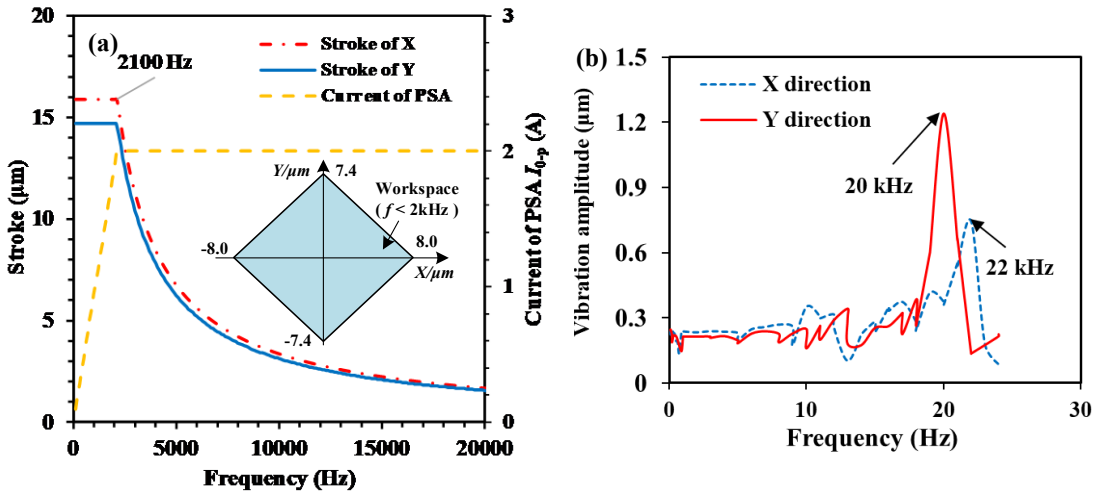

Fig. 3 Performance evaluation of second-generation tool. (a) stroke vs frequency. (b) dynamic tests results

3.2. Vibration assisted surface texturing

3.1.1. Modulated elliptical vibration texturing for fast generation of hierarchical structures

The direct application of developed 2-D non-resonant tool is in surface texturing for fast generation of micro-structured surfaces. As shown in **Fig. 4,** the developed ultrafast 2-D non-resonant cutting tool can be used to combine the fast tool servo and elliptical vibration texturing. The FTS motion is used to modulate the vibration center of elliptical vbration, realizing the modulated elliptical vibration texturing process by using two frequencies input voltages. The input voltages of the two PSAs can be expressed as

$$\begin{cases} U_L(t) = U_{1L,0-p}\sin(2\pi f_1 t) + U_{2L,0-p}\sin(2\pi f_2 t) \\ U_R(t) = U_{1R,0-p}\sin(2\pi f_1 t + \alpha_1) + U_{2R,0-p}\sin(2\pi f_2 t + \alpha_2) \end{cases} \quad (2)$$

where f_1 and f_2 denote the low and high frequency respectively. $U_{1L,0\text{-}p}$ and $U_{1R,0\text{-}p}$ are the zero-peak amplitudes of the low frequency input voltages of the two PSAs respectively, $U_{2L,0\text{-}p}$ and $U_{2R,0\text{-}p}$ are the zero-peak amplitudes of the high frequency input voltages of the two PSAs respectively. α_1 and α_2 are the phase differences. Using the methods above, the elliptical vibration can be generated at the tip of diamond cutter, while its vibration center can be dynamically modulated by the fast tool servo motion. The elliptical vibration is used for surface texturing of first hierarchical structure, the fast tool servo motion is used for the generation of second hierarchical structure.

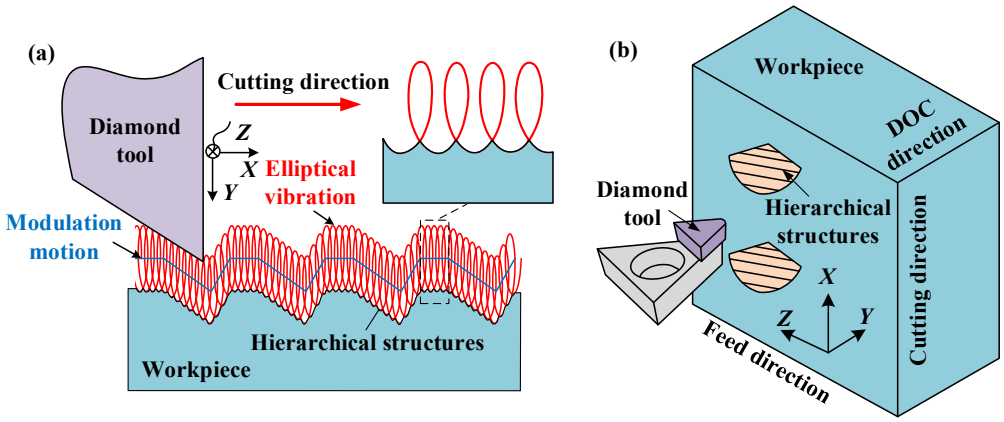

Fig. 4 Principle of hierarchical structures fabrication.

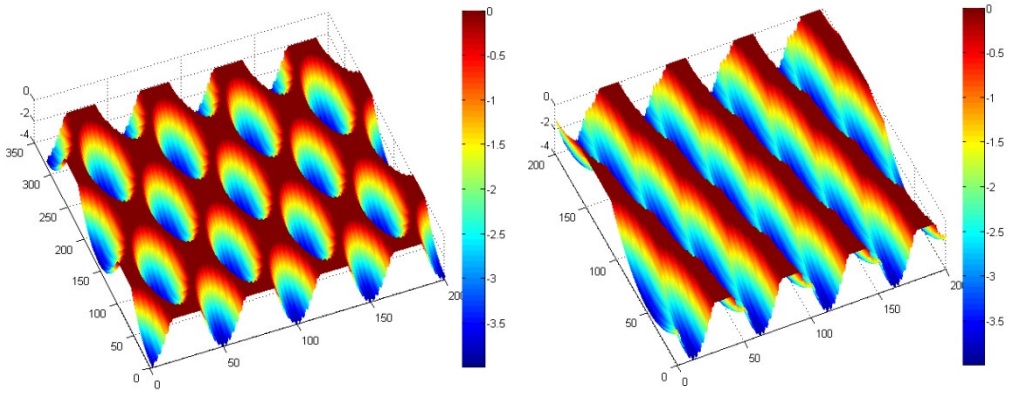

Fig. 5 Simulated results of hierarchical dimple (left) and groove (right).

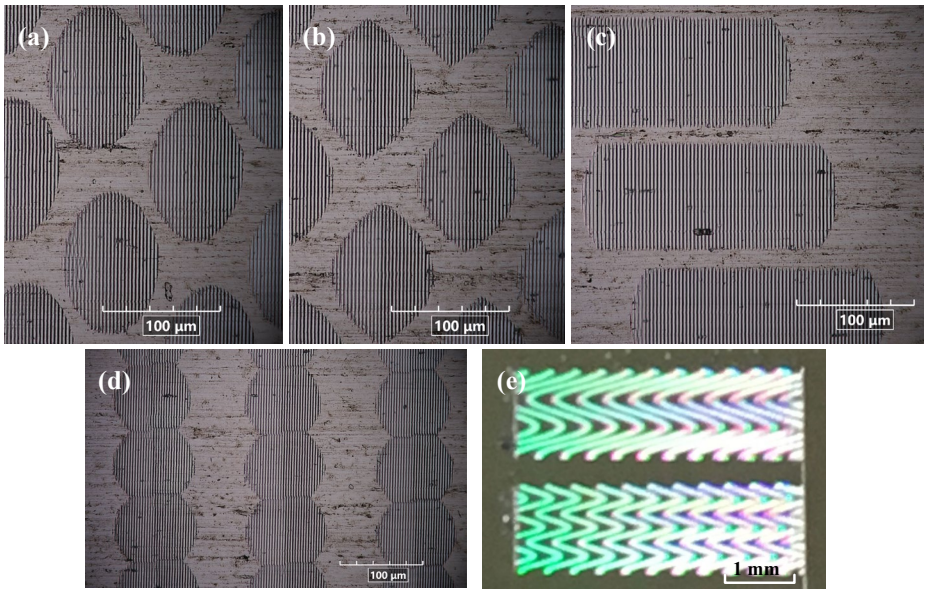

Fig. 6 machined hierarchical dimples and grooves. (a) circular dimple (b) triangle dimple (c) trapezoidal dimple (e) straight groove (e) bending groove

As shown in Fig. 4 (b), hierarchical dimples can be fast and easily generated. By carefully arrange the layout of micro dimple patterns, hierarchical grooves can also be generated. **Fig. 5** shows the simulated results and hierarchical dimple and groove. By simulation, the morphology of fabricated hierarchical structures can be predicted in advances. **Fig. 6** shows that machined micro dimples and grooves with hierarchical structures have been successfully fabricated. As shown in **Fig. 6**, by controlling the waveform of modulation motion, micro dimples with various kinds of cross-section can be obtained, such as circular, triangle and trapezoidal dimples. Moreover, by controlling the phase differences of neighboring cutting passes, bending grooves with hierarchical structures (**Fig. 6 (e)**) can be fabricated. In **Fig. 6 (e)**, the color indicates the existence of hierarchical grooves with grating constant of 3 μm.

3.1.2. Modulated elliptical vibration cutting for surface texturing on silicon and metal

The amplitude-frequency characteristic of second 2-D non-resonant tool with a ultrasonic natural frequency is schematically illustrated in **Fig. 7 (a)**, the vibration amplitude under certain frequency increases with increasing input voltages. This tool can be used to combine the ultrasonic elliptical vibration cutting and fast tool servo by two-frequencies voltages inputs are used. As shown in **Fig. 7 (a)**, one is ultrasonic frequency which is equal to the natural frequency of NVCT with tiny input voltage, resonant effect is used to amplify the small vibration of PSA for the consideration of energy saving and suppressing heat generation. The other is low frequency with relatively high input voltage, in order for generation of the fast tool servo motion. Using the methods above, the ultrasonic elliptical vibration can be generated at the tip of diamond cutter, while its vibration center can be dynamically modulated by the FTS motion as shown in **Fig. 7 (b)**. The ultrasonic elliptical vibration is used for material machinability improvement, such as increasing the nominal depth of cut in ductile regime, the fast tool servo motion is used to dynamically modulate the vibration center of ultrasonic elliptical vibration for the surface generation of micro structures.

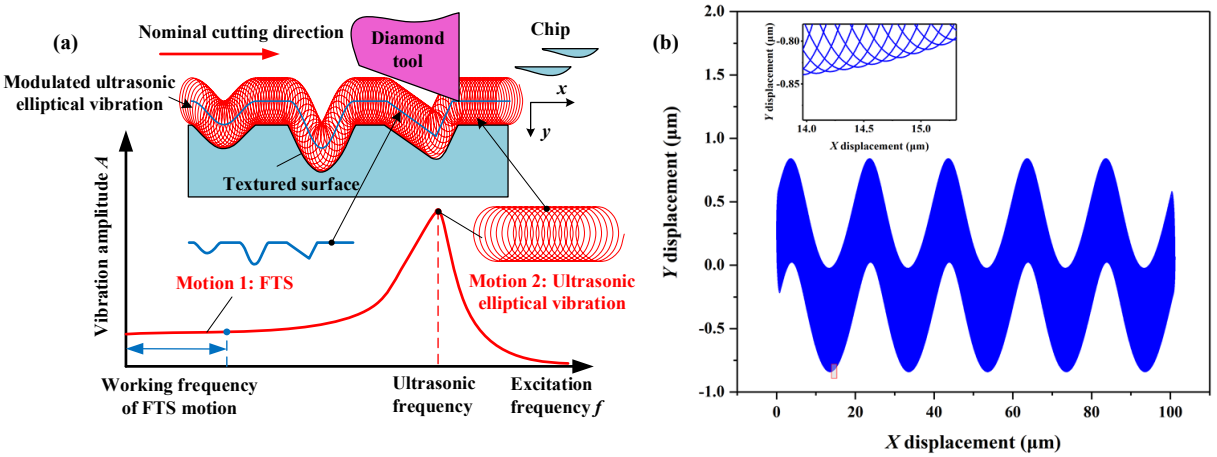

Fig. 7 (a) Principle of surface texturing of silicon, (b) tool moving trajectory, (c) machined dimple patterns

Fig. 7 (c) shows machined micro dimple patterns on silicon surface. **Fig. 8** shows the comparison of surface texturing performance with and without ultrasonic elliptical vibration. As shown in **Fig. 8**, the ductile cutting depth of micro dimples with ultrasonic elliptical vibration can be dramatically improved over that without ultrasonic elliptical vibration. When the ultrasonic elliptical vibration is employed, no severe fracture damage can be observed on the micro dimple surface even the depth of cut exceeds 1 μm. However, without ultrasonic elliptical vibration, severe and obvious fracture can be observed on the micro dimple surface just when the depth of cut is about 200 nm. Hence, the ultra-precision surface texturing of brittle materials by 2-D ultra-frequency non-resonant tool has been experimentally achieved.

The modulate elliptical vibration cutting can also be used for the integrity improvement in surface texturing of metals. **Fig. 9** shows the surface topography of machined structures, which is a sinusoidal free form surface. Of course, various kinds of textures can also be generated by employing the 2-D non-resonant tool on ultra-precision machines due to their compact designs.

Depth	0-100 nm	100-200 nm	200-300 nm	300-400 nm
With UEV	*w*= 18.9, *d*=95	*w*=25.6, *d*= 175	*w* = 31, *d* =257	*w* =35.9, *d* =343
Without UEV	*w* =13.5, *d*= 48	*w* =23.6, d= 148	*w* =31.7, *d*= 268	*w* =37.8, *d* = 380
Depth	400-500 nm	500-600 nm	600-700 nm	700-800 nm
With UEV	*w* =40.5, *d*= 437	*w* =44.5, *d* =529	*w* = 48.6, *d*=629	*w* =53.3, *d* = 758
Without UEV	*w*=40.5, *d* = 437	*w* =45.9, *d* = 561	*w* =50.0, *d*=665	*w* =52.7, *d* =739
Depth	800-900 nm	900-1000 nm	1000-1100 nm	1100-1200 nm
With UEV	*w* =57, *d* =878	*w* =59.4,*d* =941	*w* = 62.8, *d* =1051	*w* =64.8, *d* =1120
Without UEV	*w* =56.7, *d* =857	*w* =59.5, *d* =941	*w* =63, *d* =1074	*w* =66.2, *d* =1167

Fig. 8 Morphology of machined dimples with and without ultrasonic elliptical vibration (UEV), where width *w*/μm, depth *d*/nm.

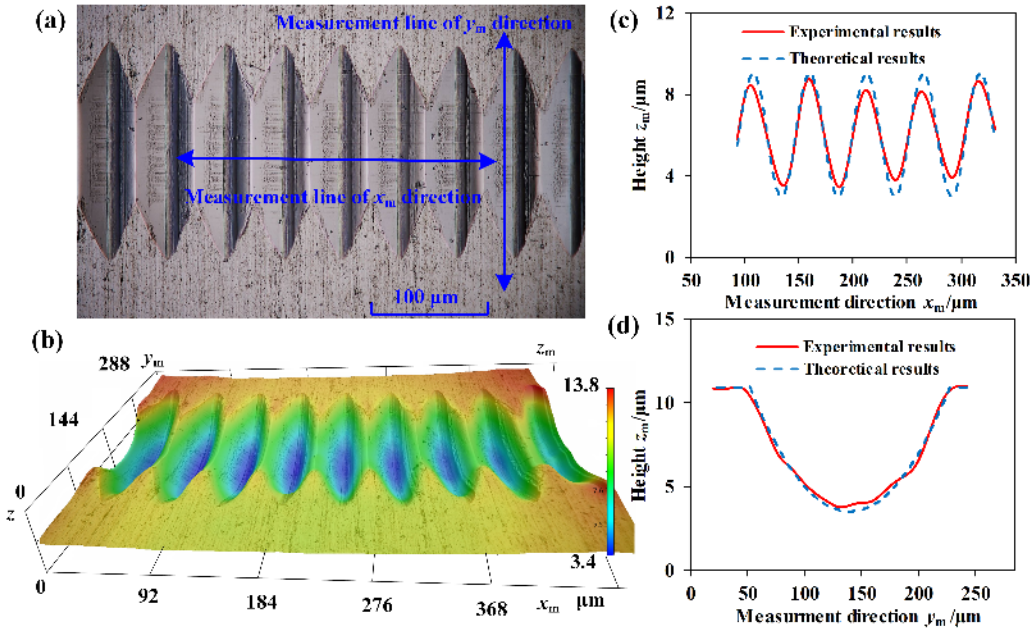

Fig. 9 (a) Measured topography of the machined texture, (b) 3D topography, (c) sectional profile of xm-direction from the measured topography, (d) sectional profile of ym- direction from the measured topography

3.1.4. Quadrate vibration texturing on metal

In this study, quadrate vibration texturing was proposed as a novel process compared with the

conventional elliptical vibration texturing. **Fig. 10** (a) demonstrates the conventional elliptical vibration texturing which can also be achieved by a resonant-type tool. By utilizing a low cutting velocity, the overlapping trajectories can generate micro-grooves on the substrate; while a higher cutting velocity results in non-overlapping trajectories to generate discrete circular dimple structures. **Fig. 10** (b) shows the unique capability of proposed 2-d non-resonant tool to machine micro-structures with an arbitrary tool trajectory thanks to its high working bandwidth. It gives the flexibility to precisely control the cross-section profiles of machined features, which is a critical factor in determining their functional performance. When a quadrate trajectory is employed, we can generate parallel grooves and dimples with a trapezoidal profile as shown in **Fig. 10** (b). These kinds of structured surfaces could find their potential applications in antibacterial application due to its capacity of surface wettability control. **Fig. 11** and **Fig. 12** shows the successful experimental results of quadrate vibration texturing.

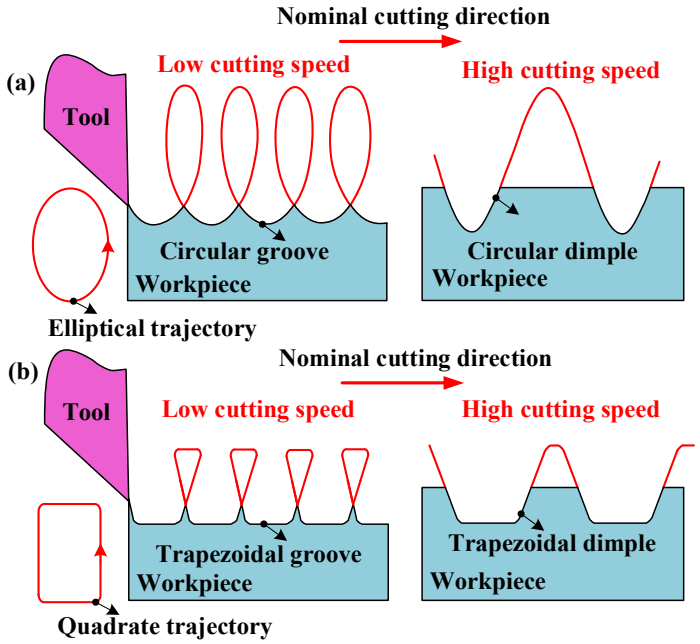

Fig. 10. Comparison of elliptical vibration texturing and quadrate vibration texturing.

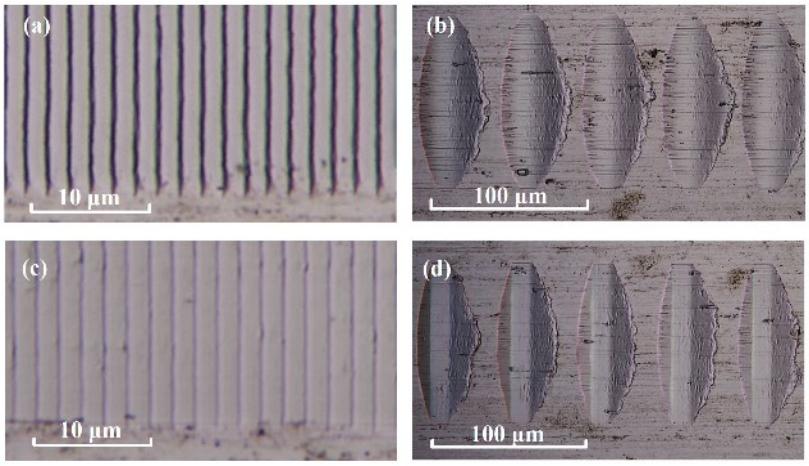

Fig. 11. Topography of textured sruface with the elliptical trajeocty at 300 Hz: (a) cutting speed of 0.6 mm/s and (b) cutting speed of 15 mm/s; with the quadrate trajectory at 300 Hz: (c) cutting speed of 0.6 mm/s and (d) cutting speed of 15 mm/s.

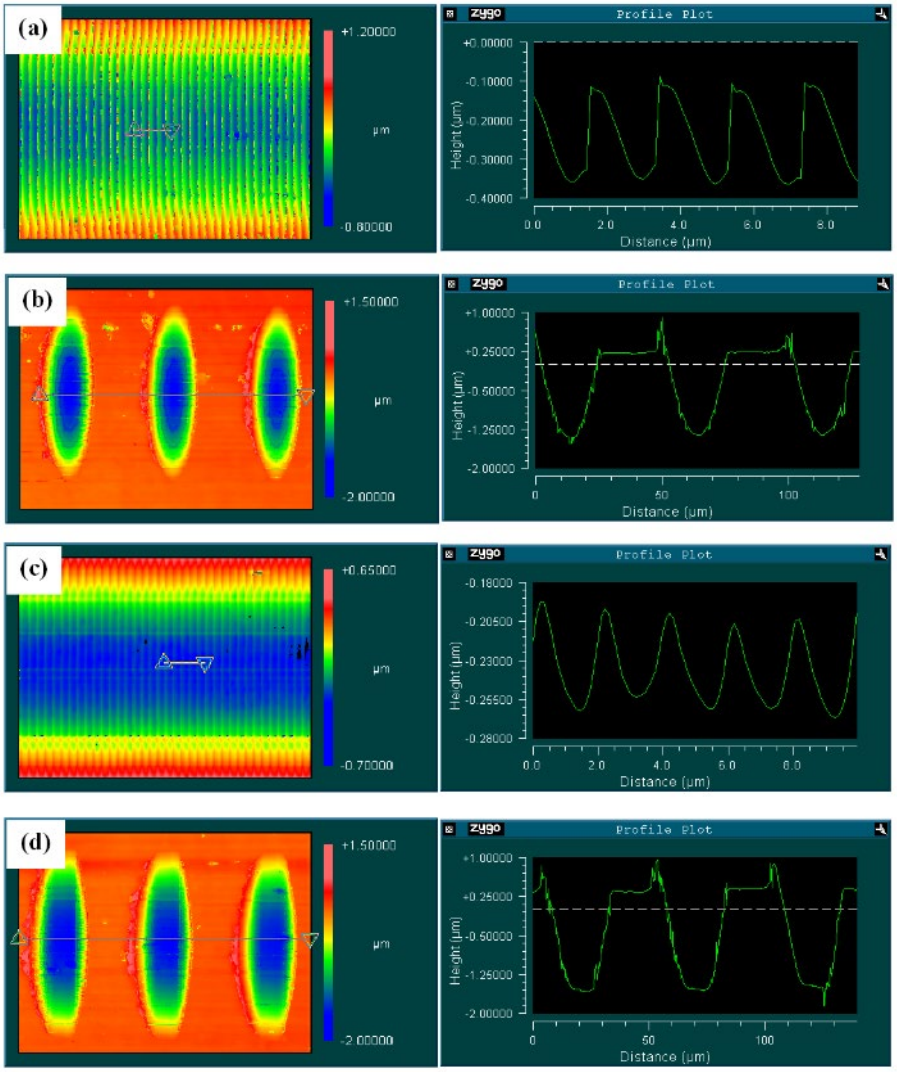

Fig. 12. Corresponding measurement results of Fig. 11 by surface profiler

3.3. Biological experiments

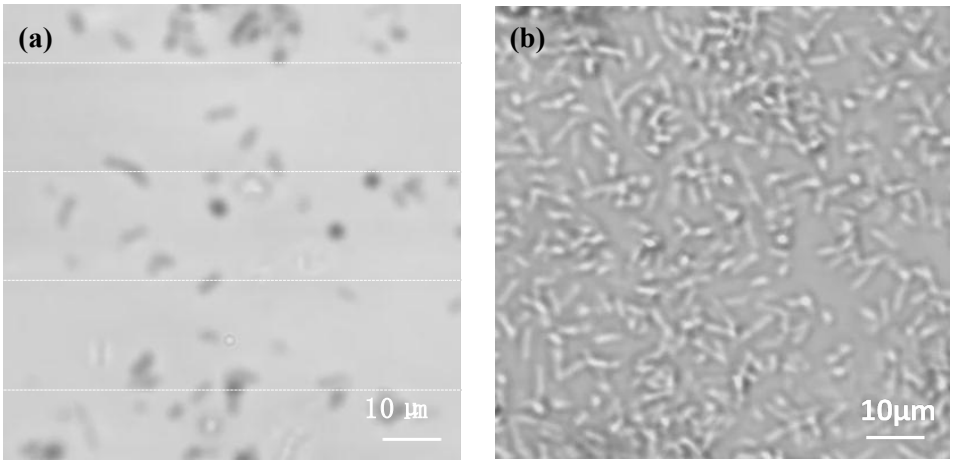

Fig. 13. Representative images taken from E-Coli attached on (a) the PDMS surface contains nanostructures. (b) the flat PDMS surface

For the ease of handling and observations, the nanostructures (nanochannels) were replicated from the copper to the PDMS following the process of soft-lithography. Same concentration of E-Coli was introduced to (1) the nanostructured surface and (2) flat surface. The E-Coli was then allowed to attach onto the surface for 15 min. Prior to the observations, the surface was then rinsed by PBS once to remove unattached E-Coli. The results are shown in **Fig. 13**, dashed lines marked where the "deeper" cuts are. The nanostructures are between the dashed lines.

As shown in **Fig. 13,** E-Coli attached on the nanostructured surface was observed less than those on the flat surface. However, the shaper cut with larger dimension (dashed lined) may confound the quantification of attachment density. Furthermore, the microscope we have handy does not have proper phase contrast module, rendering the quantification inconclusive. We also observe the movement of E-Coli. From the movement of E-Coli, the E-Coli was observed to have a different rotation pattern on the nanostructures than on a flat surface as observed by Gu et al. (Scientific Reports, vol. 6, Article number: 29516, 2016). Further investigations with high resolution microscopy may elucidate the effect of nanostructures on how bacteria land on the nanostructures and whether the altered landing scheme may affect their growth.

4. PUBLICATION AND AWARDS

Patent

1. Ping Guo and Yang Yang. "Method and apparatus for structural coloration of metallic surfaces." U.S. patent pending, No. 15/644,309.

Publications

J[1] Zhu, W. L., Zhu, Z., Guo, P., & Ju, B. F. (2018). A novel hybrid actuation mechanism based XY nanopositioning stage with totally decoupled kinematics. *Mechanical Systems and Signal Processing*, 99, 747-759.

J[2] Yeung, C. S., Yang, Y., Du, H., Wang, J., & Guo, P. (2018). Friction reduction performance of microstructured surfaces generated by nonresonant modulation cutting. *Proceedings of the Institution of Mechanical Engineers, Part C: Journal of Mechanical Engineering Science*, 0954406218796033.

J[3] You, X., Ye, C., & Guo, P. (2017). Electric field manipulation for deposition control in near-field electrospinning. *Journal of Manufacturing Processes*, 30, 431-438.

J[4] You, X., Ye, C., & Guo, P. (2017). Study of Microscale Three-Dimensional Printing Using Near-Field Melt Electrospinning. Journal of Micro and Nano-Manufacturing, 5(4), 040901.

J[5] Yang, Y., Gao, S., Chen, K., Pan, Y., & Guo, P. (2017). Vibration analysis and development of an ultrasonic elliptical vibration tool based on a portal frame structure. Precision Engineering, 50, 421-432.

C[5]Wang, J., Yang, Y., & Guo, P. (2018). Effects of vibration trajectory on ductile-to-brittle transition in vibration cutting of single crystal silicon using a non-resonant tool. *Procedia CIRP*, 71(1), 289-292.

C[6] Yang, Y., & Guo, P. (2018). Effect of elliptical vibration trajectories on grating structure formation and its application in structural coloration. *Procedia Manufacturing*, 26, 543-551.

Multimedia Technologies & AI Track

Research Reports In Multimedia Technologies and AI

Newly Funded Projects (2019-2021)	* Deep Learning Based Audio-visual Recognition of Cantonese Disordered Speech
Continuing Project (2017 - 2019)	* Achieving Simultaneous Spectral-Spatial Super-Resolution via Reconstruction from Multispectral and Hyperspectral Images

The following reports are enclosed in "Research Highlights" printed in August 2017

Completed Project (2014 - 2016)	* Managing and Analyzing Big Graph Data

The following reports are enclosed in "Research Highlights" printed in June 2015

Completed Project (2012)	* Face Recognition Across Ages Through Binary Tree Learning

The following reports are enclosed in "Research Highlights" printed in June 2014

Completed Projects (2011)	* Semantic Analysis for Image Resizing
	* Time Critical Applications over a Shared Network

	* Amplify-and-forward Schemes for Wireless Communications

The following reports are enclosed in "Research Highlights" printed in 2013

Completed Projects	
(2010)	* FADE: Secure Cloud Storage with File Assured Deletion
	* Security and Detection Protocols for P2P-Live Streaming Systems
(2009)	* An Opportunistic Approach to Capacity Enhancement in Wireless Multimedia Networks
	* Computer-Aided Second Language Learning through Speech-based Human-Computer Interaction

The following reports are enclosed in "General Report and Research Highlights 2009-2011" printed in October 2011.

Completed Projects	
(2008)	* Pattern Computation for Compression and Performance Garment
(2007)	* Real-time Transmission of High Definition (HD) 3D Video and HD Audio in Gigabit-LAN
	* High Dynamic Range Image Compression and Display
	* Multimedia Content Distribution over Hybrid Satellite-Terrestrial Communication Networks
(2006)	* Automatic Video Segmentation and Tracking for Real Time Multimedia Services
	* Information Retrieval from Mixed-Language Spoken Documents
	* Wireless Networks and Its Potential for Multimedia Applications

The following reports are enclosed in "Research Highlights 2005-2007" printed in January 2008.

Completed Projects	
(2005)	* Mobile Wireless Multimedia Communication
	* An Automatic Multi-layer Video Content Classification Framework
	* Automatic Multimedia Fission, Categorization and Fusion for Personalized Visualization in Multimedia Information Retrieval

(Funded Year)

DEEP LEARNING BASED AUDIO-VISUAL RECOGNITION OF CANTONESE DISORDERED SPEECH

Principal Investigator: Professor Xunying LIU
Department of Systems Engineering and Engineering Management, CUHK

Co-Investigator: Prof. Helen Mei-Ling MENG [1]

[1] Dept. of Systems Engineering and Engineering Management, CUHK

Project Start Date: 1 July 2019

ABSTRACT

Please state the abstract of the project in this part. The abstract should appear at the top of the report. All manuscripts must be in English.

Hyperspectral super-resolution (HSR), a recently emerged image processing technique that aims to reconstruct a spectral-spatial super-resolution image from images with either lower spectral resolution or lower spatial resolution, is expected to become a key technology soon. HSR can significantly enhance applications in areas such as computer vision, art conservation, food safety, geoscience and remote sensing, offering an imaging solution that can identify objects that are hard to see by human eyes and with fine resolutions. It holds great potential and we expect the topic will see substantial growth. The goal of this project is to investigate key fundamental problems that arise in this timely topic. Specifically, the PI will study perfect reconstruction conditions of HSR—which is an open theoretical question that none of the existing literature has been able to answer. Addressing this question satisfactorily will lead to guidelines on how to build provably correct HSR solutions, rather than relying on empirical experience which is currently the case. Furthermore, the PI will study a unified optimization framework for HSR, which is important in establishing a computationally efficient algorithmic toolset in this context.

INNOVATION AND PRACTICAL SIGNIFICANCE:

To include a paragraph to highlight specifically the innovation and practical significance of your work. Both VC and the door would like to see more research endeavors be directed to innovation and technology transfer for the betterment of mankind.

Automatic speech recognition (ASR) for disordered speech is a challenging task. Speech disorders such as dysarthria lead to severe degradation of speech quality, highly variable voice characteristics and large mismatch against normal speech. State-of-the-art speech recognition systems designed for normal speech often produce poor recognition accuracy when applied to disordered speech. Human speech production is a bimodal process based on audio-visual representation. The visual information is invariant to acoustic signal corruption and can provide complementary information to the speech recognizer. This motivates the use of visual information to improve disordered speech recognition. However, among people with speech disorders, their underlying medical conditions such as Parkinson disease and co-occurring disabilities increase the

difficulty to record high quality audio-visual data in large amounts that are necessary for audio-visual speech recognition (AVSR) system development. For example, in addition to the degradation of voice quality, head movements and different angles facing the camera are often found in recoding.

To the best of our knowledge, this project is the first attempt among the international multimedia, AI and speech technology research communities to use deep learning based AVSR approaches for disordered speech recognition. It is also the first one dedicated for Cantonese disordered speech. The outcome of this research will allow easier and more natural communication for Cantonese speaking people suffering from speech disorders with the outside world, improve their social inclusion and quality of life, and to support research and development efforts to create speech based assistive technology applications for such people. These can increase the cost effectiveness and quality of care and health service for them. This research will form a strong basis for future work on disordered speech recognition for Mandarin and other Chinese dialects to help a much larger number of similarly affected people in China.

PROJECT OBJECTIVES:

1. Using visual information to improve dysarthric speech recognition performance

2. Deriving novel deep AVSR methods to robustly model limited amounts of audio-visual disordered speech data

3. Deriving fast AVSR model adaptation methods to handle speaker dependent impairment characteristics

4. Developing exemplar AVSR systems and recipes to provide insights for designing state-of-the-art dysarthric speech recognition systems

5. Allow easier and more natural speech based communication for people suffering from speech disorders with the outside world, improve their social inclusion and quality of life

WORK IN PROGRESS

ACHIEVING SIMULTANEOUS SPECTRAL-SPATIAL SUPER-RESOLUTION VIA RECONSTRUCTION FROM MULTISPECTRAL AND HYPERSPECTRAL IMAGES

Principal Investigator: Professor Ken MA
Department of Electronic Engineering, CUHK

Research Team Members:
Qiang Li, Dr. [1], Ruiyuan Wu, Mr. [1], Qiong Wu, Ms. [1]

[1] Dept. of Electronic Engineering, CUHK

Reporting Period: 1 July 2017 – 31 May 2018
(to be completed in June 2019)

INNOVATION AND PRACTICAL SIGNIFICANCE:

This project aims to develop a theoretical framework for hyperspectral resolution, addressing why recovery of a hyperspectral super-resolution image from low resolution images can be possible in theory and further understanding how we can build better systems. While current developments in this context have shown successful results by empirical means, they are practice or intuition-driven and are unable to answer the question of why hyperspectral super-resolution works from a fundamental research viewpoint. The innovative part of this project is that the PI will depart from the standard path of the current research trends (which are somehow bottom-up) and endeavor to tackle much more challenging theoretical problems arising from this relatively new research topic (which is top-down with an emphasis on asking why, and not just how). The impacts are expected to be significant as it will lead to theoretical guidelines on designing provably good hyperspectral super-resolution algorithms and cameras, which is presently unavailable in the literature.

Moreover, the PI should emphasize that hyperspectral super-resolution is currently a rapidly emerging topic with great potential and many possibilities in applications such as computer vision, medical imaging, art conservation, to name a few. The PI sees that now is the great opportunity to investigate this timely topic, seeing the substantial impacts a theoretical framework can reshape the topic and the far-reaching implications in many applications.

ABSTRACT

Please state the abstract of the project in this part. The abstract should appear at the top of the report. All manuscripts must be in English.

Hyperspectral super-resolution (HSR), a recently emerged image processing technique that aims to reconstruct a spectral-spatial super-resolution image from images with either lower spectral resolution or lower spatial resolution, is expected to become a key technology soon. HSR can significantly enhance applications in areas such as computer vision, art conservation, food safety, geoscience and remote sensing, offering an imaging solution that can identify objects that are hard to see by human eyes and with fine resolutions. It holds great potential and we expect the topic will see substantial growth. The goal of this project is to investigate key fundamental problems that arise in this timely topic. Specifically, the PI will study perfect reconstruction conditions of HSR—which is an open theoretical question that none of the

existing literature has been able to answer. Addressing this question satisfactorily will lead to guidelines on how to build provably correct HSR solutions, rather than relying on empirical experience which is currently the case. Furthermore, the PI will study a unified optimization framework for HSR, which is important in establishing a computationally efficient algorithmic toolset in this context.

1. OBJECTIVES AND SIGNIFICANCE

Please state the objective and significance of the project in this part.

1. to analyze conditions under which perfect recovery of a super-resolution image is guaranteed, and to identify good low-rank models and provably correct formulations under such analyses

2. to establish a unified optimization framework for low-rank matrix factorization in HSR

The first objective of this project is particularly innovative. All the current developments in HSR demonstrate feasibility via empirical experiences, and the designs are intuition-driven. A theoretical framework that pins down whether and how super-resolution is possible is still missing—and the PI intends to challenge that piece of uncharted water. The outcomes, if satisfactory, will provide theory-guided designs for HSR, which has much significance from a fundamental research viewpoint and will reshape how practical researchers think when designing an HSR algorithm. The second objective is important in bringing new and computationally efficient tools for practical implementations.

2. RESEARCH METHODOLOGY

Please state the research methodology of the project in this part.

We consider low-rank matrix factorization for HSR---which is a widely adopted approach in the current HSR literature---and investigate two key aspects. First, we aim to answer an open theoretical question, namely, whether and under what conditions low-rank matrix factorization methods can guarantee perfect recovery of the true super-resolution image. Being able to address this question satisfactorily will lead to substantial impacts on developing good algorithms for HSR and on the designs of multispectral and hyperspectral camera. Currently, none of the existing literature is able to show that the low-rank matrix factorization problem can guarantee perfect recovery of the super-resolution image.

Second, we intend to establish a unified optimization framework for low-rank matrix factorization in HSR. The aim is to provide computationally efficient solutions for HSR. The problem size in HSR is large; e.g., a super-resolution image with 200 spectral bands and 1,000x1,000 pixels amounts to 200,000,000 unknowns. Careful designs that exploit problem structures are essential, and the framework should be flexible in being able to accommodate various forms of problem structure-exploiting regularizations. The outcome, if successful, will lead to a powerful computational toolset for practical implementations.

3. RESULTS ACHIEVED SO FAR

Please state the project achievement and highlight (if any) on potential for commercialization and technology transfer in this part.

Achievement 1: Efficient Optimization Schemes for HSR

In C[1], we developed novel optimization schemes for low-rank matrix factorization in HSR. The proposed schemes run many times faster than the state of the art, as our extensive numerical studies showed. We achieve this by considering a hybrid inexact alternating minimization framework. Existing studies often

employ exact alternating minimization, which incurs high computational costs at each iteration. Our idea is to replace the exact updates with inexact proximal gradient or conditional gradient updates, thereby reducing the per-iteration computational costs substantially. The proposed schemes are not just based on engineering intuitions. As a preliminary result at this moment, we showed that these schemes are equipped with theoretical guarantees on convergence.

C[1] achieves Objective 2 very well. As an ongoing work, we are consolidating our findings in C[1]. We are aiming at establishing an optimization framework—which generalizes the current hybrid inexact alternating minimization schemes—that flexibly covers a broad range of low-rank matrix factorization problems in HSR. Under this unified framework, we will provide theoretical analyses that give evidence on why the proposed framework can converge faster than the state-of-the-art. We expect that this will lead to a new standard for low-rank matrix factorization algorithm designs in HSR, and hence this will be one of the key investigations in the second year of this project. The eventual outcome will be submitted as a journal article.

Achievement 2: Guaranteed Perfect Recovery of HSR Images in Polynomial Time

In C[3], and as another signature research output, we were successful in showing a sufficient condition under which we can guarantee perfect reconstruction of the true super-resolution image. Simply speaking, our sufficient condition suggests that if the spectral resolution of the multispectral camera and the spatial resolution of the hyperspectral camera are not too coarse, then HSR perfect reconstruction is possible. This result is significant because it is the first reported result on solving the HSR perfect reconstruction problem in polynomial time—which is surprising as HSR was previously thought to be a computationally intractable (NP-hard) problem. Furthermore, our result suggested that we can, in principle, use very efficient (polynomial-time) algorithms to attain such an HSR perfect reconstruction guarantee.

While preliminary, the theory presented in C[3] is a vital milestone for Objective 1 and beyond. As an ongoing work, we are further analyzing how robust our newly developed theory is under modeling errors. This presents new analysis challenges that are unique to HSR and not seen in the current literature. Also, we are studying what new insights our result shows in terms of algorithm designs. If successful, the aforementioned studies will lead to a major breakthrough in HSR theory.

Achievement 3: A New HSR Formulation by Tensor Factorization

This is a fruitful outcome from international collaboration. The PI and his international collaborators developed a new HSR framework using tensor factorization. The existing works often treat the HSR problem as a (2D) matrix factorization problem, and none considered it as a (3D) tensor problem. Yet, super-resolution images are (3D) tensors by nature. The international collaborators are experts in tensor. The PI shared his insights and experience with the HSR problem, and by tapping on the collaborators' expertise the two sides successfully built a coupled tensor factorization framework for HSR. It is a framework not seen before (neither HSR nor tensor factorization theory), it is equipped with perfect reconstruction guarantees (like that in Achievement 2), and it was empirically found to outperform several existing matrix factorization solutions.

This part of the work leads to two accepted conference papers C[2], C[5] and one submitted journal paper J[1].

Achievement 4: HSR by Convex Optimization

As a variation on the theme of the main research undertaking, we also considered a low-rank HSR formulation using nuclear norm regularization, which led to the research output of C[4]. The idea is different from those of the previously mentioned achievements in that we adopt a convex optimization formulation. It should be noted that all the previous achievements, as well as the existing works, adopt non-convex formulations. The advantage of using a convex formulation is that it does not suffer from local minima, and

more consistent reconstruction performance may be yielded by pursuing such a formulation. Our empirical study indicated that the proposed method is more robust to noise than some state-of-the-art algorithms.

Our latest investigation reveals that the convex HSR formulation mentioned above has several advantages that deserve our further attention. Simply speaking, it works on a more relaxed model compared with the commonly adopted matrix factorization model in HSR. Hence, in practice the former may stand a better chance when the multispectral and hyperspectral images exhibit strong variabilities against the nominal model. We are currently investigating such possibilities.

Before finishing this report, the PI would like to express his gratitude to SHIAE for funding this project. The PI could not have accomplished any of the above reported results—which he believes hold much promise in immediate significance and long-term impacts—without the support of SHIAE.

4. PUBLICATION AND AWARDS

Please list out and number all the publications and/or awards produced under the funded project. All these publications must be directly acknowledged the SHIAE funding support and stated the affiliation with the Institute. The list can be numbered in alphabetic order. When referring to them for the submission in CD, name the file with corresponding reference number in square brackets as "81150xx-J[1].pdf".

C[1] R. Wu, C.-H. Chan, H.-T. Wai, W.-K. Ma, and X. Fu, "Hi, BCD! Hybrid Inexact Block Coordinate Descent for Hyperspectral Super-Resolution," IEEE International Conference on Acoustics, Speech and Signal Processing (ICASSP), IEEE, Calgary, Canada, pp. 2426-2430, April 15-20, 2018.

C[2] C. I. Kanatsoulis, X. Fu, N. D. Sidiropoulos, and W.-K. Ma, "Hyperspectral Super-Resolution via Coupled Tensor Factorization: Identifiability and Algorithms," IEEE International Conference on Acoustics, Speech and Signal Processing (ICASSP), IEEE, Calgary, Canada, pp. 3191-3195, April 15-20, 2018.

C[3] Q. Li, W.-K. Ma and Q. Wu, "Hyperspectral Super-Resolution: Exact Recovery in Polynomial Time," IEEE Statistical Signal Processing Workshop (SSP), IEEE, Freiburg, Germany, June 10-13, 2018.

C[4] R. Wu, Q. Li, X. Fu and W.-K. Ma, "A Convex Low-Rank Regularization Method For Hyperspectral Super-Resolution," IEEE Statistical Signal Processing Workshop (SSP), IEEE, Freiburg, Germany, June 10-13, 2018.

C[5] C. I. Kanatsoulis, X. Fu, N. D. Sidiropoulos, and W.-K. Ma, "Hyperspectral Super-Resolution: Combing Low Rank and Matrix Structure," to appear in IEEE International Conference on Image Processing (ICIP), IEEE, Athens, Greece, October 2018.

J[1] C. I. Kanatsoulis, X. Fu, N. D. Sidiropoulos, and W.-K. Ma, "Hyperspectral Super-Resolution: A Coupled Tensor Factorization Approach," submitted to IEEE Transactions on Signal Processing, April 2018, online available at https://arxiv.org/abs/1804.05307.

Shun Hing Distinguished Lecture Series

To achieve the Institute's mission to promote appreciation of engineering in society through education programs, the Institute has organized a Shun Hing Distinguished Lecture Series. So far, **forty-seven** distinguished lectures have been presented by renowned scholars. These lectures all were very well received and we will continue to line up and invite outstanding researchers to visit CUHK and to deliver distinguished lectures for the Institute. Here to show the **two** distinguished lectures between 2018 and June 2019.

Interpretable Convolutional Neural Networks (CNNs) via Feedforward Design

by Professor C.-C. Jay Kuo

University of Southern California
USA

Date: 4 December 2018 (Tuesday)

Abstracts

Given a convolutional neural network (CNN) architecture, its network parameters are determined by backpropagation (BP) nowadays. The underlying mechanism remains to be a black-box after a large amount of theoretical investigation. In this talk, I describe a new interpretable and feedforward (FF) design with the LeNet-5 as an example. The FF-trained CNN is a data-centric approach that derives network parameters based on training data statistics layer by layer in one pass. To build the convolutional layers, we develop a new signal transform, called the Saab (Subspace approximation with adjusted bias) transform. The bias in filter weights is chosen to annihilate nonlinearity of the activation function. To build the fully-connected (FC) layers, we adopt a label-guided linear least squared regression (LSR) method. The classification performances of BP- and FF-trained CNNs on the MNIST and the CIFAR-10 datasets are compared. The computational complexity of the FF design is significantly lower than the BP design and, therefore, the FF-trained CNN is ideal for mobile/edge computing. We also comment on the relationship between BP and FF designs by examining the cross-entropy values at nodes of intermediate layers.

Research of Smart Technology for Eldercare

by Professor Dominic K.C. Ho

Electrical Engineering and Computer Science Department
Univ. of Missouri
USA

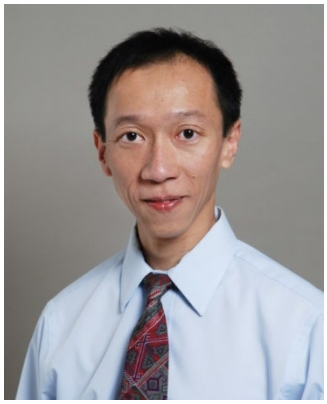

Date: 30 August 2018 (Thursday)

Abstracts

The use of technologies for health care and assisted living has attracted considerable interest in recent years. Perhaps an urgent need for this technology development is for elderly care, due to the aging population in the world and the considerable amount of financial burden incurred. A number of commercial products are available for health monitoring. Nevertheless, the wearable nature of these devices presents challenges and discomfort to the elderly. This talk introduces two low-cost, non-invasive and non-wearable sensors together with the sensor data processing for eldercare that are suitable for use in an in-home environment. One is the radar that is effective for gait monitoring and fall detection. The other is the bed sensor that is capable of heart rate tracking and relative blood pressure monitoring. The radar is mounted on the ceiling/wall and is based on the Doppler shift effect that characterizes the fall motion in terms of micro-Doppler. The bed sensor is placed under the mattress and is based on the hydraulic principle that captures the mechanical movement of the heart in terms of the Ballistocardiogram. Time-frequency analysis together with machine learning approach are used for sensor data processing. In addition to laboratory results, performance of the developed eldercare technologies in senior residence apartments will be demonstrated.

Shun Hing Institute of Advanced Engineering (SHIAE)
The Chinese University of Hong Kong
Shatin, N.T., Hong Kong

Office : Room 702, William M.W. Mong Engineering Building
Tel : (852) 3943 4351
Fax : (852) 3943 4354
Email : info@shiae.cuhk.edu.hk
Website : http://www.shiae.cuhk.edu.hk